Studies on Arabidopsis MYB Transcription Factor Genes: Potential Regulators of the Phenylpropanoid Pathway and Analysis of the Root Preferentially Expressed Gene *AtMYB68*

By
Qing Wang
Master of Agronomy, Beijing Agriculture University, Beijing, China, 1991

A THESIS SUBMITTED IN PARTIAL FULFILLMENT OF THE REQUIREMENTS FOR THE DEGREE OF DOCTOR OF PHILOSOPHY

in
THE FACULTY OF GRADUATE STUDIES
(Department of Botany)

We accept this thesis as conforming to the required standard

THE UNIVERSITY OF BRITISH COLUMBIA
April, 2003

In presenting this thesis in partial fulfilment of the requirements for an advanced degree at the University of British Columbia, I agree that the Library shall make it freely available for reference and study. I further agree that permission for extensive copying of this thesis for scholarly purposes may be granted by the head of my department or by his or her representatives. It is understood that copying or publication of this thesis for financial gain shall not be allowed without my written permission.

Department of Botany

The University of British Columbia
Vancouver, Canada

Date May 14, 03

Abstract

Genes encoding MYB transcription factors constitute a large family in Arabidopsis. With completion of the Arabidopsis genome sequence, over 130 *MYB* genes have been annotated in Arabidopsis. However functions of most of these genes are unknown.

To attempt to identify *MYB* genes involved in the regulation of the phenylpropanoid pathway, in particular, the lignin biosynthesis pathway, we took advantage of the ongoing Arabidopsis EST project at the time I started my thesis, and collected all the available 25 *MYB* EST clones. These clones represented 21 unique *MYB* genes. Expression patterns of these genes were determined by northern blot analyses to search for those that were expressed coordinately with *At4CL1*, a gene encoding one of the major enzymes in the general phenylpropanoid pathway and used as a marker for this search. Accumulation of transcripts was not detectable in the seedling and mature organs for 11 out of 21 genes. None of detected expression patterns of the *MYB* genes was similar to that of *At4CL1*. *MYB* cDNAs were then cloned from Arabidopsis bolting stems where *At4CL1* was highly expressed. A novel *MYB* gene, *STM31*, was identified. The transcript of *STM31* was accumulated ubiquitously in the seedling and all organs tested. Thus *STM31* did not appear to be a good candidate to regulate *At4CL1* transcription either.

By searching Arabidopsis T-DNA tagged populations, one T-DNA line that had the insertion in the promoter region of *AtMYB68* was identified in the Douglas laboratory. *AtMYB68* was further characterized by expression profiling. Both northern blot and RT-PCR analyses showed that the transcript of *AtMYB68* was predominantly accumulated in the root but was detectable in the seedling shoot. At the tissue and cellular level, GUS activity driven by the *AtMYB68* promoter was detected in the stele tissue of the root. A root cross-section revealed that GUS staining was more intense in the pericycle cells near the two xylem poles in the root. In the shoot, GUS staining was detected in the stomata guard cells of young leaves. GUS activity driven by the *AtMYB68* promoter was also examined in the *woodenleg* mutant background, in which the xylem was the only component in the vascular tissue of the primary root. GUS

staining was strong in the whole layer of pericycle cells and expanded to the endodermis layer in this mutant background. This result suggests that the activity of the *AtMYB68* promoter is induced by a signal from the root xylem. The level of the endogenous *AtMYB68* transcript was induced by the plant hormone IAA ~2-fold, and by ABA ~3-fold.

In order to determine *AtMYB68* function, transgenic lines overexpressing and underexpressing *AtMYB68* were generated in Arabidopsis. In addition, by searching several T-DNA tagged populations, one knockout line for *AtMYB68* was identified. In this line, the level of the *AtMYB68* transcript was very low. Phenotypes of both the overexpression line and the knockout line were examined. No morphological changes were found in either mutant line, and no phenotypic changes in response to external stimuli examined were observed. Expression patterns of the members in the *AtMYB68* phylogenetic subgroup were determined by RT-PCR. At least one more member, *AtMYB36*, had the organ-specific expression pattern very similar to that of *AtMYB68*. These results suggest that functional redundancy may exist in this subgroup.

Taken together, the data of expression profiling suggest that *AtMYB68* may play a role in the pericycle cell identity adjacent to the xylem pole. In the future, *atmyb68* double or triple mutants with closely related members might reveal a precise role of *AtMYB68*. In addition, characterization of *AtMYB68* downstream target genes can be done by using the microarray analysis.

Table of Contents

List of Tables

List of Figures

Abbreviations

4CL	4-coumarate:CoA ligase
ABA	abscisic acid
ABRC	Arabidopsis Biological Resource Center
ABREs	ABA-responsive elements
ACC	1-aminocyclopropane-1-carboxylic acid
ADH	alcohol dehydrogenase
Am	*Antirrhirum majus*
AN	ANTHOCYANIN
AP2	APETALA2
AS1	ASYMMETRICAL LEAVES1
ASA	anthranilate synthase α-subunit
At	*Arabidopsis thaliana*
ATR1	ALTERED TYPTOPHAN REGULATION1
B1	BOOSTER1
BAN	BANYULS
BAP	6-benzylaminopurine
bHLH	helix-loop-helix
BSA	bovine serum albumin
C1	COLORLESS1
C4H	cinnamate 4-hydroxylase
CAD	cinnamyl alcohol dehydrogenase
CaMV	35S cauliflower mosaic virus 35S promoter
CCA1	CIRCADIAN CLOCK ASSOCIATED1
CHS	chalcone synthase
CNBr	cyanogen bromide
Col	Arabidopsis Columbia ecotype
CPC	CAPRICE
DFR	DIHYDROFLAVONOL-4-REDUCTASE
DIC	Differential Interference Contrast
EDTA	ethylenediaminetetra-acetic acid
EREBP	ethylene-responsive-binding element protein
EST	Expressed Sequence Tag
GA3	gibberelic acid
GL1	GLABROUS1
GUS	β-glucuronidase

HR	hypersensitive response
IAA	indole-3-acetic acid
ICK	interactors of Cdc2 kinase
IPTG	isopropyl-β-D-thiogalactopyranoside
Kan	kanamycin
Kb	kilobase
KDa	kiloDalton
KNOX	knotted1-like homeobox
LC-MS	liquid chromatography-mass spectrometer
LHY	LATE ELOGATED HYPOCOTYL
MES	2[N-Morpholino]ethansulfonic Acid
MOPS	3-[N-Morpholino]propanesulfonic acid
MPSS	Massively Parallel Signature Sequencing
MS	Murashige and Skoog
MSA	M-specific activator
MYB3R	MYB homologue with three MYB repeats
MYBR1	MYB homologue with a single MYB repeat
ORF	Open Reading Frame
Pl	PURPLE LEAF
PAGE	polyacrylamide gel electrophoresis
PAL	phenylalanine ammonia-lyase
PAP	PRODUCTION OF ANTHOCYANIN PIGMENT
PBS	phosphate-buffered saline
Pc	*Petroselinum crispum*
PCR	Polymerase Chain Reaction
PEG	polyethylene glycol
Ph	*Petunia hybrida*
PHAN	PHANTASTICA
PMSF	phenylmethylsulfonyl fluoride
PVDF	polyvinylidene difuoride
RTBP1	RICE TELOMERE-BINDING PROTEIN 1
R1	RED1
RACE	Rapid Amplification of cDNA Ends
RNAi	RNA interference
RS2	ROUGH SHEATH2
RT	reverse transcription
SD	standard deviation
SDS	sodium dodecyl sulphate
shr	short-root
SOS	Salt Overly Sensitive
SSC	standard saline citrate buffer

STM	SHOOT MERISTEMLESS
T-DNA	transferred-DNA
TILLING	Targeting Induced Local Lesions in Genomes
TMRI	Torrey Mesa Research Institute
TOC1	TIMING OF CAB 1
TT	TRANSPARENT TESTA
TTG	TRANSPARENT TESTA GLABROUS
WER	WEREWOLF
wol	woodenleg
WS	Arabidopsis Wassilewskija ecotype
Zm	*Zea mays*

Acknowledgements

I would like to thank my supervisor Dr. Carl Douglas for his supervision, patience and encouragement throughout the duration of my PhD study, and for accepting me as a student first of all. I would like to thank my committee members Dr. B. Green, Dr. G. Haughn and Dr. J. Kronstad for their guidance and suggestion. Thank you, the Douglas lab former and current members for a co-operative and friendly environment, and members in the Haughn and Kunst labs. Dr. A. Pri-Hadash initiated the second project presented in my thesis. Dr. J. Ehlting is always willing to help, and Dr. D.K. Ro is so supportive during my thesis writing.

Thank you, my mom and dad. Although they are far away from me, they have been trying to give me a hand financially and mentally as always. During my study, I hardly got a chance going back to see them. I feel sorry for this. Special thanks to my husband Jing for being fundamental in helping me to achieve my degree. He experienced his mother and sister lost in last few years, but he showed me to be optimistic and open-minded to difficulty. During my study, I gave birth to my daughter Angie. She is a really great gift. Definitely she adds more work on me, but she is the light during these years' frustration.

From knowing nothing about Arabidopsis, to my thesis is full of Arabidopsis, I went through a hard journey. 'No pain, no gain', I wish it's true to me.

Chapter 1 General Introduction

1.1 The Phenylpropanoid Pathway

The phenylpropanoid pathway is required for the biosynthesis of a series of natural products based on a phenylpropane skeleton derived from L-phenylalanine. These phenylpropanoid products play important roles in higher plants. They serve as low molecular weight pigments, antibiotics (phytoalexins), UV protectors, insect repellents, and signal molecules in plant defense. They also function as polymers in surface and support structures, such as suberin, lignin (Hahlbrock and Scheel, 1989; Dixon and Paiva, 1995).

The flow of carbon from primary metabolism into an array of secondary phenylpropanoid products is through the general phenylpropanoid pathway (Figure 1-1). The specific branch pathways derive their basic phenylpropanoid unit from this core reaction (Hahlbrock and Scheel, 1989; Douglas, et al., 1992). This pathway is composed of three enzymes, phenylalanine ammonia-lyase (PAL), cinnamate 4-hydroxylase (C4H) and 4-coumarate:CoA ligase (4CL). PAL catalyzes the first step, the de-amination of L-phenylalanine to produce cinnamic acid. Cinnamic acid is then hydroxylated at the para-position by C4H, a cytochrome P450 mono-oxygenase. The product is further modified by other hydroxylases and O-methyltransferase. The enzyme 4CL catalyzes the formation of CoA esters of cinnamic acids, and these activated intermediates serve as the substrates for specific branch pathways, such as those leading to the synthesis of flavonoids and lignin.

With the large structural and functional diversity of these phenylpropanoid compounds, their temporal and spatial distributions are very different during development. For example, biosynthesis and deposition of lignin are developmentally regulated, and occur in tracheary elements during xylem differentiation. The flavonoid pigment deposition in plant organs also occurs in a cell type specific manner, such as in the epidermal cells of petals and in the aleurone

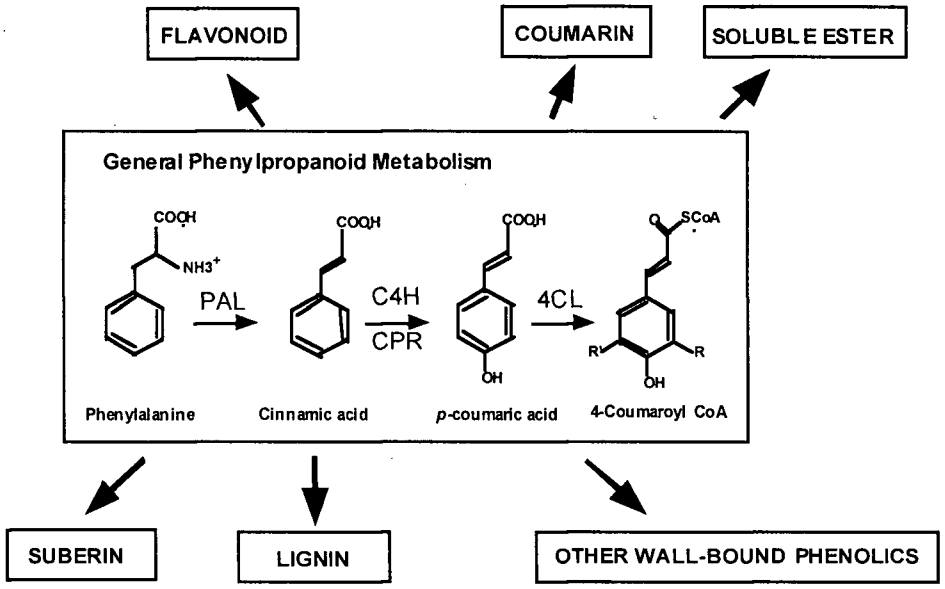

Figure 1-1. Reactions of General Phenylpropanoid Metabolism (according to Hahlbrock and Scheel et al., 1989).
Thicker arrows indicate branch pathways emanating from the general pathway. PAL, phenylalanine ammonia-lyase; C4H, cinnamate 4-hydroxylase; 4CL, 4-coumarate:CoA ligase.

layer of maize kernels. The biosynthesis of phenylpropanoid compounds is also induced upon environmental stimuli such as wounding, pathogen infection, and UV irradiation (Hahlbrock and Scheel, 1989; Douglas, et al., 1992; Dixon and Paiva, 1995).

Genes encoding the enzymes in the general phenylpropanoid pathway and some branch pathways have been isolated from many plant species (Dixon and Harrison, 1990). In many cases it has been shown that the gene transcripts accumulate in a tissue/cell type specific manner during plant development, and that expression is activated in response to different environmental stimuli (Hahlbrock and Scheel, 1989; Dangl, 1991; Douglas et al., 1992; Dixon and Paiva, 1995). This point can be illustrated using the example of *4CL* genes. *4CL* genes have been cloned from Arabidopsis and other plant species (Lee et al., 1995; Douglas et al., 1992). In all these plants, 4CLs are encoded by a small gene family. In Arabidopsis, in addition to At4CL1,

two more *4CL* genes, *At4CL2* and *At4CL3*, have been identified. *At4CL1* and *At4CL2* cDNAs share 80% identity (Ehlting et al., 1999). It has been shown that expression of *At4CL1* is correlated with lignin deposition during seedling development. In the mature plant, *At4CL1* is strongly expressed in bolting stems compared to leaves and flowers. The expression of *At4CL1* is also induced by wounding and bacterial pathogen infection (Lee et al., 1995).

It has been demonstrated that expression of genes encoding enzymes in the phenylpropanoid pathway is coordinately regulated. In Arabidopsis, expression of *PAL*, *C4H* and *4CL*, the genes encoding enzymes in the general phenylpropanoid pathway, is coordinately induced by wounding (Lee et al., 1997). Similar results are also obtained upon wounding, elicitor or UV irradiation in other plant species (Fahrendorf et al., 1995; Gorlach et al., 1995; Logemann et al., 1995).

It is believed that the phenylpropanoid pathway is regulated primarily through control of transcription initiation. The presence or activity of transcription factors is modulated by developmental and environmental signals, and these factors in turn regulate the expression of sets of genes encoding enzymes in the phenylpropanoid pathway, and thus the activity of the pathway (Hahlbrock and Scheel, 1989; Douglas et al., 1992).

In vivo footprinting and deletion analyses have defined putative cis-elements, which are conserved in the promoters of genes encoding enzymes in the phenylpropanoid pathway. In particular, the conserved motifs, P- and L-boxes have been found in the promoters of *PAL*, *4CL* and other structural genes in the phenylpropanoid pathway (Lois et al., 1989; Logemann et al., 1995; Douglas, 1996). These common cis-elements provide a basis for the coordinate regulation of the transcription of structural genes in the phenylpropanoid pathway.

1.2 Plant Transcription Factors

A 'transcription factor' is a protein that regulates the transcription frequency of a target gene (Stracke et al., 2001). A transcription factor usually displays a modular structure, and can

be a transcription activator, repressor, or both. Transcription factor genes comprise a substantial fraction of all eukaryotic genomes. On the basis of similarity in the sequence of the DNA-binding domain, the majority of transcription factors can be classified into a limited number of different families (Pabo and Sauer, 1992; Riechmann and Ratcliffe, 2000. Table 1-1).

Table 1-1. Major Gene Families of Arabidopsis Transcription Factors in Comparison to Other Species (According to Riechmann and Ratcliffe, 2000)

Gene Family	Predicted Gene Number in Genomes			
	Arabidopsis	*Drosophila*	*C. elegans*	*S. cerevisiae*
MYB	~130	35	16	19
AP2/EREBP	150	0	0	0
NAC	105	0	0	0
bHLH/MYC	100	61	38	8
bZIP	100	24	18	15
HB	90	113	88	10
Z-C_2H_2	85	352	138	47
MADS	80	2	2	4
WRKY	75	0	0	0
ARF	42	0	0	0
Dof	41	0	0	0

ARF, auxin response factor; EREBP, ethylene-responsive-binding element protein; HB, homeobox; Z-C_2H_2, zinc-finger protein of the C_2H_2 type.

With the completion of the *Arabidopsis thaliana* genome sequence, it is estimated that there might be more than 1,600 transcription factor genes in Arabidopsis, which represents about 6% of the total ~26,000 genes in this plant species (Riechmann and Ratcliffe, 2000), as compared to 700 in *Drosophila* and 500 in the *C. elegans* genome, which respectively represent 5% and 2.7% of the total genes in each genome (Rubin et al., 2000). These numbers suggest that Arabidopsis is comparable to *Drosophila* in terms of gene regulatory networks. It has been noted that many families of transcription factors exhibit great variation in numbers among different eukaryotes, and some families are organism-specific (Rubin et al., 2000). From Table 1-1, it can be seen that some classes of transcription factors are plant-specific, such as AP2/EREBP and NAC. For some classes of transcription factors, such as the MYB and MADS-box classes, the

numbers are significantly higher in plants. Among these transcription factors, *MYB* genes comprise one of the largest gene families in Arabidopsis.

1.3 MYB Transcription Factors: Structure

The first *MYB* gene identified was *v-myb*, a chicken oncogene derived from the avian myeloblastosis virus, which causes acute myeloblastic leukemia (Klempnauer et al., 1982). *v-myb* is a truncated version of the wild type gene *c-myb*. *c-myb* is well conserved in all vertebrates examined to date. *A-Myb* and *B-Myb* are two homologs of *c-myb* in vertebrates. The proteins encoded by these genes contain the conserved MYB DNA-binding domain and share limited homology in other regions (Weston, 1998). Deletion analysis of these members has revealed three functional domains: an amino-terminal DNA-binding domain, a central transcription activation domain and a carboxyl-terminal negative regulatory domain (Thompson and Ramsay, 1995). The DNA-binding domain is generally composed of three imperfect repeats of 51-52 amino acids. Each repeat includes three regularly spaced tryptophan residues, and forms three alpha helical bundles around hydrophobic cores of the conserved tryptophan residues (Thompson and Ramsay, 1995). The three repeats in c-Myb are referred as R1, R2 and R3 (Thompson and Ramsay, 1995; Weston, 1998).

Proteins containing the MYB DNA-binding domain are also found in plants, including Arabidopsis, maize, *Anthirrhinum* and rice (Romero et al, 1998; Rabinowicz et al., 1999; Jackson et al., 1991; Locatelli et al., 2000). Compared to MYB factors in vertebrates, most plant MYB homologs contain two repeats in the DNA-binding domain, corresponding to the R2 and R3 repeats in c-Myb (R2R3-type MYB).

Genes encoding the conserved MYB DNA-binding domain usually constitute large gene families in plants. In Aradidopsis, there are a total of 125 R2R3-type *MYB* genes annotated on the basis of the completed genome sequence (Stracke et al., 2001. Table 1-2). The large size of the *MYB* gene family is also confirmed in maize, in which 97 R2R3-type *MYB* genes have been

identified so far (Rabinowicz et al., 1999). According to the similarity of amino acid sequences outside the MYB DNA-binding domain, Arabidopsis MYB factors have been categorized into 22 phylogenetic subgroups (Kranz et al., 1998; Stracke et al., 2001). In contrast to intensive sequence information available, functions of most of these genes are not known yet.

Table 1-2. Genes Encoding MYB3R- and R2R3-Type MYB Transcription Factors in Arabidopsis (According to Stracke et al., 2001)

Gene Name	Gene Number
***AtMYB3R* genes:** *AtMYB3R1* to *AtMYB3R5*	5
R2R3-type genes: *AtMYB0* to *AtMYB124*	125
'Unusual' *MYB* genes: *AtMYBCDC5* *AtMYB4R1*	2

1.4 Plant MYB Transcription Factors: Functions

1.4.1 Plant MYB Factors with One Repeat

Gene encoding proteins with only one MYB repeat (MYB1R) have been identified from several plant species, including potato, Arabidopsis, parsley and rice (Baranowskij et al., 1994; Kirik and Baumlein, 1996; Feldbrugge et al., 1997; Lu et al., 2002). This group of MYB-like proteins is fairly divergent, and has low identity (30%-40%) to either the second (R2) or the third repeat (R3) of the MYB DNA-binding domain in the human c-Myb. Over 9 genes encoding MYB1R proteins are detected in the Arabidopsis genome (Carre and Kim, 2002).

Arabidopsis MYB1R proteins LHY and CCA1 have been found to be related to the circadian clock. Accumulation of *LHY* and *CCA1* transcripts is closely associated with the

circadian rhythm (Schaffer et al., 1998; Wang et al., 1997). Overexpression of either gene abolishes rhythmic expression of a set of circadian genes. These two genes are also able to regulate negatively their own transcription. LHY and CCA1 share high similarity at the amino acid level and might be functionally redundant (Wang and Tobin, 1998; Schaffer et al., 1998). They have been proposed to interact with the other regulator TOC1 as components of the Arabidopsis circadian oscillator (Alabadi et al., 2001).

MYBR1 proteins have also been found to be involved in other developmental processes. For instance, PcMYB1 from parsley interacts with a light-regulatory cis-element (Feldbrugge et al., 1997), and Arabidopsis CPC is a positive regulator of root hair formation (Wada et al., 1997). TRIPTYCHON, a homolog of CPC, regulates trichome formation in the leaf epidermis in Arabidopsis (Schellmann et al., 2002). Three cDNAs encoding the single MYB repeat have been identified from rice. Their products bind to the conserved cis-element in the promoter of an α-amylase gene and may contribute to gibberellin and sugar regulation of α-amylase gene expression (Lu et al., 2002).

MYB1R proteins also include telomeric DNA binding proteins. For example, RTBP1 identified in rice binds to the conserved tandem repeat sequence in plant telomeric DNA (Yu et al., 2000). The single MYB DNA-binding domain in RTBP1 is well conserved in the telomeric DNA binding proteins identified from different species, such as yeast and mammals (Broccoli et al., 1997; Spink et al., 2000; Vassetzky et al., 1999). Interestingly, unlike canonical MYB transcription factors, the single MYB repeats in the telomeric DNA binding proteins are located at the carboxy-ternimi. The binding of proteins to telomeric DNA is proposed to maintain chromosome integrity and protect telomers from degradation and end fusion (Greider, 1996).

1.4.2 Plant MYB Factors with Three Repeats

Through genome sequencing, genes encoding three MYB repeats (MYB3R) have been identified from Arabidopsis (Braun and Grotewold, 1999). Such genes have been also detected

in all the major plant lineages, including mosses, ferns and monocots. These genes constitute a small gene family in plant lineages, which is similar in size to the families in vertebrates and *Drosophila* (Kranz et al., 2000). Five MYB3R genes are annotated in the Arabidopsis genome (Stracke et al., 2001. Table 1-2). The plant MYB3R proteins and the vertebrate c-Myb share a high degree of amino acid identity in the MYB DNA-binding domain (over 60%, compared to 40%-60% between the R2R3-type proteins and the vertebrate c-Myb) (Braun and Grotewold, 1999). The intron-exon structures are also conserved in MYB3R genes from vertebrates and plants (Braun and Grotewold, 1999; Kranz et al., 2000).

In vertebrates, MYB transcription factors play an important role in the control of cell proliferation, differentiation and cell death through the cell cycle regulation (Thompson and Ramsay, 1995; Weston, 1998). The closer relationship between the plant MYB3R proteins and vertebrate MYB proteins in sequence suggests that the plant MYB3R proteins may have similar functions. In support of this speculation, three MYB3R proteins identified in tobacco have been found to bind to the conserved cis-element MSA in the promoters of plant B-type cyclin genes and modulate the promoter activity (Ito et al., 2001). However, the exact function of plant MYB3R proteins is not known yet.

1.4.3 R2R3-Type Plant MYB Factors

R2R3-type MYB genes constitute a large gene family and are only present in the plant lineage (Riechmann et al., 2000). However functions of these genes are poorly understood. From known cases, they are involved in many aspects of plant growth and development, and appear to regulate plant-specific processes.

(1) Regulation of phenylpropanoid metabolism. Extensive genetic and molecular studies have shown that the accumulation of specific flavonoid end products, such as anthocyanins and flavonols in plants, is under the control of MYB transcription factors. It was first revealed in maize that anthocyanin biosynthesis requires the interaction of the MYB factor

C1/Pl with the basic helix-loop-helix (bHLH, Myc) member R1/B1 (Cone et al., 1986; Paz-Ares et al., 1987; Ludwig et al., 1989). Each family contains several alleles and multiple paralogs to control pigmentation in different tissues and organs. For instance, C1 is required for anthocyanin accumulation in the aleurone layers, whereas Pl controls pigmentation in other mature tissues (Dooner and Robbin, 1991). In contrast to C1/Pl, the MYB factor P acts alone to regulate a subset of the structural genes in the flavonoid pathway, leading to the biosynthesis of phlobaphene, another flavonoid product that accumulates in the maize kernel pericarp and floral organs (Grotewold et al., 1994).

The biosynthesis of flavonoids in dicots is also under the control of MYB factors. In petunia, expression of the late flavonoid genes in flowers is controlled by at least three regulatory genes, *AN1* (encoding a bHLH factor), *AN2* (encoding a MYB factor), and *AN11* (encoding a WD40 repeat protein) (Quattrocchio et al., 1993, 1999; de Vetten et al., 1997; Spelt et al., 2000). Expression of *AN2* is essentially restricted to the corolla limb. The MYB gene *AN4* in petunia might be a paralog of *AN2* in the control of pigmentation in anthers (Spelt et al., 2000).

In Arabidopsis, the control of flavonoid synthesis follows a similar scenario. At least three regulator genes, *TTG1*, *TT8* and *TT2* are required for flavonoid synthesis in seeds. Similar to petunia, they encode a WD40 protein, a bHLH factor and a MYB factor, respectively (Nesi et al., 2000, 2001). Seeds of *tt2* (*atmyb123*) mutants are yellow or buff in color as a result of the lack of proanthocyanidin in the seed coat. Expression of late flavonoid biosynthesis genes, such as *DFR* and *BAN*, are dramatically down-regulated in the mutant. *TT2* expression is restricted to the seed during early embryogenesis, which is consistent with expression of the structural gene *BAN* and proanthocyanidin deposition. Overexpression of *TT2* is able to induce the ectopic expression of *DFR* and *BAN*, but is not sufficient for the ectopic accumulation of the proanthocyanidin product (Nesi et al., 2001). These data suggest that *TT2* plays a key role in the control of the spatial and temporal expression of flavonoid biosynthesis genes and thus proanthocyanidin accumulation.

Interestingly, overexpression of *PAP1* (*AtMYB75*) by activation tagging, a member closely related to *TT2* in Arabidopsis, results in intense purple pigmentation in the whole plant. Many other phenylpropanoid products are also increased. Expression of the general phenylpropanoid pathway genes, such as *PAL*, and genes specific for anthocyanin synthesis and transport, such as chalcone synthase (*CHS*), are also massively enhanced. Ectopic expression of *PAP1* and the most closely related member *PAP2* (*AtMYB90*) in tobacco causes the same phenotype. These results suggest that these two *MYB* genes are involved in the regulation of the phenylpropanoid gene expression. *PAP1* and *PAP2* may be functionally redundant (Borevitz et al., 2000). A *MYB* gene that controls the specific structural gene expression in anthocyanin biosynthesis has been also demonstrated in grape (Kobayashi et al., 2002).

In addition to the flavonoid pathway, other phenylpropanoid branch pathways are also under the control of *MYB* genes. Ectopic expression of *Antirrhirum MYB308* in tobacco results in significant reduction of all major soluble phenolic compounds and lignin. Expression of the structural genes in the phenylpropanoid pathway, *C4H*, *4CL*, *CAD* (encoding cinnamyl alcohol dehydrogenase, a key enzyme in lignin synthesis), and *CHS* (encoding a key enzyme in flavonoid synthesis) are all down-regulated in the transgenic tobacco plant. In addition, the plant is developmentally retarded (Tamagnone et al., 1998). These results suggest that an *AmMYB308* ortholog in tobacco may play a role in negatively regulating the phenylpropanoid pathway.

The function of *AtMYB4*, an *AmMYB308* ortholog in Arabidopsis, has been characterized by a knockout mutation. The level of sinapoyl malate, the major soluble phenolic compound in Arabidopsis leaves, is significantly increased in the *atmyb4* insertion-knockout. The increase of the sinapoyl ester causes the mutant plant to be more resistant to UV-B irradiation. AtMYB4 appears to be a transcriptional repressor, functioning principally to down-regulate *C4H* expression. This is the first direct evidence to show that an *AtMYB* gene regulates expression of one of the structural genes in the general phenylpropanoid pathway. However, expression of the other two structural genes in this pathway, *PAL* and *4CL*, is not changed in the *atmyb4* knockout mutant (Jin et al., 2000).

Besides the phenylpropanoid pathway, MYB transcription factors are also involved in regulating other metabolic pathways. AtMYB61 controls the accumulation of polysaccharides in the seed coat. Seeds of *atmyb61* insertion-knockout mutants are deficient in seed mucilage extrusion. Accordingly, *AtMYB61* is preferentially expressed in siliques, and the expression is localized in the seed coat (Penfield et al., 2001). ATR1 (AtMYB34) is involved in the regulation of the tryptophan pathway by up-regulating *ASA1* expression, a gene encoding the catalytic subunit of the first enzyme in the tryptophan pathway (Bender and Fink, 1998). In plants, tryptophan provided by the tryptophan pathway serves as a precursor for protein synthesis and the biosynthesis of an array of metabolites, such as the plant hormone indole-3-acetic acid (Radwanski and Last, 1995). This demonstrates that transcriptional control by MYB factors is not limited to genes in secondary metabolic pathways.

(2) Control of the development and determination of cell fate and identity. MYB factors GL1 (AtMYB0) and WER (AtMYB66) have been well characterized for their roles in control of trichome and root atrichoblast specification. In Arabidopsis, GL1 specifies trichome formation on the surface of leaves and stems. Expression of *GL1* is restricted to the epidermal cells in developing shoot tissues. *gl1* mutations generate a non-trichome leaf phenotype (Koornneef et al., 1982; Oppenheimer et al., 1991; Larkin et al., 1993). WER is required for non-hair cell (atrichoblast) identity in the root epidermis. Accordingly, expression of *WER* is limited to a subset of developing epidermal cells in the root and hypocotyl. *wer* mutations generate extra-hairy roots (Lee and Schiefelbein, 1999). GL1 and WER share a high degree of amino acid identity. Either gene promoter driving the other gene could functionally complement for each other (Lee and Schiefeldein, 2001). The MYB factor MIXTA from *Antirrhinum* affects epidermal cell shape in the petal. In the *mixta* mutant, the epidermal cells of the petal fail to form the normal conical shape (Noda et al., 1994).

The genetic locus *ASYMMETRICAL LEAVES1* (*AS1*) in Arabidopsis has been found to encode a MYB factor (AtMYB91) (Byrne et al., 2000). *AS1* negatively interacts with *KNOX* genes to identify stem cells and lateral organ founder cells within the shoot meristem in

Arabidopsis. In stem cells, the *KNOX* gene *STM* negatively regulates *AS1*. In founder cells, the reduced *STM* expression allows *AS1* is expressed. *AS1* in turn down-regulates another two *KNOX* genes, *KNAT1* and *KNAT2* (Byrne et al., 2000). *AS1* is an ortholog of *Antirrhinum PHAN* and maize *RS2*. Their products share a high degree of amino acid identity throughout the entire sequences (Timmermans et al., 1999).

(3) Participation in plant response to environmental stimuli and in mediating plant hormone actions. A gibberellin (GA) responsive *MYB* gene *GAMYB* has been identified from barley aleurone layers. *GAMYB* expression is an early event in GA-regulated gene expression during seed germination and precedes α-amylase gene expression. GAMYB is able to bind to the α-amylase gene promoter and activates the promoter activity (Gubler et al., 1995). Recently, three rice *MYB* cDNAs encoding single MYB repeat proteins were proposed to have the similar function of regulating α-amylase gene expression in response to GA and sugar (Lu et al., 2002).

In Arabidopsis, expression of *AtMYB2* is induced by abscisic acid (ABA), dehydration and salinity treatments (Urao et al., 1993). AtMYB2 along with the bHLH factor AtMYC2 binds to the promoter of the Arabidopsis dehydration-responsive gene *rd22* to activate the promoter activity (Ade et al., 1997). AtMYB2 also binds to the promoter of the alcohol dehydrogenase gene *AtADH1* to activate this promoter activity (Hoeren et al., 1998). Transgenic Arabidopsis plants overexpressing both *AtMYB2* and *AtMYC2* are more sensitive to exogenous ABA. Accordingly, ABA-induced expression of *rd22* is at a higher magnitude. Expression of *AtADH1* is also strongly increased in the double-overexpression line (Abe et al., 2003).

AtMYB30 is proposed to be a positive regulator during hypersensitive response (HR) signaling. *AtMYB30* expression is rapidly induced during hypersensitive cell death upon bacterial attack (Daniel et al., 1999). Overexpression of *AtMYB30* in Arabidopsis and tobacco accelerates the plant HR and increases resistance to bacterial and fungal pathogens. Suppression of *AtMYB30* expression by antisense RNA in transgenic Arabidopsis strongly decreases hypersensitive cell death (Vailleau et al., 2002). Elicitor and wounding responsive *MYB* genes have also been described in tobacco and rice (Sugimoto et al., 2000; Lee et al. 2001). *NtMYB2*

from tobacco has been shown to activate the *PAL* promoter activity, and overexpression of *NtMYB2* in transgenic tobacco plants induces *PAL* expression (Sugimoto et al., 2000). These results suggest that *NtMYB2* is involved in defense response by regulating gene expression in the general phenylpropanoid pathway.

It is interesting to see that functionally related *MYB* genes cluster together in phylogenetic trees (Stracke et al., 2001). This point can be illustrated in several phylogenetic subgroups. In subgroup 5, both members *TT2* (*AtMYB123*) and *ZmMYBC1* control pigmentation in Arabidopsis seeds and maize kernels. When expanded to the closely related subgroup 6, it can be seen that three members in this subgroup, *PhMYBAN2*, *PAP1* (*AtMYB75*) and *PAP2* (*AtMYB90*) are also involved in regulating plant pigmentation in petunia and Arabidopsis. In subgroup 15, *WER* (*AtMYB66*) and *GL1* (*AtMYB0*) both control epidermal cell differentiation in different organs of Arabidopsis and are functionally equivalent. Their different biological functions are solely caused by their different spatial expression patterns, which are conferred by specific regulatory sequences (Lee and Schiefelbein, 2001). Another example is *AS1* (*AtMYB91*), *AmMYBPHAN* and the closely related gene *ZmMYBRS2*. These genes negatively interact with *KNOX* genes to distinguish the stem cell and founder cell identity in shoot meristems in different plant species. The above data suggest a way to approach plant *MYB* gene functional studies. For example, although the function of *AtMYB113* in the subgroup 6 and *AtMYB23* in the subgroup 15 are unknown, it may be related to those of other subgroup members. Indeed, it has been shown that overexpression of *AtMYB23* can partially rescue the *gl1* mutant phenotype. This result implies that *AtMYB23* may have partial functional overlap with *GL1* (Kirik et al., 2001).

1.5 Combinatorial Control: Protein-Protein Interactions

Transcriptional control of a given gene usually requires the combined action of several transcription factors in eukaryotes (Riechmann and Ratcliffe, 2000). This combined action involves interactions between multiple proteins to give the specificity of regulatory effects, or

modulate transcription activities with a limited number of transcription factors (Singh, 1998). The yeast-based two-hybrid system provides a useful tool to study protein-protein interactions (Field and Song, 1989).

Several examples of physical interactions between MYB and other transcription factors have been described in plants. Extensive studies have shown that in maize, the MYB factor C1/Pl requires the bHLH factor R/B in the regulation of anthocyanin biosynthetic genes. Using the yeast two-hybrid system, a direct interaction between C1 and B factors in the regulation of the target promoter has been demonstrated. The MYB DNA-binding domain of C1 and the amino-terminal region of B are required for the interaction (Goff et al., 1992).

The maize MYB protein P controls another branch of flavonoid metabolism. P and C1 activate expression of some common genes in the flavonoid biosynthesis pathway, such as *A1*, by binding to an identical cis-element with different affinities. However, C1 in association with the R/B factor can activate additional genes specific for anthocyanin synthesis, such as *Bz1*, which P can not, although P and C1 share nearly 80% identity in the MYB DNA-binding domain (Grotewold et al., 1994). These data indicate that a MYB transcription factor can obtain a new DNA binding specificity by interacting with another transcription factor. The amino acid residues in the first helix of the MYB R3 repeat are critical for the interaction of C1 and R. Substitution of these residues in P is sufficient for conferring the regulatory specificity of C1to the P factor (Grotewold et al, 2000). This further demonstrates that the MYB DNA-binding domain is important for the protein-protein interaction.

In Arabidopsis, several developmental processes are regulated by MYB proteins in cooperation with other regulatory factors. For example, the MYB protein GL1 with TTG1, GL3 in the control of trichome cell fate (Oppenheimer et al., 1991), and AtMYB61 with TTG1 and CL2 in the regulation of seed mucilage extrusion (Penfield et al., 2001). It has been demonstrated that the bHLH protein GL3 physically interacts with the MYB protein GL1, similar to the interaction between B and C1 in maize, in the regulation of trichome cell development (Payne et al., 2000). The promoter of the dehydration responsive gene *rd22* has

both the MYB and bHLH binding sites. Overexpression of both *AtMYB2* and *AtMYC2* enhances the ABA-induced expression of *rd22* (Abe et al., 1997 and 2003). These results also suggesting that these two proteins might have physical interaction.

1.6 The Way Forward in Plant *MYB* Gene Functional Studies

Currently, sequence analysis of genes is more advanced than their functional characterization. A variety of reverse genetic approaches provide useful tools for functional studies of genes identified by sequencing of the plant genome. The most common method involves large populations of mutants created by either T-DNA, or transposon insertions (Maes et al., 1999; Walbot, 2000; Krysan et al., 1999). Originally, these populations were used to screen for insertion mutations in a particular gene using a PCR-based strategy with a gene specific primer in combination with T-DNA (or transposon) border primers. It is calculated that Arabidopsis T-DNA insertion lines generated by seed transformation have an average of 1.5 T-DNA inserts per line (Krysan et al., 1996). Thus, by searching a large enough insertion population, one should be able to find an insertion in any gene of interest.

In one of the first uses of reverse genetic approaches, T-DNA insertions within any member of the Arabidopsis actin gene family were identified in a single screen using gene degenerate primers. By searching 5,300 Arabidopsis T-DNA insertion lines, insertions in two actin genes were found out of a total of 10 (McKinney et al., 1995). Using gene-specific primers to screen 9,100 Arabidopsis T-DNA lines, insertions in seventeen genes were found in a total of 63 genes examined (Krysan et al., 1996). A systematic screen for insertion mutations in a large gene family has been carried out in the Arabidopsis P450 gene family (Winkler et al., 1998).

Recently, T-DNA collections have been generated in which T-DNA insertion junctions are sequenced and compiled in databases. These databases can be easily searched on-line for potential T-DNA insertions in a gene of interest.

To dissect Arabidopsis R2R3-type *MYB* gene functions, a systematic screen for *MYB* gene insertion mutations has been performed with several T-DNA or transposon tagged populations. This resulted in the identification of 47 insertions in 36 genes by searching a total of 73 *MYB* genes (Meissner et al., 1999). So far insertion knockouts in only one gene, *AtMYB61*, exhibited a mutant phenotype (Penfield et al., 2001). The lack of phenotypic changes is probably due to functional redundancy in the family members. The *AtMYB4* function has also been elucidated by an insertion knockout (Jin et al., 2000).

Another common method in plants for producing loss-of-function mutants for a specific gene is the use of antisense RNA or RNA interference (RNAi) to suppress gene expression (Schuch, 1991; de Lange et al., 1995; Hamilton et al., 1995; Finnegan et al., 1996). This method is based on interfering with gene expression. Using this approach, combined with overexpression, *AtMYB30* has been functionally characterized (Vaiieau et al., 2002). The efficiency of antisense RNA suppression is usually low. A new approach to suppress gene expression is RNAi. In this method, double-strand RNA is used to block gene expression (Bosher and Labouesse, 2000). Gene repression using RNAi in a sequence-specific manner has been reported in Arabidopsis. RNAi transformants exhibited mutant phenotypes at a much higher frequency than the plants transformed with either the antisense or the sense gene alone (Chuang and Meyerowitz, 2000). However its efficacy is not yet clear. Epigenetic phenotypes could be a problem in this method (Que and Jorgensen, 1998). However, with the use of loss-of-function approaches, a gene with redundant functions can not be easily characterized.

A gain-of-function in which a gene is constitutively expressed is another approach for a functional study. One of the methods is using T-DNA carrying the 35S enhancer as an activation tag (Weigel et al., 2000). Using this approach, *PAP1* (*AtMYB75*) and *PAP2* (*AtMYB90*) have been successfully identified (Borevitz et al., 2000). However, a phenotype revealed in this way may not truly reflect gene function, since it could be caused by interference with other genes. The study of *AtMYB4* by its knockout mutation has shown that *AtMYB4* primarily negatively regulates *C4H* expression. However, when overexpressing *AtMYB4* under the control of the 35S

promoter, not only *C4H*, but also *4CL* and *CHS* are down-regulated (Jin et al., 2000). This suggests that the specificity of a transcription factor might be reduced under conditions of overexpression. Thus, gene function revealed by a gain-of-function allele should be interpreted with caution.

1.7 Research Objectives and Approaches

In this thesis, based on evidence revealed at the time (reviewed in Section 3.1), I set out to identify *MYB* genes involved in the regulation of transcription initiation of genes encoding enzymes in the lignin biosynthetic pathway in Arabidopsis, using *At4CL1* as a marker. Taking advantage of the ongoing Arabidopsis Expressed Sequence Tag (EST) project that was revealing new *MYB* genes at the time I started my thesis, my objective was to search for *MYB* genes that had expression patterns similar to that of *At4CL1*. Alternatively, I would clone *MYB* cDNAs from Arabidopsis bolting stems, where *At4CL1* was highly expressed, and then characterize these genes. This approach appeared to be reasonable, since in some cases, such as the examples reviewed in this chapter, expression of regulatory genes occurred coordinately with expression of target structural genes.

In a second project, a *MYB* gene with a T-DNA insertion in its promoter region was identified by Dr. Aviva Pri-Hadash in the Douglas laboratory, which was a potential gene knockout. My further study showed that this gene had an interesting expression pattern. I set out to continue characterization of this gene by its expression profiling, and to characterize its function using reverse genetic approaches.

Chapter 2 Materials and Methods

2.1 Plant Material Preparation

2.1.1 Plant Growth Conditions

For growing seedlings on defined media, *Arabidopsis thaliana* seeds were surface-sterilized with 20% bleach plus 0.02% Triton-X100, and then planted on AT (ABRC) or MS salt (Murashige and Skoog, 1962) plus 1% sucrose media. In the experiments where the harvesting or observation of roots was necessary, seedlings were grown vertically in square plates. All plates were put in a growth chamber at 20°C under continuous light. For hydroponic cultures, seedlings were grown in AT liquid media plus 0.5% sucrose in a growth chamber at 20°C with 16 h light / 8 h dark cycle. Plants were grown to maturity in soil in a growth chamber at 20°C with continuous light or a 16 h light / 8 h dark cycle.

2.1.2 Plant Treatments

Expression of *AtMYB68* in response to external stimuli was examined as follows. In the following treatments, AT liquid media plus 0.5% sucrose and 23 mM MES served as basic media. Seedlings were treated under the light period, except as indicated otherwise.

For the NO_3^- treatment, Arabidopsis seedlings were grown in AT liquid media in the absence of NO_3^- for 4 days. KNO_3 was added to the media to a final concentration of 2 mM. Whole seedlings were harvested after a 6-hour treatment. Seedlings maintained in the medium without KNO_3 served as a control.

For the plant hormone treatments, seven- or eight-day old Arabidopsis seedlings grown in AT media were transferred to new media supplemented with IAA, BAP, GA_3, ABA or ACC respectively. Each plant hormone was made to a final concentration of 10 μM in the medium,

except IAA at 100 μM. Whole seedlings were harvested after a 6-hour treatment respectively. Seedlings in the medium without any plant hormones served as a control.

For the cold treatment, seven-day old Arabidopsis seedlings grown in AT liquid media without MES were transferred to a 4^0C dairy fridge for 24 hours. For the desiccation treatment, seedlings from the same batch were removed from the medium, put on Whatman paper in a Petri dish and left room temperature 30 minutes (Kranz et al., 1998). For the salinity treatment, seedlings from the same batch were transferred to the new medium supplemented with NaCl in a concentration of 200 mM for 6 hours. Whole seedlings were harvested after each treatment. Seedlings grown in AT media under the normal conditions served as a control.

AtMYB68 overexpression and knockout lines were examined for phenotypes as follows. In the following treatments, MS media supplemented with 1% sucrose served as basic media. Seedlings were grown under continuous light. Primary root length was measured using a ruler. Lateral root numbers were visualized under a dissecting microscope.

ABA treatment: four-day old seedlings grown on MS plates were transferred to plates supplemented with 1.0 μM ABA. Seedlings were grown vertically on the ABA plates. Measurements were taken after 6 or 7 days.

IAA treatment: seven-day old seedlings grown on MS plates were transferred to plates supplemented with 1.0 μM IAA. Seedlings were grown vertically on the IAA plates. Measurements were taken after 5 days.

Salinity stress: four-day old seedlings grown on MS plates were transferred to plates supplemented with a series of concentrations (50, 100 and 150 mM) of NaCl. Seedlings were grown vertically with roots upside down on the NaCl plates (Wu et al., 1996), for observing root-bending.

Drought stress: 20-day old soil-grown plants were not watered for 2 weeks. To minimize variation, the same number of plants was grown in each pot.

The root obstacle-touching response was examined as described by Rutherford and Masson (1996).

2.1.3 Plant Transformation

Arabidopsis Columbia (Col) plants were transformed according to the protocol described by Clough and Bent (1998). Briefly, *Agrobacterium* GV3303 strains carrying binary vectors with inserts were grown in LB media plus kanamycin (100 mg/L), gentamycin (25 mg/L) and rifampicin (25 mg/L) to OD_{600} ~0.8. The *Agrobacterium* cells were collected by centrifugation then resuspended in 5% sucrose. Silwet L-77 was added to a concentration of 0.05%. Aerial parts of plants with many immature flower clusters and few siliques were dipped in the *Agrobacterium* solution. The plants were then covered by Saran wrap and kept under a lab bench for a day. The transformation procedure was repeated once after a 3-day interval for the antisense *AtMYB68* transformation. Seeds of transformed plants (T1 generation) were harvested and plated on kanamycin-containing (50 mg/L) AT media to identify transformants.

2.2 General Molecular Methods

2.2.1 Plasmid DNA Preparation and DNA Sequencing

Plasmid DNA was prepared by the alkaline-lysis/PEG precipitation procedure (the NAPS laboratory of the University of British Columbia, 1995), or using the QIAprep Spin Miniprep Kit (QIAGEN), following the manufacture's instructions. DNA sequencing was done using the BigDye™ Terminators Sequencing Kit and carried out in the NAPS laboratory.

2.2.2 Plant Genomic DNA Isolation

Plant genomic DNA was isolated according to the 'Short DNA Quick-Prep' protocol from the University of Wisconsin Biotechnology Center (http://www.biotech.wisc.edu).

2.2.3 Total RNA and Poly(A)$^+$ RNA Isolation

Total RNA was extracted from Arabidopsis seedlings and mature organs using the RNeasy™ Plant Mini Kit (QIAGEN), following the manufacture's instructions. Poly(A)$^+$ RNA was prepared using the Dynabeads™ Oligo $(dT)_{25}$ (DYNAL), following the manufacture's instruction.

2.2.4 Northern and Southern Blot Analysis

Total RNA or poly(A)$^+$ RNA was separated on 1.2% agarose gels containing 0.22 M formaldehyde in 1X MOPS buffer. After separation, the gel was washed in water for 1 hour, and then blotted on Hybond™-N nylon membranes (Amersham) in 10X SSC. RNA samples were fixed by baking blots at 80°C for 2 hours. ^{32}P-radiolabeled probes were hybridized to blots in 0.25 M sodium phosphate buffer (pH 7.2) containing 7% SDS (Church and Gilbert, 1984), at 65°C in a hybridization oven overnight. The blots were washed at low stringency (2X SSC, 0.1% SDS at 65 °C) and high stringency (0.2X SSC, 0.1% SDS at 65 °C). Signals were detected by exposure to an x-ray film (Kodak).

For Southern blot analyses, DNA was separated on 1% agarose gels, and then blotted on Hybond™-N+ nylon membranes (Amersham) in 0.4 M NaOH. Blots were hybridized and washed at the same conditions as those in northern blot analyses. Signals were detected as above.

Hybridization probes used in northern and Southern blot analyses were generated from PCR fragments, cDNAs, or genomic DNA, as indicated in each experiment. ^{32}P-radiolabeled probes were generated using the Random Primers DNA Labeling System (Gibco BRL) according to the manufacturer's instructions.

Blots were sometimes stripped for re-hybridization. For RNA blots, the blots were stripped by incubating blots in 5 mM Tris (pH 8.0) buffer containing 2 mM EDTA and 0.1 X Denhardt at 65 °C for 2 hours. For DNA blots, blots were stripped by pouring boiling 0.1% SDS on the blots, and then allowing the solution to cool to room temperature. This procedure was sometimes repeated. Successful stripping was ensured by exposure to an x-ray film before the blots were used for the next hybridization.

2.2.5 Quantitative RT-PCR Analysis

Total RNA (100 ng) was used in reverse transcription (RT) followed by PCR amplification using the QIAGEN™ OneStep RT-PCR Kit (QIAGEN), except for *AtMYB84* where 2-step RT-PCR was used. One gene-specific primer (forward) was designed to span an intron to avoid amplification from any contaminating DNA. The QuantumRNA™ 18S Internal Standards (Ambion) were used as an internal control. The products were separated on 3.5% mini polyacrylamide gels, and then post-stained by Syber green I (Molecular Probes) for 30 minutes. Fluorescent signals were detected and quantified using a Storm Phosphorimager and the ImageQuant software (Amersham-Pharmacia).

First, the PCR linear amplification range for each target gene was determined, in which PCR products were increased exponentially with the cycle number. This was done by performing identical RT-PCR reactions for different numbers of PCR cycles. The results were quantified and plotted. An example of such an experiment is shown in Figure 2-1. A cycle number close to the middle of the linear range was used in the experiment. Second, the optimal ratio of 18S primers to Competimers™ in the kit (Ambion) was determined. This was done by performing several RT-PCR reactions with different ratios of 18S primers to Competimers at the number of PCR cycles determined above. The results were assessed on a gel. The ratio that gave a level of 18S product similar to that of the gene specific product was chosen.

Primers for each gene used in the quantitative RT-PCR analyses are listed in Table 2-1.

Table 2-1. Primers Used in Quantitative RT-PCR Analyses

Gene	Primer	Product Size (bp)
AtMYB68	Forward 5'-GCCTCAGAAAATTGGTTTAAGG-3'	1008
	Reverse 5'-TACACATGATTTGGCGCATTGA-3'	
AtMYB84	Forward 5'-TTGGTAGCAGGTGGTCTATAATC-3'	750
	Reverse 5'-TCCATATATACGTTACGTACCCCC-3'	
AtMYB36	Foreard 5'-TGCCTCAGAAAATTGGGCTGAAG-3'	930
	Reverse 5'-TTATCCATCCCTATAGTTACGCA-3'	

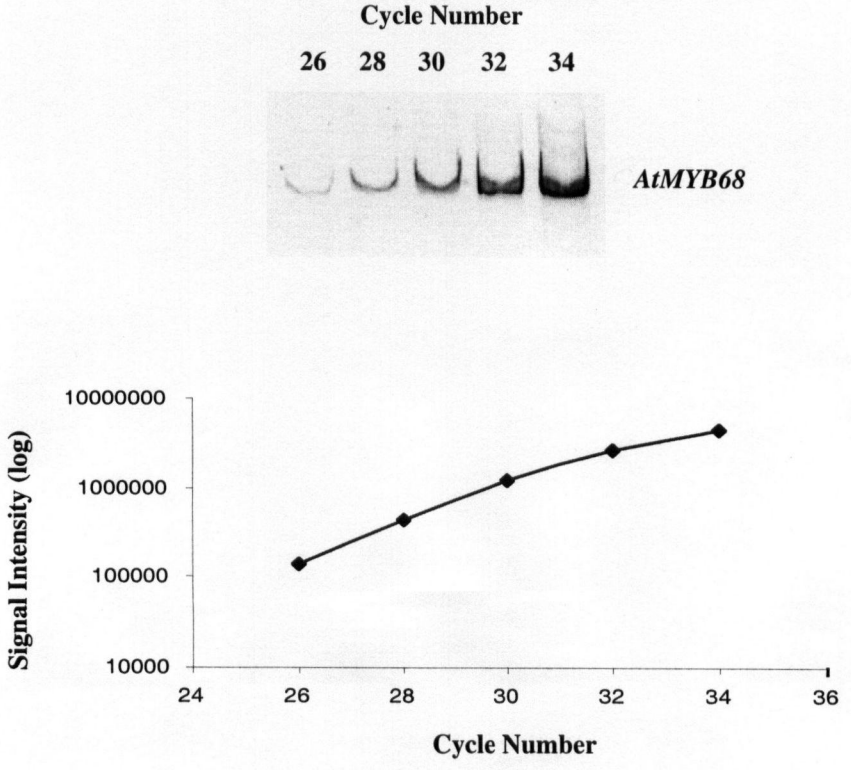

Figure 2-1. Determination of the Linear Range for RT-PCR.
Total RNA from 4-day old Col seedlings was used in RT-PCR to determine the linear range for *AtMYB68* amplification. RT-PCR aliquots were removed from the thermocycler at the indicated cycle numbers and resolved on a polyacrylamide gel. Cycle numbers are plotted against the log scales of signal intensity.

2.3 Cloning

2.3.1 Cloning of *MYB* cDNAs

Poly(A)$^+$ RNA (1 μg) extracted from Arabidopsis Col bolting stems was used to generate *MYB* cDNAs, using the Marathon™ cDNA Amplification Kit (CLONTECH) following the manufacture's instructions. The 5' regions of *MYB* cDNAs were amplified using 5'-RACE. A *MYB* degenerate primer corresponding to the region in the MYB R3 repeat, 5'-TTGAC(T)T(CA)T(G)CA(G)TTG(A)G(T)CG(AT)GTC(T)CT(G)TCC-3', was used in 5'-RACE. The amplified products were separated on a gel and tested by a Southern blot analysis. A mixture of cDNA fragments corresponding to the MYB DNA-binding domain was used as a probe. These cDNA fragments were derived from MYB EST clones 95L7T7, 106H10T7 and 1B4T7P by first digesting with *Hin*dIII then with *Sal*I (see Figure 2-2-A). The *SalI/Hin*dIII fragments were recovered from a gel. The 5'-RACE products of the predicted size were cloned into the TA vector (Invitrogen) and sequenced.

The 3' region of the *STM31* cDNA was amplified using 3'-RACE, with the Expand™ High Fidelity PCR System (Boehringer Mannhein). A gene-specific primer, 5'-TAGAGCACCGTGCTTTTTCGCAG-3', was used in 3'-RACE. The amplified fragment was also cloned into the TA vector and sequenced. The full-length *STM31* cDNA was generated by joining the 5'-cDNA and the 3'-cDNA at the *Sac*I site in the overlapping region.

2.3.2 Generation of the *AtMYB68::GUS* Construct

PCR was used to generate a 1.9 kb *AtMYB68* promoter fragment with *Hin*dIII and *Bam*HI sites on the 5' and 3' ends respectively from Arabidopsis Col genomic DNA, using the Expand™

High Fidelity PCR System (Boehringer Mannhein). Primers, 5'-ctcaagCTTCTTTTCATCTCTTTTGG-3', and

*Hin*dIII

5'-tgcggaTCCCATTTTCTTGATTCTTG-3', were used for PCR. The

*Bam*HI

PCR fragment was cloned into the pBluescript KS vector, and sequenced to ensure no mutations were introduced during amplification. A 1.9 kb fragment was released by *Bam*HI digestion and *Hin*dIII partial digestion. This fragment was inserted 5' to the *GUS* gene in the pBI121 binary vector (CLONTECH), replacing the 35S promoter (Figure 2-2-E). The *AtMYB68* promoter was translationally fused to the *GUS* in the vector. The plasmid was transformed into the *Agrobacterium* GV3303 strain.

2.3.3 Cloning of the *AtMYB68* cDNA into *E. coli* Expression Vectors

The 3' cDNA of *AtMYB68* was derived from the EST clone 110F12T7 by *Hin*dIII digestion. A fragment of ~880 bp was recovered from a gel and cloned into the *Hin*dIII site of the expression vector pQE-30 (QIAGEN) (Figure 2-2-D). The sense orientation clone was selected by *Xba*I digestion. The clone was also sequenced to confirm that the cDNA was in frame with the ATG from the vector. This plasmid was transformed in the *E. coli* M15[pREP4] strain using a method recommended by the manufacture. The empty vector pQE-30 in M15[pREP4] was used as a negative control.

2.3.4 Generation of Constructions to Sense and Antisense *AtMYB68*

A sense construct for overexpression of *AtMYB68* was generated as follows. The full-length *AtMYB68* cDNA was released from EST clone 110F12T7 by *Sal*I/*Not*I digestion. Two overhangs were removed by Klenow, and then the cDNA was inserted into the *Sma*I site behind the 35S promoter of the pRT101 vector (Topfer et al., 1987) (Figure 2-2-B). The sense

orientation clone was selected by *Hin*dIII digestion. A 35S-*AtMYB68*-poly-A cassette was released by *Hin*dIII partial digestion. A fragment of ~2 kb was selected and inserted into the *Hin*dIII site of the pBin19 binary vector.

An antisense *AtMYB68* construct was generated as follows. The 3' cDNA of *AtMYB68* was released from EST clone 110F12T7 by *Hin*dIII digestion. Two overhangs were removed by Klenow, and then the cDNA was inserted into the *Sma*I site behind the 35S promoter of the pRT101 vector (Figure 2-2-C). The antisense orientation clone was selected by *Hin*cII digestion. A 35S-*AtMYB68* (-)-poly-A cassette was released by *Hin*dIII digestion and then inserted into the same site of the pBin19 binary vector.

Both sense and antisense constructs in pBin19 were transformed into the *Agrobacterium* GV3303 strain.

2.4 Protein Analysis

2.4.1 Protein Extraction

The recombinant AtMYB68 protein was prepared and purified according to the QIAexpressionist™ instructions (QIAGEN). Briefly, an *E. coli* culture of 500 ml (OD_{600}=0.7-0.9) containing the expression plasmids was induced by 1 mM IPTG for 2 hours. The bacterial pellet was collected by centrifugation. The recombinant protein was extracted and purified under denaturing conditions as follows. The pellet was resuspended and lysed in 6 M guanidine-HCl buffer. The recombinant protein was purified with Ni-NTA resin (QIAGEN) columns, and finally eluted with 8 M urea buffer (pH 4.5).

Plant proteins were extracted by grinding tissues in a buffer containing 25 mM Tris (pH 8.0), 10 mM NaCl, 10 mM MgCl2, 5 mM EDTA, 10 mM β-mercaptoethanol, 1 mM PMSF (Kwok et al., 1998), plus 1 tablet Complete™ (Roche) per 10 ml buffer to prevent protein degradation. The homogenate was centrifuged at 4 °C to remove cellular debris.

A

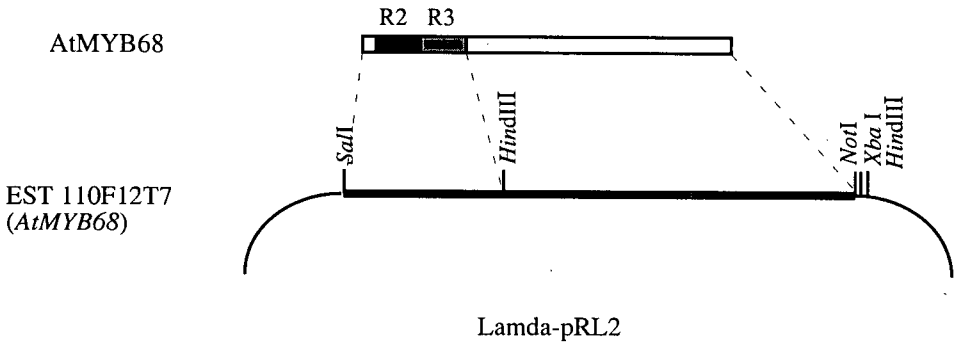
AtMYB68
R2 R3
EST 110F12T7
(AtMYB68)
SalI
HindIII
NotI
Xba I
HindIII
Lamda-pRL2

B

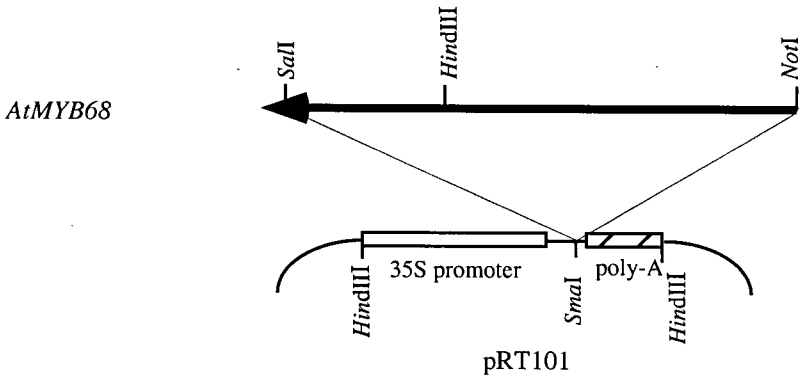
AtMYB68
SalI
HindIII
NotI
HindIII
35S promoter
SmaI
poly-A
HindIII
pRT101

C

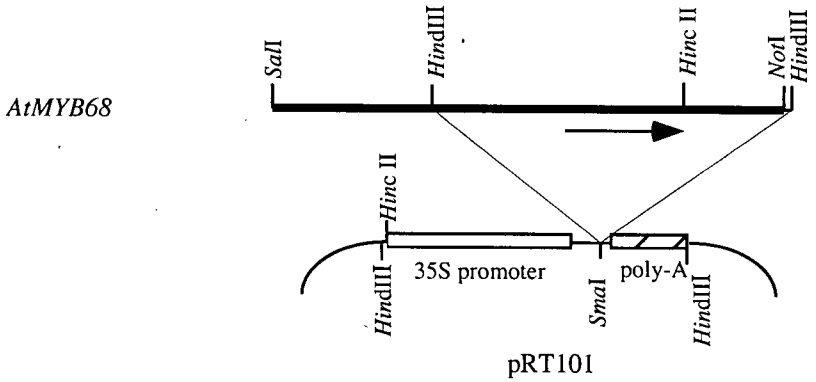
AtMYB68
SalI
HindIII
Hinc II
NotI
HindIII
Hinc II
HindIII
35S promoter
SmaI
poly-A
HindIII
pRT101

D

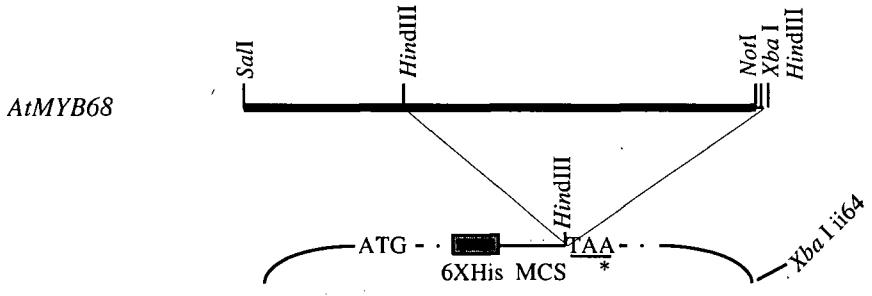

pQE-30

E

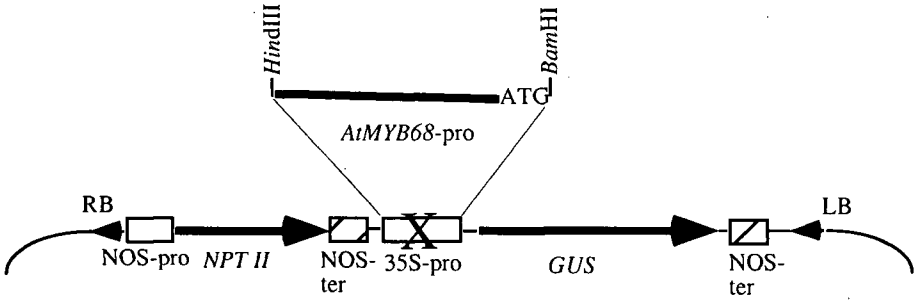

pBI121

Figure 2-2. Plasmids Generated for Various *AtMYB68* Constructs.
(A) The predicted AtMYB68 protein from the cDNA is shown on the top. Black and grey boxes represent the MYB R2 and R3 repeats.
(B) *AtMYB68* sense DNA construct.
(C) *AtMYB68* antisense DNA construct.
(D) *AtMYB68* expression construct. The grey box represents 6X histidine-tag on the vector. The translation start and stop codons are shown on the figure. MCS, multi-cloning site.
(E) *AtMYB68::GUS* construct. A 1.9 kb *AtMYB68* promoter with the ATG codon was put in frame to replace the 35S promoter. Pro, promoter. Ter, terminator.

Protein concentrations were quantified by the Bradford (1976) method using the Bio-Rad Protein Assay Solution™ (Bio-Rad) with BSA as a standard.

2.4.2 Generation of Anti-Serum against the AtMYB68 Recombinant Protein

Polyclonal antibodies were raised in New Zealand White rabbits, cared for at the Animal Care Center in the University of British Columbia. Two female rabbits were pre-bled and the pre-immune sera were tested for cross-reaction to *E. coli* and plant proteins. The two rabbits were injected with ~100 μg purified recombinant AtMYB68 (in the urea buffer) mixed with Complete Freund's Adjuvant in the total volume of 1 ml. They then received two subsequent booster injections of ~100 μg recombinant AtMYB68 mixed with Incomplete Freund's Adjuvant at about 3-week intervals. The rabbits were sacrificed and their blood was recovered. The blood was placed in Falcon tubes with toothpicks at the edge at 37 °C for 1 hour, then transferred to 4 °C overnight to induce clotting. The clot was removed and the serum were centrifuged to remove blood cell debris. A few crystals of sodium azide were put in the serum to prevent contamination. The serum was stored at -80 °C.

2.4.3 AtMYB68 Antiserum Purification

The antiserum from one of the rabbits was purified using a CNBr-activated Sepharose™ 4B (Pharmacia Biotech) affinity column, according to a protocol described by Fuller et al. (1997), combined with the CNBr-activated Sepharose™ 4B manufacture's instructions. The purified recombinant AtMYB68 protein in the urea buffer was concentrated and changed to the coupling buffer (0.1 M $NaHCO_3$, pH 8.3, 0.5 M NaCl) before it was bound to the Sepharose. This was done by ultrafiltration using the Ultrafree™-4 Centrifugal Filter Unit (MWCO 10,000, Millipore). The concentrated recombinant protein was finally dialyzed in the coupling buffer overnight. CNBr-activated Sepharose 4B powder (1.5 g) was swollen and washed by 1 mM HCl followed by the coupling buffer, and then mixed with recombinant AtMYB68 at a concentration

of ~2.4 mg/ml in 10 ml coupling buffer overnight at 4 °C. The gel was washed with the coupling buffer, and then incubated with 15 ml of 1 M ethanolamine (pH 8.0) for 5 hours at 4 °C to block excess remaining active groups. The gel was washed alternatively with the coupling buffer (pH 8.3) and the wash buffer (0.1 M sodium acetate, 0.5 M NaCl, pH 4.0) for three cycles to remove excess of uncoupled antigen. The gel slurry was prepared in PBS buffer at the ratio 3:1, and then packed in a 20 cm-long glass column and equilibrated with PBS buffer. The antiserum (8 ml) was diluted in 3X volume of PBS buffer and filtered through a 0.2 μm filter, and then loaded to the column. The flow rate was controlled at ~200 ml/hr. The column was washed by PBS buffer until an $A_{280} < 0.005$ was present in the wash. The bound antibody was eluted by glycine-HCl buffer (pH 2.3) and neutralized in 1/4 volume of 0.5 M sodium phosphate buffer (pH 7.7). The purified antibody was finally concentrated to ~0.1 μg/μl using the Ultrafree™-15 Centrifugal Filter Device (MWCO 10,000, Millipore), and examined on SDS-PAGE.

2.4.4 Western Blot Analysis

Bacterial or plant proteins were separated on 10% SDS-polyacrylamide separating gels (Laemmli, 1970), and then blotted on PVDF membranes (Amersham-Pharmacia) at 30 V overnight. Duplicated gels were stained by 0.1% Coomassie Brilliant Blue as loading controls. Signals were detected by using ECL Plus™ detection reagents (Amersham-Pharmacia) according to the manufacturer's instruction. The blots were reacted with a 1:1000 dilution of the rabbit antiserum raised against the recombinant AtMYB68, or a 1:5000 dilution of the purified antibody. Horseradish peroxidase (HRP) conjugated anti-rabbit IgG (Amersham-Pharmacia) was used as the secondary antibody at a 1:20000 dilution. Chemiluminescent signals were detected by exposure to x-ray films. ECL protein molecular weight markers (Amersham-Pharmacia) were also loaded on the blots.

2.5 Histology and Histochemistry

2.5.1 Histochemical GUS Staining

Seedlings were incubated in a GUS reaction solution, containing 0.5 mM X-Gluc substrate in 0.1 M sodium phosphate buffer (pH 7.0), and 0.5 mM each potassium ferri- and ferrocyanide as an oxidation catalyst, plus 10 mM EDTA and 0.1% Triton X-100, at 37 °C overnight (Stomp, 1992). Stained seedlings were then cleared as described by Malamy and Benfey (1997) and mounted in 50% glycerol on glass microscope slides. Samples were observed under a dissecting microscope. Pictures were taken with Ektachrome Tungsten films (Kodak).

2.5.2 Root Section Preparation

Two-three days old Col seedlings harboring the *AtMYB68::GUS* fusion, or 7-day old *wol* seedlings harboring the same fusion were pre-stained for GUS activity as described above for 9 hours, and then fixed in 4% formaldehyde in PBS buffer overnight at 4 °C. The seedlings were dehydrated via an ethanol series at room temperature, 30%, 50%, 70%, 85%, 95%, 100%, 30 minute in each, 100% ethanol for 1 hour. Ethanol exchanged for Spurr resin by passing through a series of ethanol:resin mixtures, 3:1, 1:1, 1:3, 100% resin (X2), 1 hour in each, and then embedded in 100% resin and baked at 65 °C overnight. The Spurr resin was prepared following a recipe in the EM facility of the University of British Columbia. The seedling root was sectioned to ~3 μm on the Ultracut microtome E (Reichert-Jung), and mounted on glass slides. Samples were observed under a Leitz microscope with the DIC field.

2.6 Primers Used in Screening T-DNA Tagged Populations

AtMYB68 primers used for screening for *AtMYB68* knockout mutations in various T-DNA tagged populations are listed in Table 2-2. T-DNA border primers used in the screens were specified by the generator of each collection.

Table 2-2. *AtMYB68* Primers Used for Screening T-DNA Tagged Populations

Name	Primer	T-DNA Population Screened
myb13-3	Reverse 5'-TTCTACCACTCCCTAAAGACACAG-3'	Jack (ABRC)
m13295	Forward 5'-CCATCCTCCTCATTCTCTTCATCATCAAC-3'	Wisconsin (U of
m13293III	Reverse 5'-AACTTTTCTACCACTCCCTAAAGACACAG-3'	Wisconsin)
m13293	Nested 5'-AGAAAACCCCTCTTTATGTATGTAAGTAC-3'	
m13293III (to confirm)		Garlic (TMRI)

Chapter 3 Searching for Arabidopsis *MYB* Genes Involved in Regulation of the Phenylpropanoid Pathway

3.1 Introduction

MYB transcription factors appear to play an important role in the regulation of phenylpropanoid metabolism. A random-binding site selection experiment has shown a core binding site of the maize MYB protein P (Grotewold et al., 1994). This core binding sequence conforms to the conserved cis-elements P- and L-box present in *PAL*, *4CL* and other genes encoding enzymes in phenylpropanoid metabolism (Table 3-1, Douglas, 1996). A tobacco MYB related protein has been also shown to bind to a similar sequence (Sablowski et al., 1994). Ectopic expression of the *Antirrhinum MYB* gene *AmMYB305* can activate the bean *PAL2* promoter activity in tobacco mesophyll cells (Sablowski et al., 1995).

Table 3-1. Conserved Cis-Elements in Promoters of Phenylpropanoid Genes and MYB P Binding Site (According to Douglas, 1996)

Sequence	Cis-Element	Gene	Plant
ACCAACCC (T) (A)	Core binding site	*P* (*MYB*)	Maize
ACCAACCC	FP4	*4CL1*	Parsley
ACCAACCC	FP8	*4CL1*	Parsley
ACAAACCC	P Box	*PAL1*	Parsley
ACCTACCA	L Box	*PAL1*	Parsley
ACCTACCA	AC-I	*PAL1*	Bean
ACCAACCC	AC-II	*PAL1*	Bean
ACCTAACT	AC-III	*PAL1*	Bean
AACAACCC	AC	*CAD*	*Eucalyptus gunnii*

A few years ago, based on the analysis of cis-elements in the promoters of the genes encoding enzymes in phenylpropanoid metabolism, we hypothesized that MYB transcription factors were involved in the regulation of tissue/cell type-specific expression of the genes

encoding enzymes in phenylpropanoid metabolism. Recent research on Arabidopsis *MYB* genes has revealed several *AtMYB* genes, such as *AtMYB4* and *TT2*, are involved in the regulation of different branch pathways in phenylpropanoid metabolism (reviewed in Chapter 1). However, another important branch pathway, that of lignin biosynthesis, has not been reported to be under the control of MYB proteins. Lignin biosynthesis requires the coordinate action of both the enzymes in the general phenylpropanoid pathway (PAL, C4H and 4CL) and the enzymes specific for lignin biosynthesis, such as CAD (Hahlbrock and Scheel, 1989). The MYB binding site has been found in the promoters of the genes encoding these enzymes (Douglas, 1996; Table 3-1). Therefore we expect to see that coordinate control of gene transcription initiation, which brings about coordinate enzyme action in this pathway, is under the control of MYB transcription factors. The Arabidopsis bolting stem is a major site for lignin biosynthesis, and *At4CL1* is a good marker for lignin biosynthesis since its expression is temporally and spatially coordinated with lignin deposition (Lee et al., 1995).

In this chapter, I describe the initial work to identify *AtMYB* genes involved in the regulation of expression of the genes encoding enzymes required by lignin biosynthesis. I searched for representative *AtMYB* genes in the publicly available EST database at the time that had expression patterns similar to that of the marker gene *At4CL1*. I also tried to identify such *AtMYB* genes through cloning *MYB* cDNAs from the bolting stem, where *At4CL1* was strongly expressed. Before doing these experiments, I first characterized differential expression patterns of Arabidopsis *4CL* genes.

3.2 Expression of Arabidopsis *4CL* and *4CL*-Like Genes

Since *At4CL1* and *At4CL2* cDNAs shared a high degree of identity, I first needed to know how similar they were in expression patterns. The expression pattern of *At4CL1* was determined before (Lee et al., 1995). The expression pattern of *At4CL2* was examined in seedlings and mature organs by a northern blot analysis. A ~1.5 kb genomic DNA fragment of

At4CL2 containing the 1st exon and a ~400 bp upstream region was used as a probe. This fragment did not hybridize to the *At4CL1* cDNA as tested on a Southern blot (data not shown). For comparison, the *At4CL1* cDNA was hybridized to the same blot after the *At4CL2* probe was removed.

Figure 3-1-A shows that the level of the *At4CL2* transcript was generally lower than that of *At4CL1* (probes were labeled to have similar specific activities). Both had similar expression patterns in seedlings. Accumulation of the transcripts was increased as the seedling grew from 2-day old to 3-day old. It was noted that some seedlings at this age accumulated anthocyanin pigments in the cotyledons and hypocotyls under the light conditions used. Among organs, the *At4CL1* transcript accumulated highly in bolting stems. In contrast, the level of the *At4CL2* transcript was low in this organ. Both had moderate expression in the root, but had low expression in rosette leaves, flowers and siliques.

At the time, by searching the Arabidopsis EST database, we found that EST clone 139B10T7 had some similarity to *At4CL1* (now, with completion of the Arabidopsis genome project, this gene is known to be one of many related to *4CL*). The predicted protein has 41.5% identity to At4CL1. It contains a partially conserved sequence 'GEICIRG' (motif II), common to all 4CL enzymes (Becker-Andre et al., 1991), and the motif I, which was postulated to be part of the AMP-binding domain that is common to ATP-dependent enzymes (Schroder, 1989) (Figure 3-2). Thus, the expression pattern of this *4CL*-like gene was also examined. A northern blot analysis showed that the transcript of this gene accumulated ubiquitously at a low level in all the tissues/organs tested. The transcript level was slightly higher in 3-day old seedlings. This could be related to light induced anthocyanin synthesis in these seedlings (Figure 3-1, B).

3.3 Expression Patterns of Arabidopsis *MYB* Genes

When this project was started in 1995, a search of the Arabidopsis EST database revealed 25 MYB related EST clones (Table 3-2). These clones were ordered from the ABRC Stock

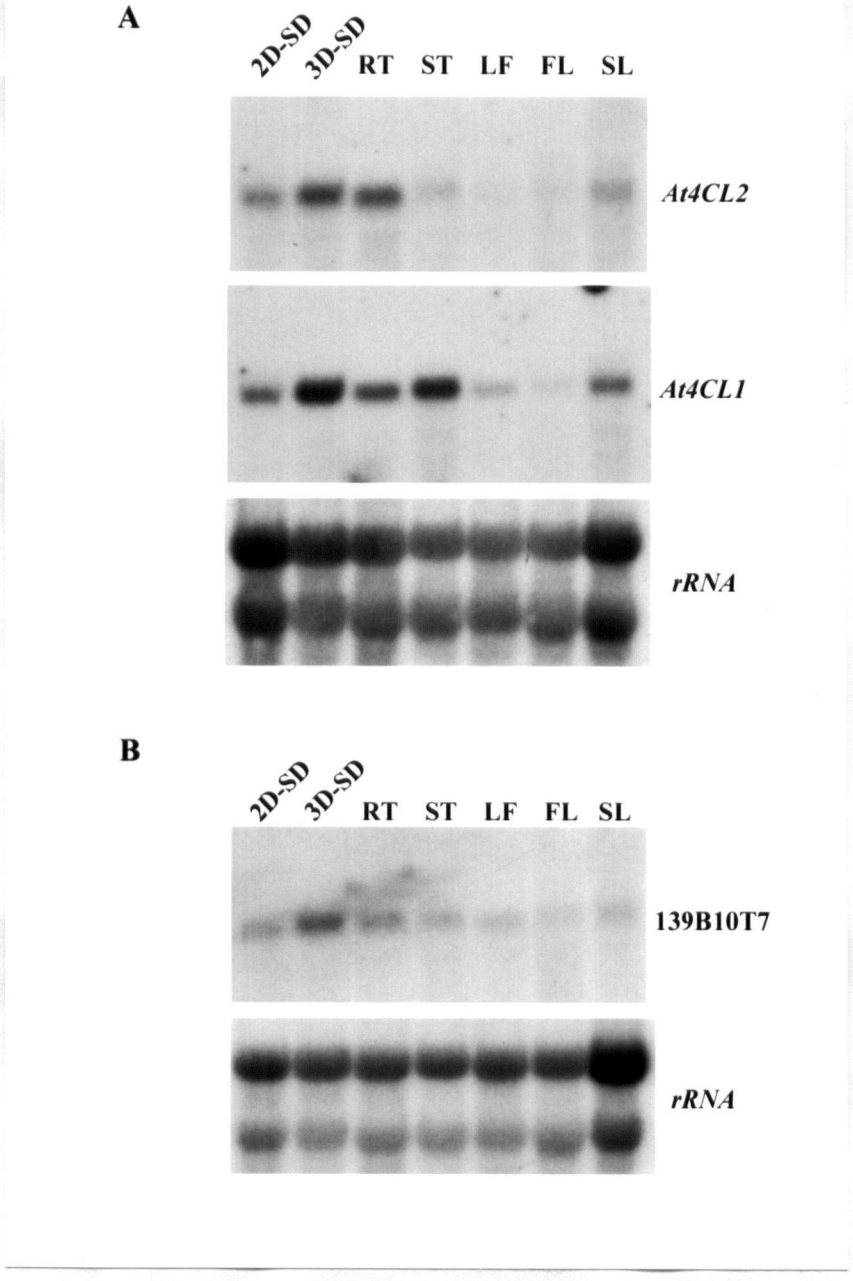

Figure 3-1. Northern Blot Analysis of Expression Patterns of Arabidopsis *4CL* Genes.
(A) Expression patterns of *At4CL1* and *At4CL2*. The *At4CL1* cDNA was hybridized to the same blot after the *At4CL2* probe was removed.
(B) Expression Pattern of *4CL*-like EST 139B10T7.
Total RNA was extracted from Col seedlings and mature organs. 10 μg total RNA was loaded on each lane. 2D-SD, 2-day old seedlings. 3D-SD, 3-day old seedlings. RT, 10-day old seedling roots. ST, bolting stems. LF, rosette leaves. FL, flowers. SL, siliques. A ribosomal RNA probe was hybridized to the same blot as a loading control after a blot was striped. Blots were washed at high stringency.

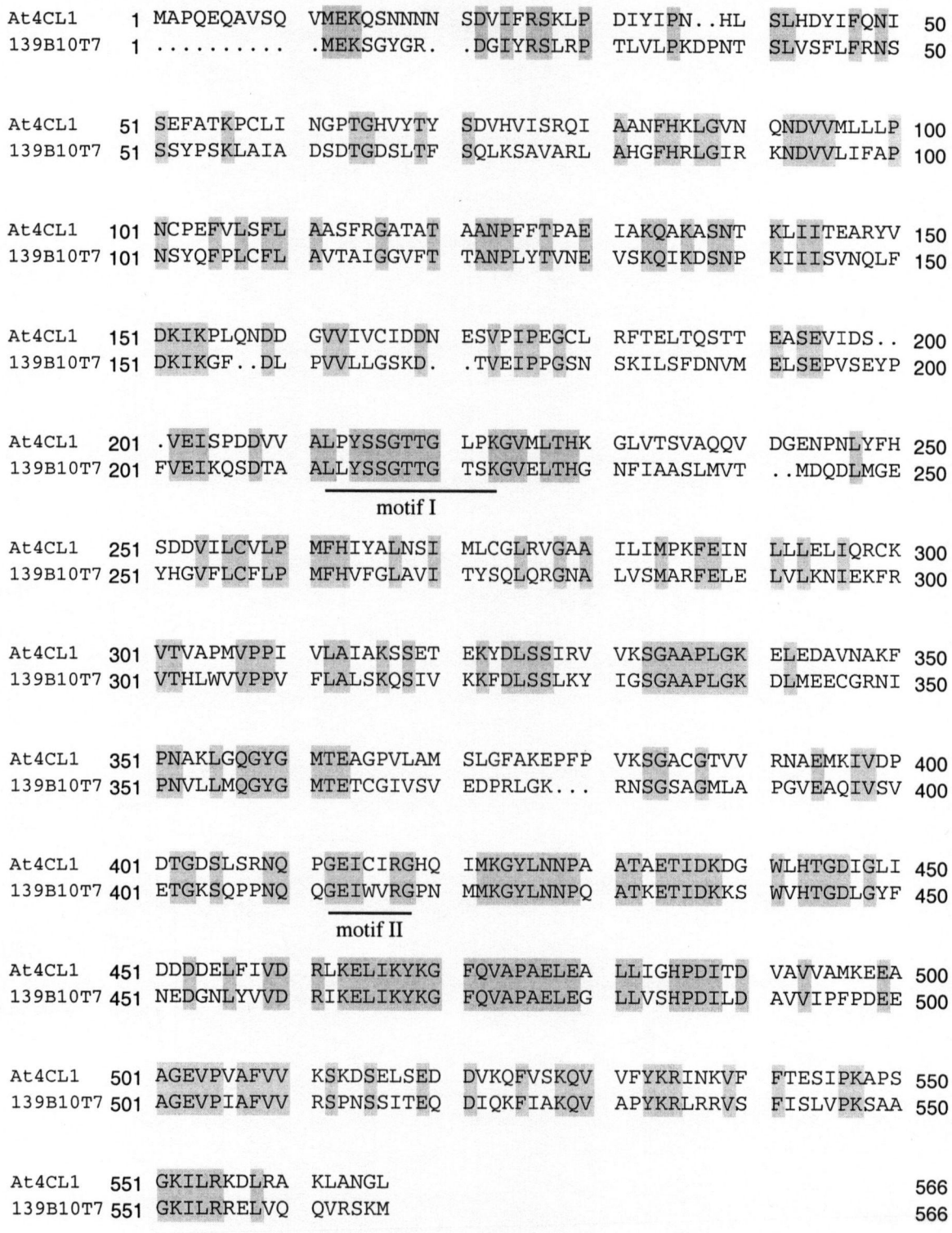

Figure 3-2. Alignment of At4CL1 and the 4CL-Like Protein Encoded by EST 139B10T7. The shaded area indicates conserved amino acids in both proteins. Motif I and II are conserved in all 4CLs.

Center, and checked by sequencing to ensure that the right clones had been received. They represented 21 unique genes since redundancy existed in three pairs of ESTs (clones 4 and 7; 6 and 21; and 16 and 23), and one EST clone (clone 20) can no longer be assigned as a *MYB*-related gene, as most of Arabidopsis genes have been annotated today. Three (clones 3, 18 and 25) were not R2R3-type *MYB* genes.

Table 3-2. Examined Arabidopsis *MYB* EST Clones

Douglas Lab No.	EST Clone	GenBank Accession for EST Clone	Corresponding Gene#	Gene Code
1	165L19T7	R30551	*AtMYB47*	At1g18710
2	170K1T7	R65084	*AtMYB45*	At3g48920
4	111E18T7	T42232	*AtMYB94* (*AtMYBCP70*)	At3g47600
7	111F18T7	T42245	*AtMYB94*	At3g47600
5	178M4T7	H36793	*AtMYB93*	At1g34670
6	95L7T7	T21333	*AtMYB44* (*AtMYBr1*)	At5g67300
21	93E13T7	T21228	*AtMYB44*	At5g67300
8	99M15T7	T22593	*AtMYB51*	At1g18570
9	99P9T7	T22223	*AtMYB75* (*PAP1*)	At1g56650
10	106H10T7	T22697	*AtMYB63*	At1g79180
11	157G9T7	T88197	*AtMYB92* (*AtMYB64*)	At5g10280
12	122N17T7	T43719	*AtMYB6*	At4g09460
13	110F12T7	T42065	*AtMYB68*	At5g65790
14	1B4T7P	T04118	*AtMYB3*	At1g22640
15	186O19T7	R89962	*AtMYB16* (*AtMIXTA*)	At5g15310
16	114F24T7	T42666	*AtMYB59*	At5g59780
23	206N11T7	N37592	*AtMYB59*	At5g59780
17	156O4T7	T88476	*AtMYB36*	At5g57620
19	220A8T7	N38154	*AtMYB4*	At4g38620
22	193M15T7	H76020	*AtMYB90* (*PAP2*)	At1g66390
24	E11A6T7	AA041019	*AtMYB96* (*mybcov1*)	At5g62470
3*	109M16T7	T41952	Encoding MYB-like protein	At4g17780
18*	135E3T7	T46559	Encoding putative MYB protein	At1g71030
25*	130A10T7	T44683	Encoding Myb-related transcription activator-like protein	At5g47390
20*	226M4T7	N65339	?	

#*AtMYB* gene systematic name in Stracke et al. (2001).

*EST clones not included in the Stracke et al. (2001) *AtMYB* gene list.

The non-conserved 3' region of each clone was PCR amplified using a degenerate primer corresponding to the end of the conserved MYB DNA-binding domain and a vector primer. No product was amplified from clone 25. The PCR fragments were gel-purified and used as probes for northern analyses. For clone 25, the whole cDNA fragment was used as a probe.

The results of northern blot analyses are summarized in Table 3-3, and accumulation of the transcripts detected by northern blot analyses is shown in Figure 3-3. Total RNA from 2- and

Table 3-3. Expression Patterns of Examined Arabidopsis *MYB* Genes

EST Clone (Gene)	Tissue Detected						
	2D-Seedlings	3-4D-Seedlings	Roots	Bolting Stems	Rosette Leaves	Flowers	Siliques
165L19T7 (*AtMYB47*)	—	—	N/A	—	—	—	N/A
170K1T7 (*AtMYB45*)	—	—	N/A	—	—	—	N/A
111E18T7 (*AtMYB94*)	Not Done						
111F18T7 (*AtMYB94*)	—	—	—	—	—	—	N/A
178M4T7 (*AtMYB93*)	—	—	N/A	—	—	—	N/A
95L7T7 (*AtMYB44*)	+	++	+++	++	+++	+	+
93E13T7 (*AtMYB44*)	+	++	N/A	+++	+++	+	N/A
99M15T7 (*AtMYB51*)	—	—	N/A	—	+	—	N/A
99P9T7 (*AtMYB75*)	+	—	N/A	—	—	—	N/A
106H10T7 (*AtMYB63*)	—	—	N/A	—	—	—	N/A
157G9T7 (*AtMYB92*)	—	—	N/A	—	—	—	N/A
122N17T7 (*AtMYB6*)	—	—	N/A	—	—	—	N/A
110F12T7 (*AtMYB68*)	—	+	++	—	—	—	—
1B4T7P (*AtMYB3*)	N/A	—	—	—	—	—	—
	N/A*	+	N/A	+	+	N/A	N/A
186O19T7 (*ATMYB16*)	++	++	N/A	—	—	+	N/A
114F24T7 (*AtMYB59*)	—	—	N/A	—	—	—	N/A
206N11T7 (*AtMYB59*)	—	—	N/A	—	—	—	N/A
156O4T7 (*AtMYB36*)	N/A	+	++	—	—	—	—
220A8T7 (*AtMYB4*)	+	++	++	+	+	+	++
193M15T7 (*AtMYB90*)	—	—	N/A	—	—	—	N/A
E11A6T7 (*AtMYB96*)	—	—	N/A	—	—	—	N/A
109M16T7	—	—	N/A	—	—	—	N/A
135E3T7	N/A	—	—	—	—	—	—
	N/A*	+	N/A	+(-)	+	N/A	N/A
130A10T7	+	++	+	+	++	+	+

+++, moderate; ++, weak; +, very weak; +(-), just detectable; -, not detectable; N/A, not done.

* Signal detected on poly(A)$^+$ RNA blot.

3-day old seedlings, bolting stems, rosette leaves and flowers was commonly examined. Total RNA from roots and siliques was only examined with 3 clones (expression of *AtMYB68* is shown in Chapter 4).

The transcript levels of these MYB-homolog genes were generally low, except that the level of the *AtMYB44* transcript was relatively high. Of all 21 genes examined, expression of 13 genes was not detectable in the tissues/organs tested on the total RNA northern blots.

Expression of 8 genes was detectable by a northern analysis with various expression patterns (Figure 3-3). In particular, expression of 99M15T7 (*AtMYB51*) was only detected in rosette leaves (Figure 3-3, C), and 99P9T7 (*AtMYB75*) expression was only detected in 2-day old seedlings (Figure 3-3, D). Expression of 156O4T7 (*AtMYB36*) was mainly detected in roots, and detectable in 3 day-old seedlings (Figure 3-3, F). This pattern is the same as that of 110F12T7 (*AtMYB68*) (Chapter 4). Expression of 186O19T7 (*AtMYB16*) was relatively high in seedlings, and just detectable in flowers (Figure 3-3, E). 95L7T7 (and 93E13T7 for *AtMYB44*), 220A8T7 (*AtMYB4*) and 130A10T7 had more or less constitutive expression patterns (Figure 3-3, A, B and G). In these, expression of *AtMYB44* was higher in roots and rosette leaves, and expression of *AtMYB4* was higher in roots, as compared to other organs.

Expression of 135E3T7 and 1B4T7P (*AtMYB3*) was tested using both total RNA and poly(A)$^+$ RNA on a northern blot. Neither was detectable using total RNA. Using poly(A)$^+$ RNA, both had constitutive expression patterns in the tissues/organs tested, including 4-day old seedlings, bolting stems and rosette leaves (Figure 3-3, H).

Among all the above *AtMYB* genes tested, none had an expression pattern that coordinated with that of *At4CL1*, which was most highly expressed in bolting stems among organs. Thus, none of these *MYB* genes were obvious candidates in my search for a regulator of the expression of *At4CL1*, or a set of genes encoding the enzymes in the lignin biosynthesis pathway.

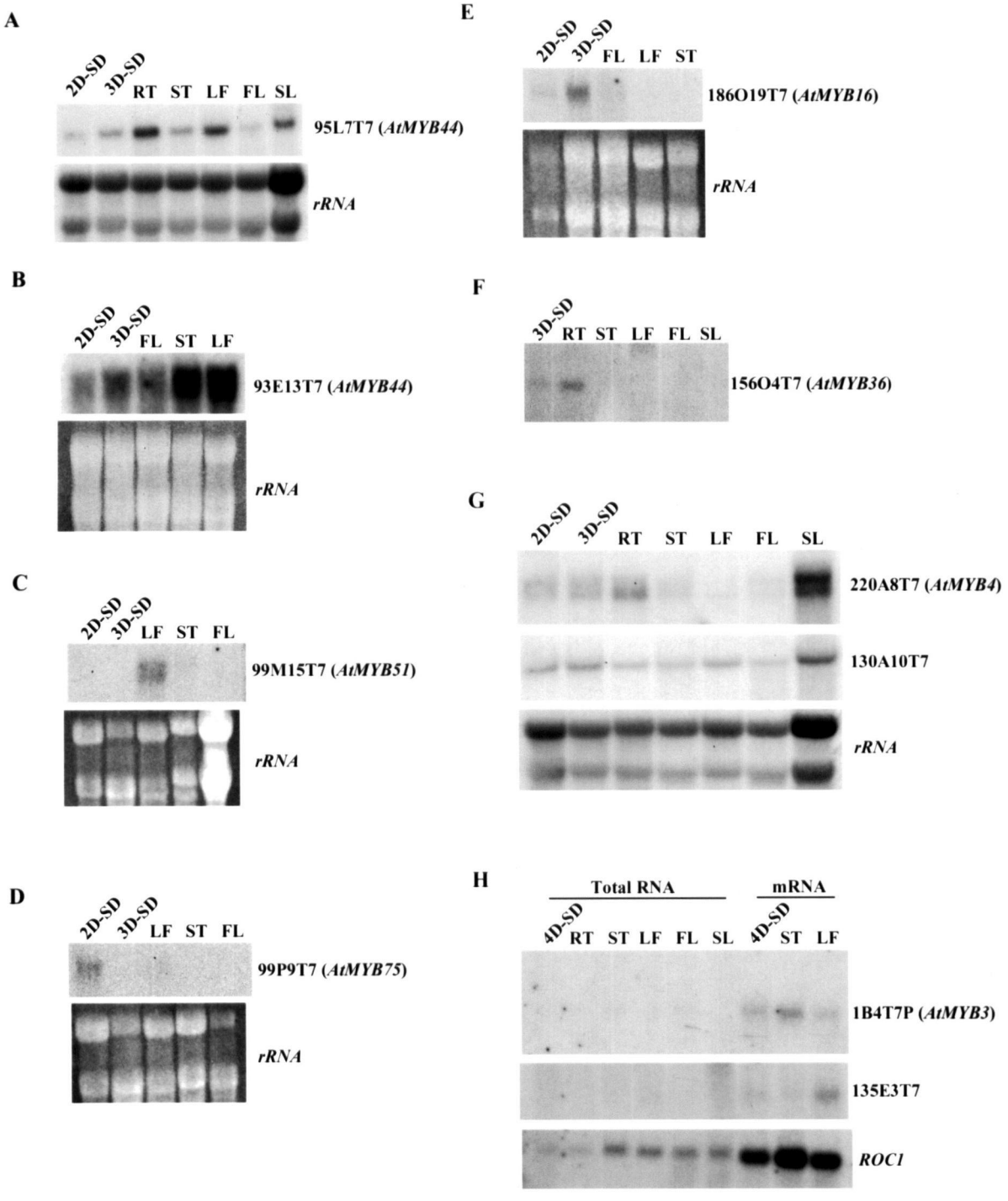
A
2D-SD
3D-SD
RT ST LF FL SL
95L7T7 (AtMYB44)
rRNA
B
2D-SD
3D-SD
FL ST LF
93E13T7 (AtMYB44)
rRNA
C
2D-SD
3D-SD
LF ST FL
99M15T7 (AtMYB51)
rRNA
D
2D-SD
3D-SD
LF ST FL
99P9T7 (AtMYB75)
rRNA
E
2D-SD
3D-SD
FL LF ST
186O19T7 (AtMYB16)
rRNA
F
3D-SD
RT ST LF FL SL
156O4T7 (AtMYB36)
G
2D-SD
3D-SD
RT ST LF FL SL
220A8T7 (AtMYB4)
130A10T7
rRNA
H
Total RNA
mRNA
4D-SD
RT ST LF FL SL
4D-SD
ST LF
1B4T7P (AtMYB3)
135E3T7
ROC1

3.4 Cloning *MYB* cDNAs from Arabidopsis Bolting Stems

Using the EST clones available at the time, I did not find any *AtMYB* genes that were coordinately expressed with *At4CL1*. Since a characteristic of *At4CL1* was high expression in bolting stems, likely associated with lignin biosynthesis, I tried to clone new *AtMYB* cDNAs from bolting stems where they might be specifically or preferentially expressed, and potentially involved in regulating expression of *At4CL1* and other genes in the lignin biosynthetic pathway.

Poly(A)$^+$ RNA isolated from Arabidopsis bolting stems was used for reverse transcription to generate cDNAs. The 5' regions of cDNAs encoding the conserved MYB DNA-binding domains were amplified by 5'-RACE using a *MYB* degenerate primer. The predicted size for an amplified fragment corresponding to the R2R3-type MYB DNA-domain was ~400 bp. Several distinct PCR fragments ranging in size from 300 bp to 450 bp were observed by gel electrophoresis (data not shown). These fragments were tested on a Southern blot using a *MYB* cDNA probe. The Southern blot analysis showed hybridization signals from the fragments (data not shown), which were then cloned into TA vectors (Invitrogen). The cloned inserts were also tested on Southern blots. Nine out of 54 clones tested had inserts that hybridized to the *MYB* probe (data not shown). These 9 positive clones were sequenced. Seven of them had identical sequences corresponding to the conserved MYB DNA-binding domain, and the longest sequence

---

Figure 3-3. Northern Blot Analysis of Expression Patterns of Arabidopsis *MYB* Genes. Total RNA was extracted from Col (except RNA on blot H from WS ecotype) seedlings and mature organs. 10 μg total RNA (except 20 μg on blot B) was loaded on each lane. Poly(A)$^+$ RNA was extracted from WS seedlings and selected mature organs. ~2 ug poly(A)$^+$ RNA (blot H) was loaded on each mRNA lane. 2D-SD, 2-day old seedlings. 3D-SD, 3-day old seedlings. RT, 10-16 days old seedling roots. ST, bolting stems. LF, rosette leaves. FL, flowers. SL, siliques. For blots A and G, a ribosomal RNA probe was hybridized to the same blot as a loading control after the blot was striped. For blots B, C, D and E, ribosomal RNA bands were stained by ethidium bromide as a loading control. For blot H, *ROC1* cDNA (encoding Arabidopsis cytosolic cyclophilin) was hybridized to the same blot as a loading control after the blot was striped.

was 414 bp in length (data not shown). This *MYB* sequence was not identical to any known *MYB* EST or gene at the time.

The 3' region of the cDNA was amplified by 3'-RACE using a gene-specific primer. An amplified fragment was cloned into the TA vector. Three clones were sequenced and had identical sequences. The full-length cDNA was generated by joining the 5'-clone and 3'-clone together. This gene was designated as *STM31*. The ORF encoded 320 amino acids (Figure 3-4). Later, this *MYB* gene was also identified by another group (Romero, et al., 1998). In that study this gene was systematically named as *AtMYB73* (At4g37260).

The other two positive clones identified on the Southern blot had sequences identical to the known EST clone 1B4T7P in the MYB DNA-binding domain (data not shown). Thus 3' cloning for this gene was not carried out.

The expression pattern of *STM31* was examined by a northern blot analysis. The analysis showed that *STM31* had a constitutive expression pattern in various tissues/organs tested, including 2-day and 3-day old seedlings, seedling roots, bolting stems, rosette leaves, flowers and siliques (Figure 3-5). Expression of the EST clone 1B4T7P, identical to the second clone identified from the 5'-RACE, is shown in Figure 3-3-H.

Thus, these two *MYB* genes cloned as cDNAs from Arabidopsis bolting stems did not have expression patterns similar to *At4CL1*, making it unclear whether they could be involved in regulating *At4CL1* expression.

A

```
TTTCTTCCCA ACACACACAA AAAAAAAAAC TGTAACGACC AAAAAAAAAG AGGACGCGTT AGAAGAAAAA
AAAAGAACAA TCCGATAAAA AGATCCGGCG ATGTCAAACC CGACCCGTAA GAATATGGAG AGGATTAAAG
GTCCATGGAG TCCAGAAGAA GATGATCTGT TGCAGAGGCT TGTTCAGAAA CATGGTCCGA GGAACTGGTC
TTTGATTAGC AAATCAATCC CTGGACGTTC CGGCAAATCT TGTCGTCTCC GGTGGTGTAA CCAGCTATCT
CCGGAGGTAG AGCACCGTGC TTTTTCGCAG GAAGAAGACG AGACGATTAT TCGAGCTCAC GCTCGGTTTG
GTAACAAGTG GGCTACGATC TCTCGTCTTC TCAATGGACG AACCGATAAC GCTATCAAGA ATCATTGGAA
CTCGACGCTG AAGCGAAAAT GCAGCGTCGA AGGGCAAAGT TGTGATTTTG GTGGTAATGG AGGGTATGAT
GGTAATTTAG GAGAAGAGCA ACCGTTGAAA CGTACGGCGA GTGGTGGTGG TGGTGTCTCG ACTGGCTTGT
ATATGAGTCC CGGAAGTCCA TCGGGATCTG ACGTCAGCGA GCAATCTAGT GGTGGTGCAC ACGTGTTTAA
ACCAACGGTT AGATCTGAGG TTACAGCGTC ATCGTCTGGT GAAGATCCTC CAACTTATCT TAGTTTGTCT
CTTCCTTGGA CTGACGAGAC GGTTCGAGTC AACGAGCCGG TTCAACTTAA CCAGAATACG GTTATGGACG
GTGGTTATAC GGCGGAGCTG TTTCCGGTTA GAAAGGAAGA GCAAGTGGAA GTAGAAGAAG AAGAAGCGAA
GGGGATATCT GGTGGATTCG GTGGTGAGTT CATGACGGTG GTTCAGGAGA TGATAAGGAC GGAGGTGAGG
AGTTACATGG CGGATTTACA GCGAGGAAAC GTCGGTGGTA GTAGTTCTGG CGGCGGAGGT GGCGGTTCGT
GTATGCCACA AAGTGTAAAC AGCCGTCGTG TTGGGTTTAG AGAGTTTATA GTGAACCAAA TCGGAATTGG
GAAGATGGAG TAGAGTGATA AGAACAAGTT TTCCCTCTGT TTCTCGGGAA AATAAAAGTT TCAGGCTTTT
CATGTATAGA GCCAGTAGTA GGGACGACGA AAGGAGGAAG CGAAATCAAA AAATGTTTTG TTATCATCAT
CATATGATCT TCTTTCGTGA TTCAATTAAA AGCAAAGCAA GATCACTTAT TAAAAAAAAA AAAAAAAA 1258
```

B

```
MSNPTRKNME RIKGPWSPEE DDLLQRLVQK HGPRNWSLIS KSIPGRSGKS CRLRWCNQLS
PEVEHRAFSQ EEDETIIRAH ARFGNKWATI SRLLNGRTDN AIKNHWNSTL KRKCSVEGQS
CDFGGNGGYD GNLGEEQPLK RTASGGGGVS TGLYMSPGSP SGSDVSEQSS GGAHVFKPTV
RSEVTASSSG EDPPTYLSLS LPWTDETVRV NEPVQLNQNT VMDGGYTAEL FPVRKEEQVE
VEEEEAKGIS GGFGGEFMTV VQEMIRTEVR SYMADLQRGN VGGSSSGGGG GGSCMPQSVN
SRRVGFREFI VNQIGIGKME *
```

Figure 3-4. Nucleotide and Deduced Amino Acid Sequences of Arabidopsis *MYB STM31* (*AtMYB73*).

(A) The DNA sequence. Shaded nucleotides indicate the putative translation start and stop sites.

(B) The deduced amino acid sequence. Grey amino acids, the dark grey (R2) and the light grey (R3) indicate the conserved MYB binding domain.

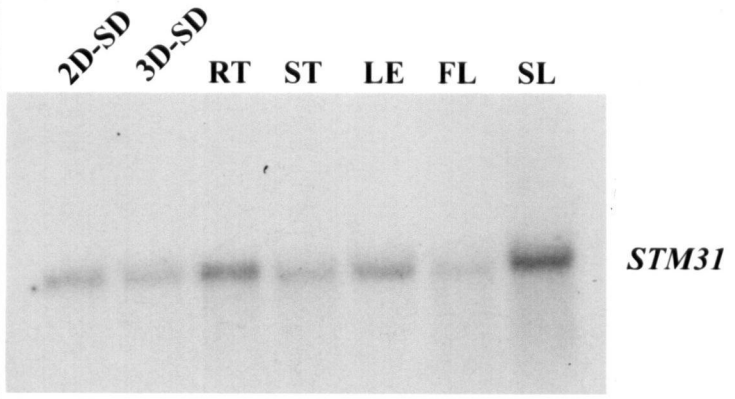

Figure 3-5. Northern Blot Analysis of *STM31*Expression.
Total RNA was extracted from Col seedlings and mature organs. 10 μg total RNA was loaded on each lane. 2D-SD, 2-day old seedlings. 3D-SD, 3-day old seedlings. RT, 10-day old seedling roots. ST, bolting stems. LF, rosette leaves. FL, flowers. SL, siliques. A ribosomal RNA probe was hybridized to the same blot as a loading control after the blot was striped.

3.5 Discussion

Strikingly, among various organs, *At4CL1* is strongly expressed in the bolting stems but not *At4CL2*. This data plus enzyme activity analyses (Ehlting, et al., 1999), suggest that although *At4CL1* and *At4CL2* share a high degree of similarity, *At4CL1* is the only member in the Arabidopsis *4CL* gene family that plays a primary role in phenylpropanoid metabolism in bolting stems, a major site for lignin synthesis. Both genes also have moderate expression in seedling roots. This result suggests that *At4CL1* and *At4CL2* might have overlapping functions in the root, which may reflect an evolutionary adaptation of roots for response to stress. Various phenolic compounds derived from the phenylpropanoid pathway appear to play an important role in the

plant defense response (Dixon and Paiva, 1995). Both *At4CL1* and *At4CL2* expression are induced by pathogen infection, wounding and UV irradiation (Lee, et al., 1995; Ehlting, et al., 1999).

The protein encoded by the *4CL*-like EST clone 139B10T7 is only partially conserved in the two motifs present in 4CL enzymes. Thus it was not surprising to see that this 4CL-like protein did not have 4CL enzyme activity (Samaeian and Douglas, unpublished data). What biochemical function this 4CL-like protein has needs to be tested further, but is not apparent from its expression pattern.

Of the125 Arabidopsis R2R3-MYB genes, I examined expression of 19 genes by northern blot analyses (plus one by RT-PCR, Chapter 5). These represent 16% of the members of the Arabidopsis R2R3-*MYB* gene family. These genes are scattered in different phylogenetic subgroups. For 13 out of 21 *MYB* genes examined here, expression was not detectable using total RNA on northern blots. This result indicates that *AtMYB* transcripts generally accumulate at a low level. It also should be noted that for most of the genes, the expression was not examined in roots and siliques. The reason for this was that in my screen for *AtMYB* genes involved in the regulation of the phenylpropanoid pathway, the bolting stem was our primary target. Thus, it can not be excluded that some of these *AtMYB* genes are specifically or preferentially expressed in roots or siliques, such as *AtMYB68* and *AtMYB36*. Another possibility for not seeing the expression is that the transcription of some of the genes may be induced under specific conditions. These conditions were not included in my assays.

Three years after I started this project, expression patterns of Arabidopsis *MYB* genes were systematically tested by 'reverse northern' analyses (Kranz, et al., 1998). Most of my gene expression data matches their results with minor exceptions. Currently, examination of gene expression profiles on a large scale can be much more easily achieved by using the microarray technique. However, either reverse northern or RNA-array data should be interpreted with caution, since in these techniques, sizes of transcripts are not included and therefore the problem of cross-hybridization to other genes can be involved (Kranz, et al., 1998). Recently, expression

patterns of over 95% of Arabidopsis genes have been examined by using the MPSS (Massively Parallel Signature Sequencing) technique, a more precise and sensitive way to quantify gene expression (Brenner et al., 2000a and 2000b; http://mpss.ucdavis.edu). My expression data also matches MPSS data. For some of the *MYB* genes, expression was not detectable in my study, it was also not detectable or detected at a very low level by MPSS.

Some of the *MYB* genes, examined for the expression pattern in this study, have also been analyzed in other groups later. In particular, *AtMYB4* has been found to negatively regulate the biosynthesis of sinapate ester, a UV protector in Arabidopsis leaves (Jin et al., 2000). My data and MPSS data revealed that this gene has a more or less constitutive expression pattern. Expression of both *AtMYB90* and *AtMYB75* are not detectable by MPSS. In my experiment, the *AtMYB75* transcript was only detected at a very low level in 2-day old seedlings. It is interesting to see that overexpressing these two genes with such a low expression level, results in dramatic increase of a set of phenylpropanoid products (Borevitz et al., 2000). Expression of *AtMYB44* has also been found to increase at late stages of embryogenesis, and AtMYB44 maybe related to embryogenesis (Kirik, et al., 1998).

Here I described one approach to identify a regulatory gene, by searching for coordinate expression with a target gene. In some cases, this approach could work because gene function can be reflected from its expression pattern. *AtMYB* genes *TT2* and *AtMYB61* are such examples. Both are involved in different aspects of seed development. Accordingly, the expression is seed specific or preferential (Nesi et al., 2001; Penfield et al., 2001). However, this is not always necessary true. Studies of animal and plant MYB transcription factors, such as the maize C1, revealed that the activity of some MYB factors requires interactions with partner proteins (Weston, 1998; Goff et al., 1992). In this case, expression of one of the regulatory genes may not be similar to that of a target gene, since the combination of transcription factors leads to gene regulation. This could be the case in regulation of gene expression in the phenylpropanoid pathway. Thus other ways to identify a *MYB* gene involved in the regulation of the phenylpropanoid pathway should be considered.

Another approach used in this study was to clone *MYB* cDNAs preferentially expressed in the bolting stem, where *At4CL1* was most highly expressed. However, neither cDNA identified was preferentially expressed in this organ. Thus, like the other *AtMYB* genes analyzed in this study, there were no obvious candidates for genes regulating gene expression in the lignin biosynthetic pathway. In addition, interesting results were obtained with another *AtMYB* gene (described in Chapter 4 and 5), therefore I did not study these genes further.

Now we know there are over 130 *MYB* genes in Arabidopsis (Stracke, et al., 2001). However, using the RACE method, I only obtained two clones from the bolting stem, obviously missing some. The problem could be caused by the *MYB* degenerate primer used in the 5'-RACE. Although the primer was designed corresponding to the highly conserved amino acid stretch in the MYB R3 repeat, it may not have been able to amplify all the members of such a big gene family. On the other hand, this result also reflected low expression of *AtMYB* genes in general. Another study in which Arabidopsis *MYB* genes were systematically identified by a PCR-based strategy revealed the same thing. More than twice as many genes were amplified from a genomic library than from cDNA libraries despite different combinations of several degenerate primers used (Romero et al., 1998).

Chapter 4 *AtMYB68*: a Root Preferentially Expressed *MYB* Gene — Expression Profile Studies

4.1 Introduction

Plant roots are adapted for growing through soil and absorbing water and mineral nutrients. Roots grow and develop from their distal ends. The external morphology of the root tip can be divided into four distinct but overlapping zones: the root cap, the meristematic zone, the elongation zone and the maturation zone (Figure 4-1, A). The meristematic zone is characterized by small cells overlaid by the root cap. The elongation zone is the site of rapid and extensive cell elongation. Both the meristematic zone and the elongation zone are about a quarter of a millimeter long in the Arabidopsis root. The maturation zone is the region in which the elongated cells acquire their differentiated characteristics. Differentiation may begin earlier, but the cells do not achieve the mature state until they reach this zone (Dolan et al., 1993; Taiz and Zeiger, 2002)

Transverse sections reveal that the Arabidopsis root has a simple and radial organization. A typical section from the mature region of the root is composed of the central vascular core surrounded by four radial cell layers (Figure 4-1, B). From the outside, they are the epidermis, cortex, endodermis and pericycle. Each cell type is present in a single layer. In Arabidopsis, there are usually 8 and 12 cells in the endodermis and pericycle respectively. The central vascular core is composed of the phloem and xylem. The xylem axis consists of two types of cells, the protoxylem cells at two ends and the central metaxylem cells. Two poles of the protoxylem cells are adjacent to pericycle cells (Dolan et al., 1993; Cano-Delgado et al., 2000).

Longitudinally, each cell type forms a vertical file of cells that can be traced to meristematic initials in the root apical meristem. There are four sets of meristematic initials in Arabidopsis roots. Respectively, these give rise to the epidermis and the lateral root-cap, the columella root cap, the cortex and endodermis, and the stele tissues including the pericycle and

vascular tissues (Dolan et al., 1993). These initials appear to be established during embryogenesis (Scheres et al., 1994).

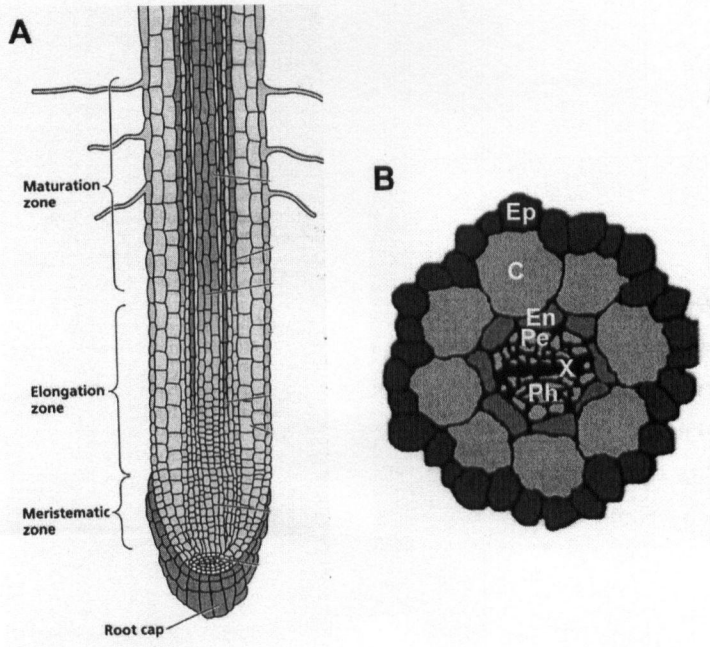

Figure 4-1. Schematic View of Root Anatomy.
(A) Stylized typical root longitudinal section (from Plant Physiology (Taiz and Zeiger), copyright © 2002 Sinauer).
(B) Arabidopsis root cross-section. Ep, Epidermis. C, Cortex. En, Endodermis. Pe, Pericycle. X, Xylem. Ph, Phloem (from Di Laurenzio et al., copyright © 1996 Cell).

The elegant simplicity of the Arabidopsis root anatomy and its clear cell lineages make it a useful tool for developmental study with the aid of mutant screening. One class of root mutations in Arabidopsis causes radial pattern defects. An example of such a mutation is *wooden leg* (*wol*), which has highly reduced root growth as compared to the wild type. The root of the *wooden leg* mutant has a reduced cell number in the vascular tissue and all these vascular cells differentiate into protoxylem, resulting in the vascular cylinder lacking phloem and consisting of

xylem only (Scheres et al., 1995). The *WOL* gene encodes a putative two component histidine kinase. The *wol-1* allele contains a single point mutation converting T_{278} to I_{278} in the WOL protein, resulting in a non-conservative amino acid change in the conserved putative extracellular receptor domain. It is postulated that the *WOL* gene product is a receptor molecule that controls the asymmetric cell divisions of the vascular initials through a certain signal transduction pathway (Mahonen et al., 2000).

Lateral root development provides an interesting example of postembryonic organogenesis in higher plants. In angiosperms, lateral roots are derived from the differentiated pericycle layer of a parent root (McCully, 1975). Their formation involves several key stages (Malamy and Benfey, 1997). First, the mature pericycle cells are stimulated and dedifferentiated. Interestingly, not all pericycle cells can become founder cells for lateral roots. Lateral roots arise only from files of pericycle cells adjacent to the two xylem poles (Steeves and Sussex, 1989; Charlton, 1991). It is not known how this bipolar pattern is established. The initiation of lateral roots occurs some distance away from the root apical meristem. There is a consistent relationship between the position of the first founder cell division and the root apex (Casimiro et al., 2001). Second, ordered cell divisions and cell differentiation occur to generate a highly organized lateral root primordium. This process is initiated from a pair of adjacent xylem pole pericycle cells in a single file that undergo several transverse divisions, followed by a periclinal division to give rise to two cell layers. This step represents the critical event during the onset of lateral root formation. Third, the lateral root primordium grows through the overlying cell layers and eventually emerges from the parent root. This process largely depends on cell expansion. In Arabidopsis, emergence of lateral roots is observed ~20 mm from the primary root apex (Casimiro et al., 2001). Fourth, an active lateral root meristem allows continued lateral root growth.

The plant hormone auxin is a key regulator of lateral root development. It is known that exogenous auxin induces lateral root primordium formation, but inhibits root elongation (Evans et al., 1994). Several auxin-related lateral root mutants have been isolated in Arabidopsis. In

these mutants, lateral root development was arrested at different stages. This suggests that indole-3-acetic acid (IAA) is required at several stages of lateral root development (Celenza et al., 1995). It is also proposed that IAA is initially required to establish a population of rapidly dividing pericycle cells and that the subsequent derivatives form a hormone-autonomous meristem (Laskowski et al., 1995).

Auxin polar transport plays an important role in lateral root formation. It has been demonstrated that blocking auxin basipetal transport (from the shoot apex toward the base) results in a reduced lateral root number in Arabidopsis seedlings (Reed et al., 1998). Another experiment shows that treating the Arabidopsis root with the auxin polar transport inhibitor arrests lateral root development at the initiation stage. Endogenous IAA is found to accumulate in the root apex while reducing in the upper zone where lateral roots initiate. This result suggests that the initiation of the xylem pole pericycle cells for lateral root formation requires a threshold concentration of auxin (Casimiro et al., 2001).

Root development including root branching is also largely depending on nutrient supply. One striking example is that many plant species respond to an uneven distribution of nutrients (e.g. NO_3^-, NH_4^+ or inorganic phosphate) by developing their lateral roots preferentially within nutrient-rich zones (Robinson, 1994; Leyser and Fitter, 1998). This is believed to be important for a plant to compete for limiting resources (Hutchings and de Kroon, 1994). However, the mechanisms are poorly understood. Studies on NO_3^- have shown that NO_3^- supply modulates lateral root growth with two opposite effects. Low concentrations of NO_3^- locally stimulate lateral root growth, but at high concentrations it has an inhibitory effect on lateral root growth (Ericsson, 1995; Zhang et al., 1999). Two distinct signal pathways have been proposed. The stimulatory effect is localized to the lateral roots directly exposed to NO_3^-. It acts through an NO_3^- specific pathway. The Arabidopsis *ANR1* gene, encoding a MADS-box transcription factor, was identified in this pathway (Zhang and Forde, 1998). In contrast, the inhibitory effect is systematic. It more likely depends on the plant N status. N sources other than NO_3^- produce a response, and this pathway might be mediated by the N/C ratio (Zhang et al., 1999).

Using a reverse genetic approach, a systematic search for knockout mutations in Arabidopsis *MYB* genes was carried out seven years ago (Pri-Hadash and Douglas, unpublished data). Screens of DuPont and Feldmann T-DNA collections for a total of 14,100 T-DNA lines were performed by PCR using a *MYB* degenerate primer corresponding to the conserved MYB binding domain. One T-DNA line with the insertion 536 bp upstream of the putative ATG translation start codon of *AtMYB68* (At5g65790) was identified from the Feldmann collection (Figure 4-2). This line was backcrossed two times to the wild type WS ecotype. Since this line had the insertion fairly close to the ATG codon in the 5' promoter region, there was high possibility that this insertion might alter the gene transcription. As well, *AtMYB68* had not been functionally studied except that the EST clone had been identified (ABRC). Based on these reasons, it was chosen for further studies. While the subsequent analysis of this *AtMYB68* T-DNA line (T-14) showed that *AtMYB68* expression was not affected (Chapter 5), my preliminary data revealed a root-dominant expression pattern of this gene. The simplicity of Arabidopsis root cell organization provides a good system to study gene expression and function during development. This chapter describes studies on expression of *AtMYB68*, as the first step towards the goal of determining gene functions.

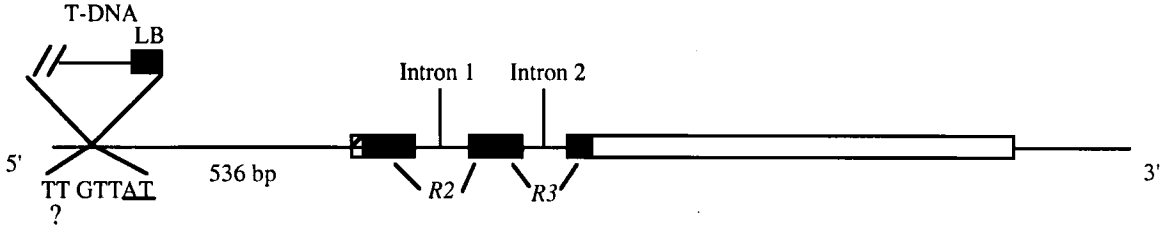

Figure 4-2. Schematic of a T-DNA Insertion within *AtMYB68* in Line T-14.
The sequence with a question mark indicates new nucleotides found at the T-DNA-*AtMYB68* junction. The sequence underlined indicates re-arrangement in *AtMYB68* at the junction. The dark and light grey boxes indicate the coding region for the two conserved MYB repeats R2, R3. The hatched box indicated the conserved 5' region. The open box indicates the non-conserved region.

4.2 Organ and Cell-Type Specific Expression of *AtMYB68*

The organ-specific expression of *AtMYB68* was examined by a northern blot analysis. The analysis of total RNA isolated from several Arabidopsis organs and seedlings showed that the *AtMYB68* transcript accumulated at a low level in roots, and was also detectable in 4-day old seedlings. It was not detectable in the other organs examined, including bolting stems, rosette leaves, flowers and siliques (Figure 4-3, left panel). Poly(A)$^+$ RNA isolated from selected samples was also prepared on the same blot. The analysis of poly(A)$^+$ RNA showed that again, the *AtMYB68* transcript was readily detectable from the 4-day old seedlings, but was still not detectable from either bolting stems or rosette leaves (Figure 4-3, right panel). These northern results were later confirmed by a RT-PCR analysis (Chapter 5).

The lower expression of *AtMYB68* in the whole seedlings (containing both shoots and roots) could be due to *AtMYB68* expression solely contributed in the seedling root, or due to the expression in the shoot as well. This was further tested using quantitative RT-PCR, a more sensitive method than a northern blot. Fourteen-day old Arabidopsis seedlings were separated as shoots (aerial part including hypocotyls) and roots. Total RNA isolated from these two separated parts was subjected to reverse transcription followed by PCR amplification. The quantitative RT-PCR analysis revealed that *AtMYB68* was expressed at a very low level in the shoot, a level about 20-fold lower than that in the root (Figure 4-4).

To determine the spatial and temporal, as well as cell-type specific expression pattern of *AtMYB68*, the β-glucuronidase (GUS) reporter gene was fused behind the *AtMYB68* promoter. GUS expression would represent where the *AtMYB68* promoter is active. A 1.9 kb *AtMYB68* promoter fragment including the ATG translation start codon was obtained by PCR amplification from Arabidopsis Col genomic DNA. This PCR product was sequenced and no PCR error was found in the fragment when compared to the Col genome sequence (data not shown). The *AtMYB68::GUS* translational fusion was generated by inserting the *AtMYB68* promoter fragment

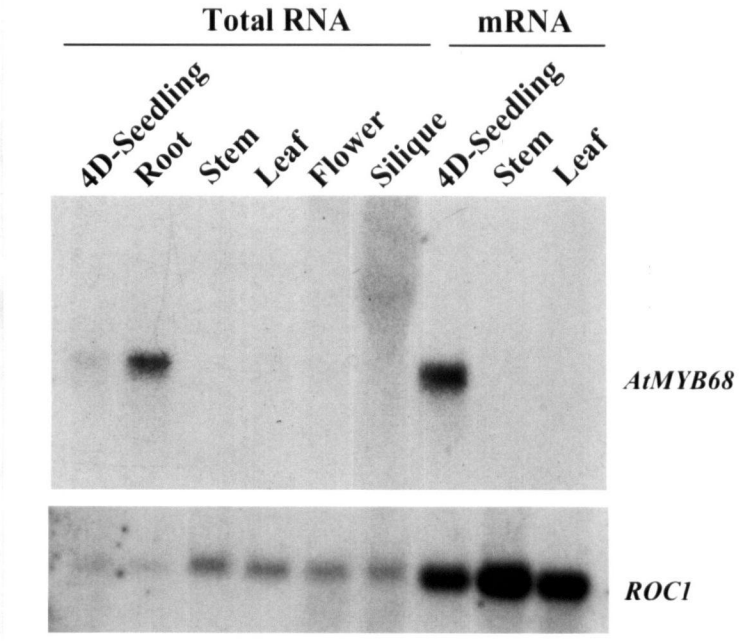

Figure 4-3. Northern Blot Analysis of *AtMYB68* Expression in Arabidopsis.
Total RNA and poly(A)$^+$ were extracted from seedlings and mature organs of Arabidopsis WS ecotype, except that roots were from 16-day old hydroponically grown seedlings. Leaves contained rosette leaves only. The left panel of the blot was loaded with 10 ug total RNA per lane. The right panel was loaded with ~2 ug poly(A)$^+$ RNA per lane. The *ROC1* cDNA (encoding Arabidopsis cytosolic cyclophilin) was hybridized to the same blot as a loading control after the blot was stripped.

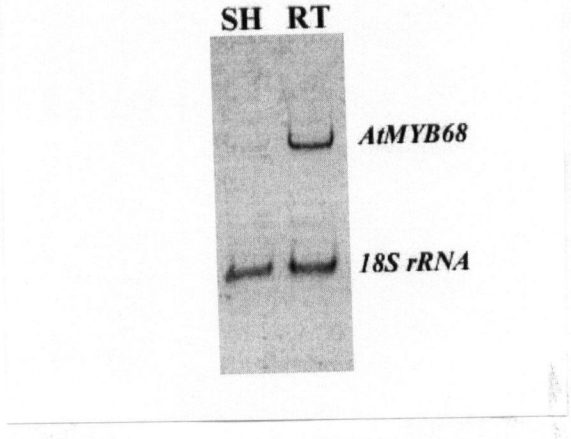

Figure 4-4. RT-PCR Analysis of *AtMYB68* Expression in Arabidopsis Seedlings.
Reverse transcription followed by PCR amplification was performed against total RNA. Total RNA was extracted from shoots and roots of 14-day old hydroponically grown seedlings. 18S ribosome RNA was used as an internal control. SH, shoot. RT, root.

into the pBI121 binary vector (CLONTECH) in place of the *35S* promoter upstream of the *GUS* gene (Figure 2-2-E). The *NPT II* gene in the pBI121 vector provided kanamycin resistance as a selectable marker.

After transformation into *Agrobacterium*, the *AtMYB68::GUS* construct was transformed into Arabidopsis Col plants by the Agrobacterium-mediated floral dip method. T1-generation transformants were selected on kanamycin plates. The transformation rate was ~0.4% (11 out of 3,000 seeds with kanamycin resistance). The kanamycin-resistant T1 plants were allowed to set seeds to generate the T2-generation. GUS activity was examined in the T2 generation. Among 4 independent transgenic lines examined, three lines had the same GUS expression pattern, in which the root was a major site of GUS expression (the other line had strong GUS expression in the hypocotyl). One of the lines had strong GUS expression and contained a single locus with the *AtMYB68::GUS* cassette, indicated by ~3:1 segregation ratio of Kan^R:Kan^S in the T2-generation (data not shown). This line was selected to generate the homozygous line, designated 12-2G, for further tests.

GUS expression driven by the *AtMYB68* promoter was first tested during seedling development. After seeds germinated on plates for 1-2 days, the radicals emerged from seed coats. At this stage, weak GUS staining was visible at and below the shoot-root junction area, apparently in the median stele tissue (Figure 4-5, A). At 3-4 days old, seedlings had two opened green cotyledons. In these seedlings, strong GUS staining was observed through the entire root except the root tip, within the stele tissue. It extended slightly into the hypocotyl (Figure 4-5, B). Two strong staining files adjacent to the xylem vessels were often observed in the upper part of the root (Figure 4-5, E). Close examination of the shoot revealed that GUS staining was also consistently present in the stomata guard cells of the cotyledons (Figure 4-5, C and D). Stained Col wild-type seedlings at the same age were also examined as a control, but no GUS staining was found anywhere in these seedlings (Figure 4-5, F and G).

When the seedling was 7-8 days old, lateral roots were emerging from the primary root. At this stage, GUS staining was seen to decline in the old part of the primary root but still

retained in the young part (as shown in the 2-week old seedling, Figure 4-5, H). As lateral roots were developing, the same GUS staining pattern as in the primary root was repeated in the lateral root (Figure 4-5, H). After emergence of true leaves, GUS staining was observed in the guard cells of young leaves but was absent in the cotyledons and old leaves (data not shown). Strong staining was also seen at the petiole bases of expanding leaves when the seedling reached about 2-week old (Figure 4-5, I). GUS activity was also tested in the mature plants. No staining was observed in any mature organs including rosette leaves, bolting stems, flowers and siliques, except in roots (data not shown).

To further determine the cellular specificity of *AtMYB68* expression, 2-3 days old GUS stained seedlings of line12-2G were embedded in Spurr resin and subjected to sectioning using a microtome. The serial root cross-sections revealed that in general GUS staining was present in the vascular, pericycle and some endodermal cells with a specific expression pattern (Figure 4-6). The staining was light in the section closest to the root tip (Figure 4-6, A). As the sectioning continued toward the older part of the root, it became obvious that the staining was higher in the cells near the two xylem poles (Figure 4-6, B and C). In the section from the upper part of the root, it was clearly shown that the staining became more restricted to the pericycle cells adjacent to the xylem poles (Figure 4-6, C). The endodermal cells adjacent to xylem side pericycle cells had some spotty staining. This was probably due to the weak staining in these large cells. The staining in the vascular parenchyma cells was generally light. At the root-hypocotyl transition area, the staining was mostly restricted to the two pairs of pericycle cells adjacent to the xylem poles (Figure 4-6, D).

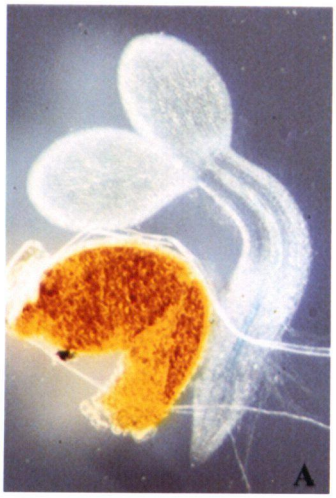
A

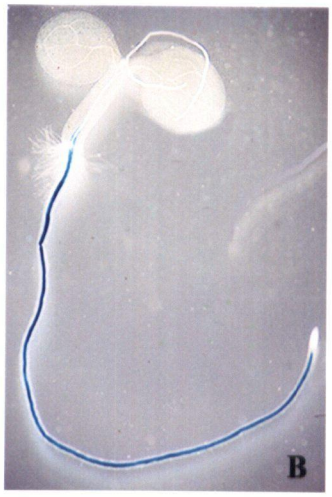
B

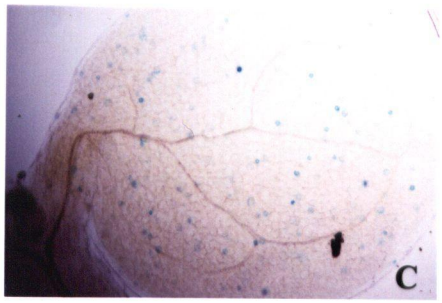
C

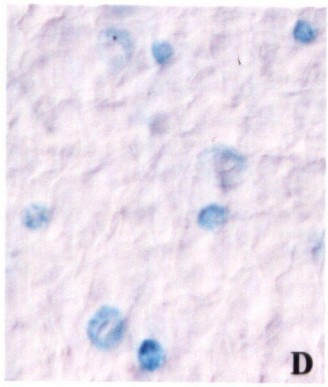
D

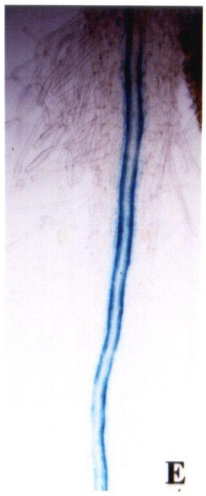
E

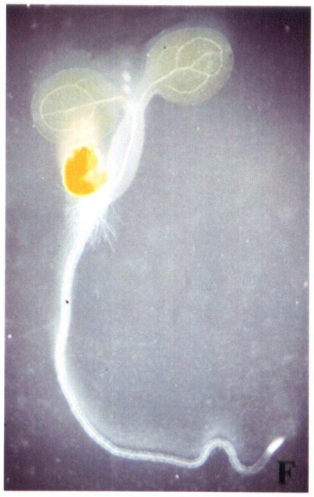
F


G

Figure 4-5. Whole-Mount Histochemical Staining of GUS Driven by the *AtMYB68* Promoter during Seedling Development in Line 12-2G.
GUS staining is shown as a blue color (dark area on the pictures) .
(A) 1-2 days old seedling.
(B) 3-4 days old seedling.
(C) Magnification of one of the cotyledons in (B).
(D) Higher magnification of (C).
(E) Upper part of the root from the 2-3 days old seedling.
(F) GUS stained 3-4 days old Col wild type seedling.
(G) Magnification of one of the cotyledons in (F).
(H) 14-day old seedling.
(I) Magnification of the petiole base region in (H).

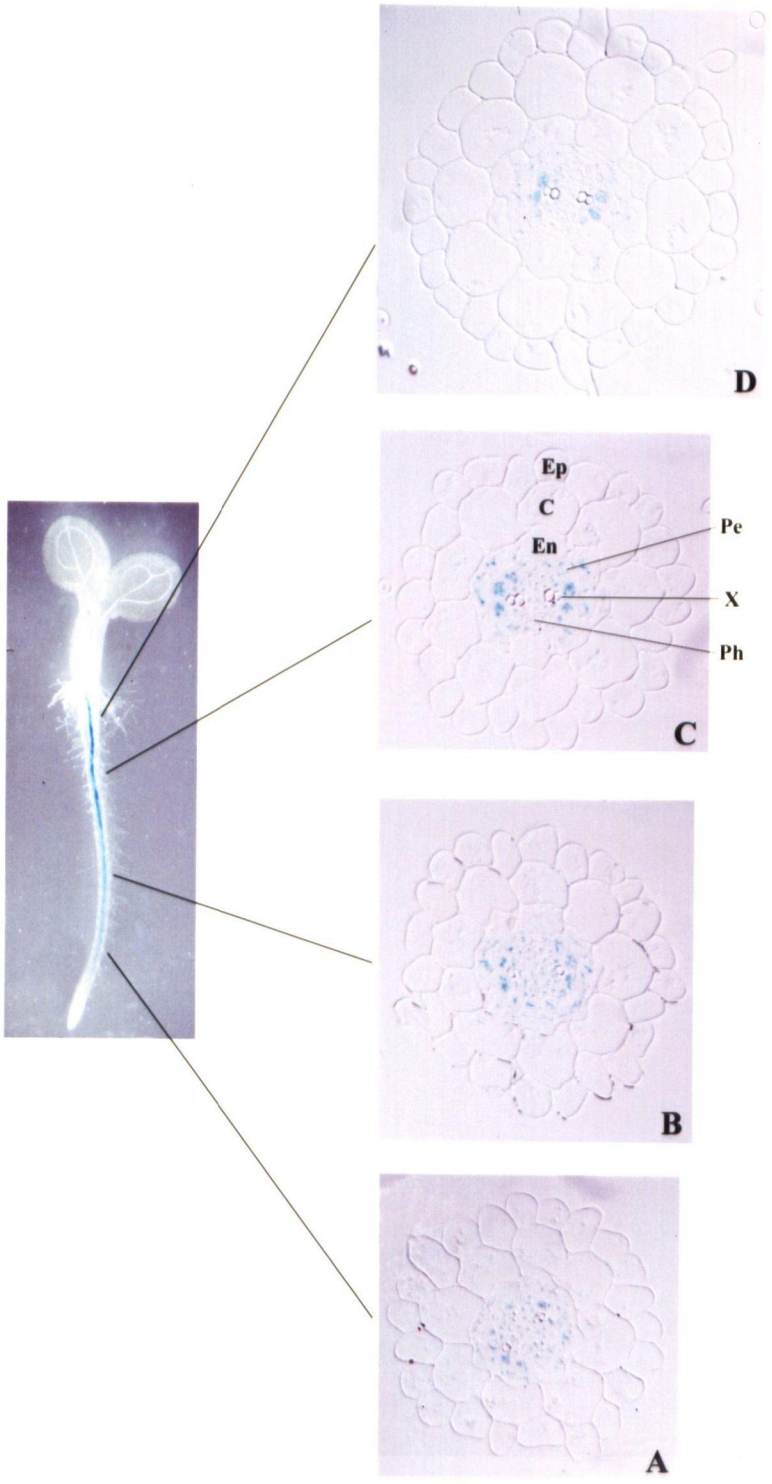

Figure 4-6. Root Cross-Sections of the *AtMYB68::GUS* Line 12-2G.
GUS staining is shown as a blue color (dark area on the pictures). The root was from the 2-3 days old seedling. Sections A to D represent the young part of the root to the root-hypocotyl junction. Ep, Epidermis. C, Cortex. En, Endodermis. Pe, Pericycle. X, Xylem. Ph, Phloem.

4.3 Expression of *AtMYB68* in the *woodenleg* (*wol*) Mutant Background

The histochemical analysis of root cross-sections revealed that expression of *AtMYB68::GUS* was higher in the pericycle cells adjacent to the xylem poles in the old part of the root. This cell type-specific pattern led to these questions: What determines this cell type-specific pattern? Do signals from the xylem specify the expression in the xylem pole pericycle cells? The Arabidopsis root mutant *woodenleg* (*wol*) provides a useful tool to test this hypothesis. In the *wol* mutant, the vascular cylinder in the primary root contains only xylem, lacking phloem (Scheres et al., 1995). By expressing *AtMYB68::GUS* in this mutant background, we would be able to see if the cell type-specific expression of *AtMYB68::GUS* is altered by the presence of the vascular tissue containing only xylem, without the symmetry of xylem poles.

The *AtMYB68::GUS* construct was introduced into the *wol* mutant by crossing the *AtMYB68::GUS* homozygous line 12-2G to the *wol-1* homozygous line. The heterozygous F1-generation plants set seeds to give rise to the F2-generation. In the F2 generation, about one quarter of seedlings (42 out of 190 examined) had the *wol* phenotype, characterized by dramatically reduced root growth. In each mutant and wild type sibling population, about 3 quarters of seedlings (31 out of 41 in the mutants and 11 out of 17 in wild-type siblings) had GUS activity, indicating that the *GUS* transgene and *WOL* segregate independently.

When seedlings were 7-day old, it was easily seen that the *wol* mutants had much shorter primary roots than wild type siblings (Figure 4-7, A and B). In the mutant seedling, GUS staining was generally in the same pattern as in the wild-type sibling used as a control (Figure 4-7, compare A and B). The staining was seen in the stele tissue through the entire root except the root tip and slightly extended to the hypocotyl. In the *wol* background, the staining appeared stronger in the region below the root-hypocotyl junction and the region just basal to the root tip (Figure 4-7, A). In the 15-day old *wol* seedling, adventitious roots had formed (Figure 4-7, C). The primary root of the *wol* mutant is not able to produce normal lateral roots, and such adventitious roots come from the hypocotyl. In contrast to the *wol* primary root, the secondary and later roots have normal vascular tissues (M.-T. Hauser, personal communication). In the *wol*

seedling, strong GUS staining was also present in the secondary roots similarly as in the primary root. As previously observed, the staining decreased in the old part of the primary root as it grew longer (Figure 4-7, C).

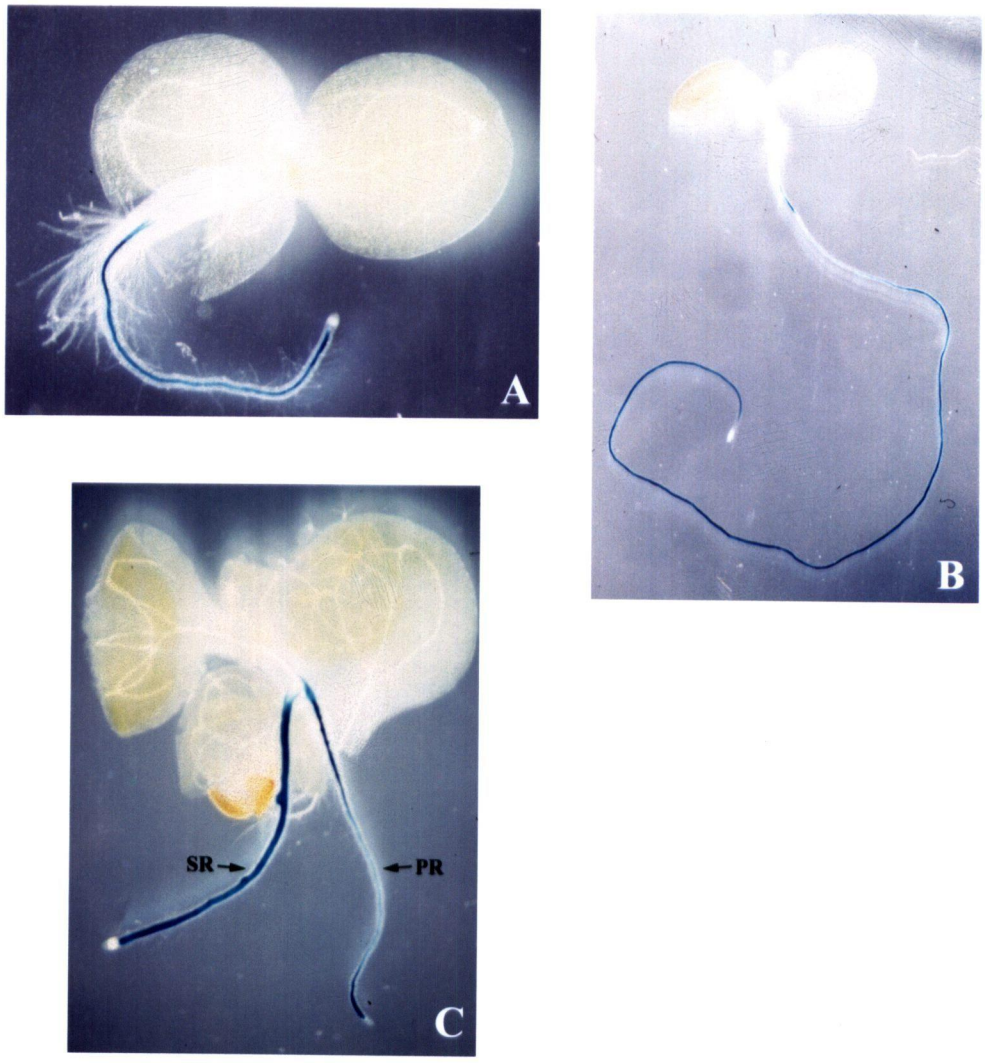

Figure 4-7. Whole-Mount Histochemical Staining of GUS Driven by the *AtMYB68* Promoter in the *woodenleg* Mutant Background.
GUS staining is shown as a blue color (dark area on the pictures).
(A) 7-day old *woodenleg* seedling containing the *AtMYB68::GUS* fusion.
(B) 7-day old wild type sibling.
(C) 15-day old *woodenleg* seedling containing the *AtMYB68::GUS* fusion. PR, primary root. SR, secondary root.

To test if the cell type-specific expression of *AtMYB68::GUS* was altered in the *wol* mutant background, it was necessary to look at the expression at the cellular level. Seven-day old *wol* seedlings harboring the *AtMYB68::GUS* fusion were stained, and then embedded in Spurr resin. These seedlings were subjected to sectioning using a microtome. The serial sections of the *wol* primary root revealed that the expression pattern of *AtMYB68::GUS* was much different from that in the wild type root. In the region just basal to the root tip, the staining was stronger than that in the wild type. Strong GUS staining was observed in all pericycle cells, and eventually extended into the whole endodermal layer as well (Figure 4-8, A and B). It was interesting to see that in the youngest section, GUS staining was also clearly present in the non-lignified xylem parenchyma cells within the vascular tissue (Figure 4-8, A). In the central region of the root, the staining was initially present in both the pericycle and endodermis, but later disappeared from the endodermis and became specific to the pericycle, where it was expressed in all the cells (Figure 4-8, C). At the root-hypocotyl transition region, strong GUS staining in the entire layer of the pericycle was maintained, and was evident again in the endodermal layer (Figure 4-8, D). Taken together, these results show that in the *wol* mutant background, the expression of *AtMYB68::GUS* was strengthened in the entire layer of pericycle cells and expanded to the endodermal layer, and was no longer restricted to the pericycle cells near the xylem poles. This novel expression pattern correlates with the over production of xylem and loss of symmetry (xylem poles) in the *wol* vascular tissue. The result suggests that a positive signal from the xylem (or a negative signal from the phloem) may be responsible for the cell type-specific expression of *AtMYB68::GUS*.

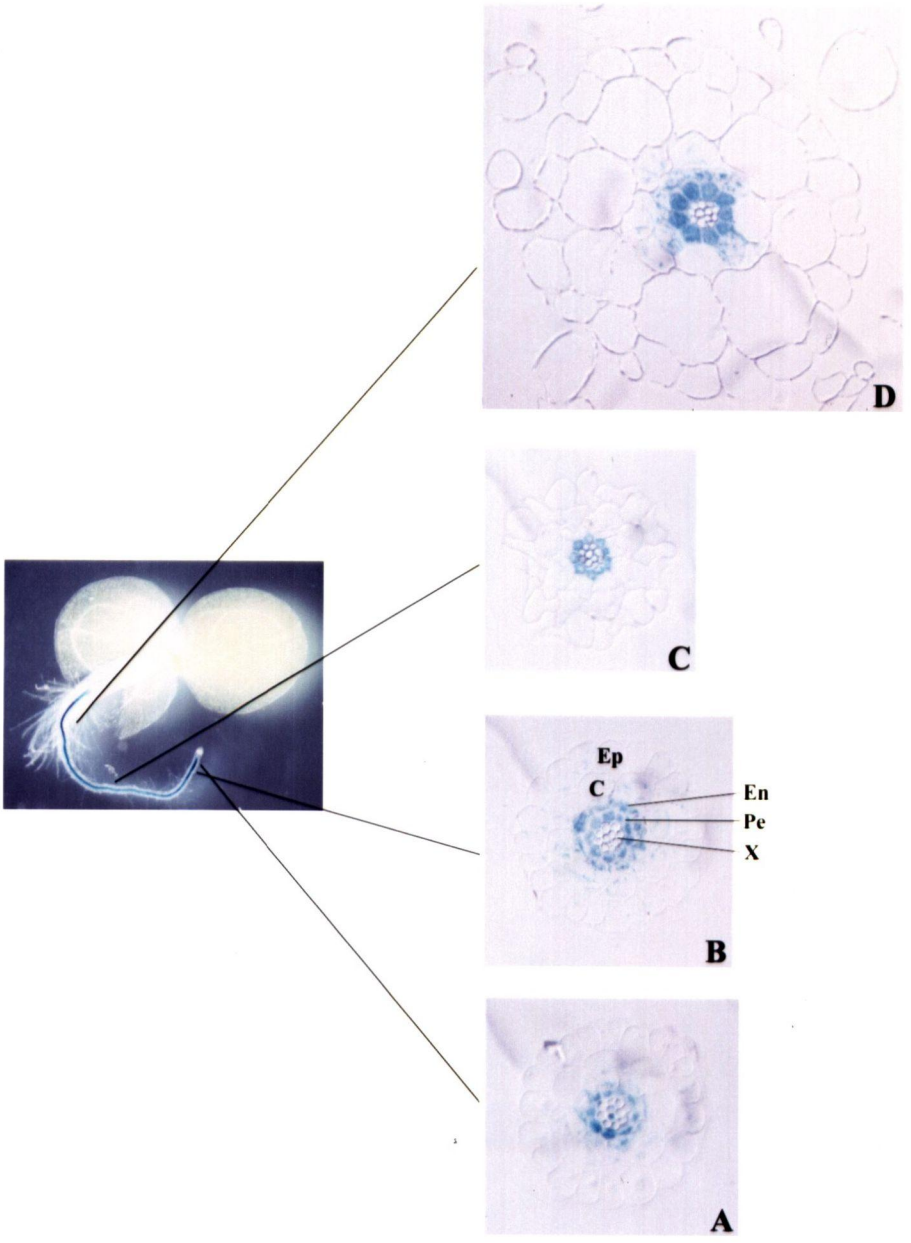

Figure 4-8. Root Cross-Sections of the *woodenleg* Seedling Containing the *AtMYB68::GUS* fusion.

GUS staining was shown as blue color (dark area on the pictures). The root was from 7 day-old seedling. Sections A to D represent the young part of the root to the root-hypocotyl junction. Ep, Epidermis. C, Cortex. En, Endodermis. Pe, Pericycle. X, Xylem. Ph, Phloem.

4.4 Expression of *AtMYB68* in Response to External Stimuli

The pericycle cells, where GUS activity driven by the *AtMYB68* promoter was higher, have a specific function — they serve as founder cells for lateral root formation (Steeves and Sussex, 1989; Charlton, 1991). This led to the question: Is *AtMYB68* related to lateral root formation? To address this question, expression of *AtMYB68* in response to NO_3^- and auxin, two key regulators of lateral root formation, was tested. Meanwhile, *AtMYB68* in response to other major plant hormones was also tested, since plant hormones are important signals in many aspects of plant growth and development. As a first step in functional studies of *AtMYB68*, these tests might give clues to its functions.

The quantitative RT-PCR method was used in examination of *AtMYB68* expression under various external stimuli. Total RNA extracted from whole seedlings was used for reverse transcription followed by PCR amplification with *AtMYB68* specific primers. 18S rRNA primers were also added in the same RT-PCR reaction as an internal control (details described in Chapter 2). The ratio of product intensity of *AtMYB68* to 18S rRNA represented the gene relative expression level. As a preliminary experiment, only one typical concentration and treating time were used for each treatment based on those in the literature.

For the NO_3^- treatment, four-day old Col seedlings grown without NO_3^- were treated with 2 mM KNO_3 for 6 hours. The RT-PCR analysis showed that the level of the *AtMYB68* transcript remained stable when seedlings were treated with NO_3^- (Figure 4-9, A).

For the plant hormone treatments, eight-day old Col seedlings were treated with IAA (a natural auxin), BAP (a synthetic cytokinin), GA_3 (gibberellic acid), ABA (abscisic acid) or ACC (a precursor of ethylene) for 6 hours. Except IAA, used at 10 μM, the other hormones were used at 100 μM in the media. RT-PCR analyses showed that accumulation of the *AtMYB68* transcript was down-regulated 2-fold by the IAA treatment, and up-regulated 3-fold by the ABA treatment, as compared to the untreated control respectively. With the other hormone treatments (BAP, GA_3

or ACC), accumulation of the *AtMYB68* transcript remained at a stable level (Figure 4-9, B). These results were repeated in two independent experiments.

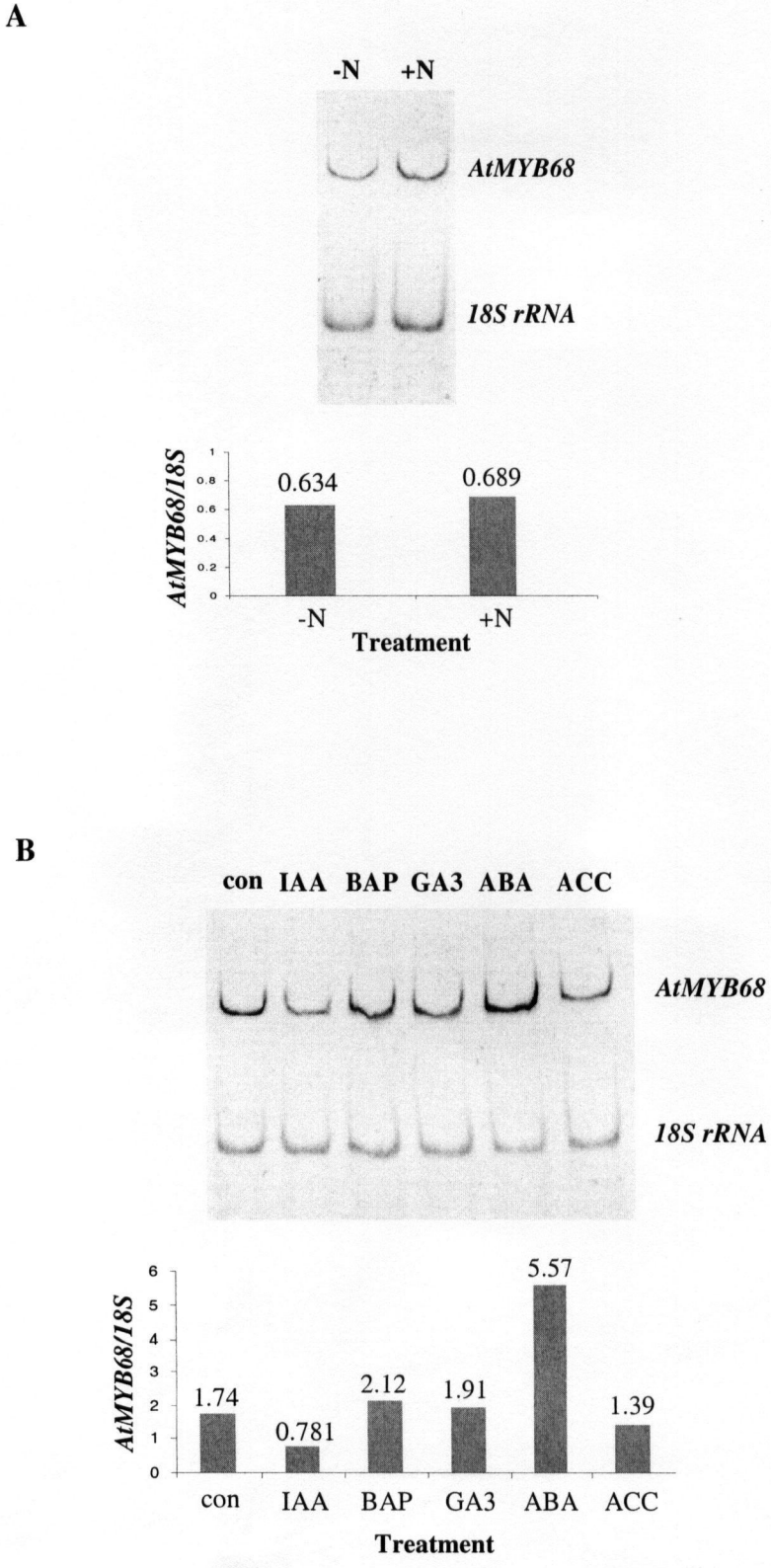

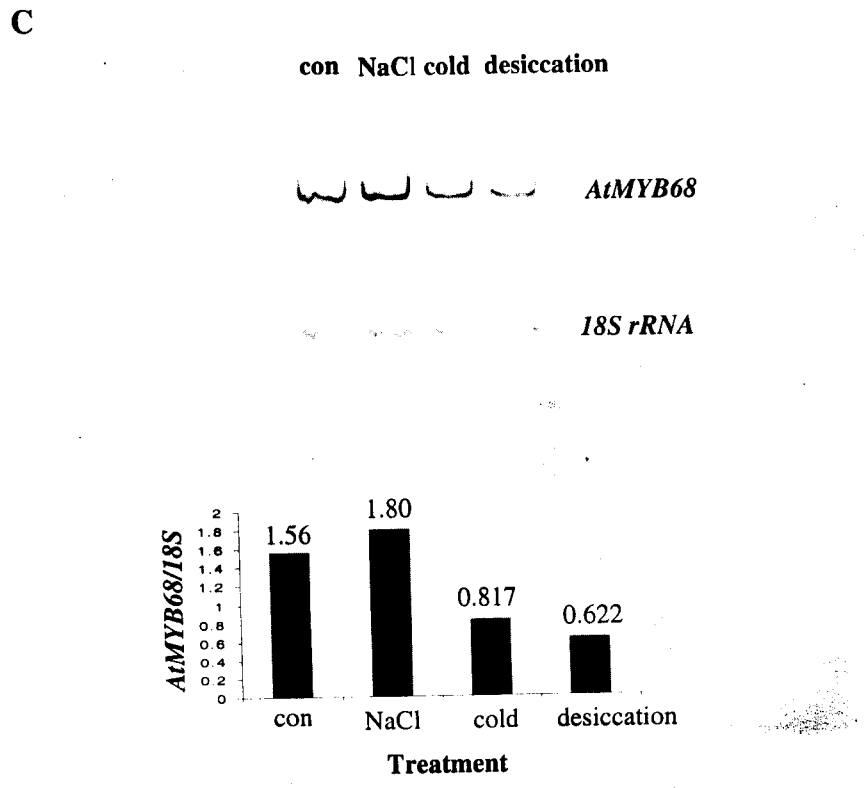

Figure 4-9. RT-PCR Analysis of *AtMYB68* Expression in Response to External Stimuli. Reverse transcription followed by PCR amplification was performed against total RNA. Total RNA was extracted from whole seedlings after treatments. 18S ribosome RNA was used as an internal control. The ratio of the intensity of *AtMYB68* to 18S rRNA represented the relative *AtMYB68* mRNA level. The ratios were visualized by bar graphs in the lower panel and values are shown above each bar. RT-PCR reactions were performed at least twice for each treatment to assess reproducibility in quantification. The results were consistent. One of them is shown here.
(A) 4-day old seedlings grown hydroponically in absence of NO_3^- were treated with 2mM KNO_3 for 6 hours (+N). –N, untreated sample.
(B) 8-day old seedlings grown hydroponically were treated with various plant hormones for 6 hours. The concentration of hormones was 100 μM except IAA in 10 μM. The control was in the medium without adding hormones (con).
(C) 7-day old seedlings grown hydroponically were treated with abiotic stresses. The seedlings were treated with 200 mM NaCl for 6 hours (NaCl), put in 4°C for 24 hours (cold), or left on Whatman paper on the lab bench for 30 minutes (desiccation), respectively. The control was grown under normal conditions (con).

The inducible expression of *AtMYB68* by ABA suggested that *AtMYB68* might be related to stress responses, since ABA plays primary regulatory roles in plant response to stress. To test this speculation, expression of *AtMYB68* in response to abiotic stresses, in particular, desiccation, cold, and salinity conditions was examined further. For the cold treatment, seven-day old Col seedlings were transferred to 4^0C for 24 hours. For the desiccation treatment, the seedlings from the same batch were put on Whatman paper for 30 minutes to induce dehydration. For the salinity treatment, the seedlings from same batch were treated with 200 mM NaCl for 6 hours. RT-PCR analyses showed that the level of the *AtMYB68* transcript was down-regulated 2-3 fold by the cold and the desiccation treatments respectively, as compared to the untreated control. The salinity treatment did not significantly change the level of the *AtMYB68* transcript (Figure 4-9, C).

4.5 Expressing AtMYB68 Recombinant Protein and Raising AtMYB68 Antiserum

To verify that the cell type-specific expression of *AtMYB68::GUS* represents native *AtMYB68* expression, the *in situ* hybridization technique was used. Unfortunately, with paraffin sectioning, sections with intact root morphology beyond the root tip region could not be obtained. Other sectioning methodologies that could preserve mature root anatomy were then considered. LR Gold™ plastic sectioning has been successfully used in protein immunolocalization (Samuels et al., 2002). This encouraged me to use this embedding technique combined with immunolocalization to detect localization of native gene expression. In order to do protein immunolocalization for AtMYB68, an AtMYB68 antibody was needed. This antibody would also be useful to detect protein expression levels in gene over-expression lines in functional studies.

To raise an AtMYB68-specific antibody, a truncated AtMYB68 recombinant protein was produced in *E. coli*. To avoid producing antibodies that might cross-react with the conserved MYB domain, the 3' region of *AtMYB68* cDNA, derived from the full-length cDNA clone, was

fused in-frame to the pQE-30 expression vector (QIAexpressionist™). This placed an additional 24 amino acids, including a 6×histidine-tag, prior to the amino-terminus of the truncated AtMYB68 (Figure 2-2-D). The 6×histidine-tag would be useful for the recombinant protein purification. This plasmid was transformed into *E. coli*, and a high level of the recombinant protein was produced upon IPTG induction. The recombinant protein was purified through Ni-NTA resin. The predicted size of the AtMYB68 recombinant protein was 31.4 kDa.

Figure 4-10 shows expression of the AtMYB68 recombinant protein in *E. coli* and the purification process. The cell lysate from the *E. coli* strain containing the empty vector was used as a control (lanes 1 and 2). Upon 1 mM IPTG induction, in the total lysate from the *E. coli* strain containing the *AtMYB68* cDNA insert, a product of about the predicted size was clearly seen (indicated by arrow in lane 4 (protein extracted at a small-scale), and lane 5 (protein extracted at a large-scale)). The *E. coli* cell lysate was passed through a Ni-NTA column for purification. The recombinant protein bound to the column and absent in the flow-through fraction (lane 6), and in the wash fraction (lane 7). With a low pH elution (pH 5.9), the recombinant protein was eluted (lane 8), and it was more abundant in a lower pH elute fraction (pH 4.5). Some carboxyl-terminal truncated recombinant proteins were also produced and eluted in this fraction (shown as smaller sizes, lane 9). The average yield of the purified recombinant protein from one liter *E. coli* culture was about 9 mg calculated by the Bradford method.

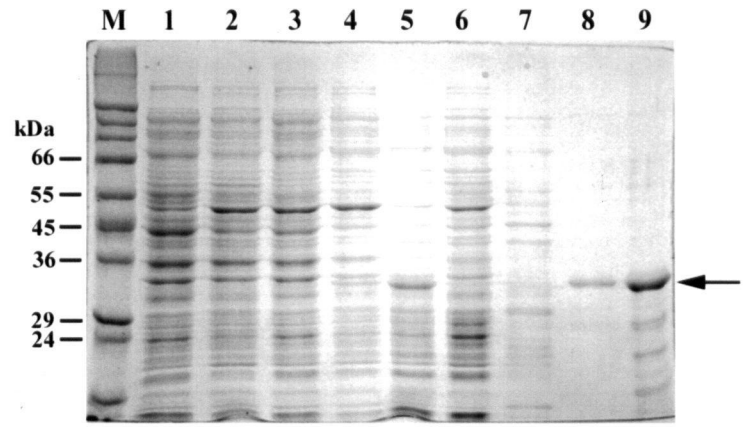

Figure 4-10. SDS-PAGE Analysis of AtMYB68 Recombinant Protein Expressed in *E. coli* and Recombinant Protein Purification.
The *AtMYB68* cDNA encoding the non-conserved region was put into the pQE-30 expression vector. Proteins in lane 1 to lane 4 were prepared at a small-scale. Proteins in lane 5 were prepared at a large-scale. Lane 1, cell lysate from the *E. coli* strain containing the empty vector (IPTG absent). Lane 2, cell lysate from the *E. coli* strain containing the empty vector (IPTG present). Lane 3, cell lysate from the *E. coli* strain containing the *AtMYB68* cDNA insert (IPTG absent). Lane 4 and 5, cell lysate from the *E. coli* strain containing the *AtMYB68* cDNA insert (IPTG present). Lane 6, fraction of flow-through Ni-NTA column. Lane 7, wash fraction. Lane 8, elution fraction at pH 5.9. Lane 9, elution fraction at pH 4.5. The arrow indicates the AtMYB68 recombinant protein. M, marker lane with sizes shown at left.

The purified AtMYB68 recombinant protein (pH 4.5 fraction) was used to immunize two rabbits. The anti-sera from both showed similar reactions to the purified recombinant AtMYB68 and *E. coli* crude extracts. Characterization of the AtMYB68 antibody by western blot analyses from one is shown here. First, the pre-immune serum was tested for cross-reactions on the western blot shown in Figure 4-11-A. This blot shows that the pre-immune serum did not react with the recombinant AtMYB68 from either the purified fraction (lane 1), or the *E. coli* total lysate (lane 3). It very slightly reacted with a few other proteins from *E. coli* total lysates (lane 2 from the strain containing the empty vector, and lane 3 from the strain containing the *AtMYB68*

insert). It also reacted with a small number of proteins from Arabidopsis shoot and root extracts (lanes 4 and 5).

The AtMYB68 antiserum from immunized rabbits was then tested on a western blot shown in Figure 4-11-B. This blot showed that the AtMYB68 antiserum reacted strongly with proteins of about the predicted size (close to 29 kDa, indicated by arrow) from both the purified fraction (lane 1), and the *E. coli* total lysates (lane 2 (IPTG absent), and lane 3 (IPTG present)). However it also cross-reacted with many other proteins in these preparations. The AtMYB68 antiserum also detected a number of proteins from Arabidopsis shoot and root extracts (lanes 4 and 5).

Cross-reactions of the AtMYB68 antiserum with many other proteins from both *E. coli* and Arabidopsis made it impossible to use in immunodetection. To purify an AtMYB68 antibody from the antiserum, antigen-Sepharose affinity methodology was used as described in Chapter 2. The purified AtMYB68 antibody was tested by the western blot shown in Figure 4-11-C. In general, the purified antibody detected much less background. It detected a single major band of the purified recombinant AtMYB68 (lane 1), and the major band of the recombinant AtMYB68 from the total lysate of the *E. coli* strain containing the *AtMYB68* cDNA insert (lane 3). The purified antibody did not react with any proteins in the *E. coli* strain containing the empty vector (lane 2). In the Arabidopsis shoot extract, one major band of ~43 kDa in size was detected by the AtMYB68 antibody (lane 4). This size was very close to the predicted size of 42 kDa for the AtMYB68 native protein. Surprisingly, however no bands were clearly detected from the Arabidopsis root extract (lane 5). This result was repeatedly seen with the AtMYB68 antibody using independent protein extracts and blots. This was an unexpected result due to its inconsistency with either northern or RT-PCR analyses, which showed that the *AtMYB68* transcript was mainly accumulated in the root but not the shoot (Figure 4-3 and 4-4).

There were several possibilities for this anomalous result. The most likely was the AtMYB68 antibody recognized another protein from the shoot. Later, an *atmyb68* knockout line, Garlic 94B-18, was identified. In this knockout line, the *AtMYB68* transcript was not detectable

(Chapter 5). Thus, the AtMYB68 protein was not expected to be detectable either. This knockout line provided a simple way to test if the anti-AtMYB68 signal from the shoot was an artifact. Protein extracts from shoots and roots of both Col and the knockout homozygous line (94B-18) were prepared. A western blot analysis of these extracts clearly showed that the signals detected by the AtMYB68 antibody were present in both wild type and the knockout shoot extracts. There was no difference in proteins detected in both root extracts either (Figure 4-12). From this, I conclude that the AtMYB68 antibody detected a non-AtMYB68 protein in the Arabidopsis shoot, and failed to detect AtMYB68 in the root. The antibody thus was not able to be used for the protein immunolocalization experiment.

Figure 4-11. Western Blot Analysis of Protein Extracts from *E. coli* and Arabidopsis Seedlings. Protein preparations were separated on SDS-PAGE then blotted on PVDF membranes. Signals were detected by the ECL Plus system then visualized by exposure to an x-ray film.
(A) The pre-immune serum was used as a probe. Lane 1, purified AtMYB68 recombinant protein (~0.05 μg). Lane 2, cell lysate from the *E. coli* strain containing the empty pQE-30 vector. Lane 3, cell lysate from the *E. coli* strain containing the *AtMYB68* cDNA insert. Lane 4, crude protein extract from 10-day old Arabidopsis seedling shoots (10 μg). Lane 5, crude protein extract from roots of the same seedlings (10 μg).
(B) The AtMYB68 Antiserum was used as a probe. Lane 1, purified AtMYB68 recombinant protein (~0.1 μg). Lane 2, cell lysate from the *E. coli* strain containing the *AtMYB68* cDNA insert (IPTG absent). Lane 3, cell lysate from the *E. coli* strain containing the *AtMYB68* cDNA insert (IPTG present). Lane 4, crude protein extract from 10-day old Arabidopsis seedling shoots (10 μg). Lane 5, crude protein extract from roots of the same seedlings (10 μg). The arrow indicates the AtMYB68 recombinant protein position.
(C) The purified AtMYB68 antibody was used as a probe. Lane 1, purified AtMYB68 recombinant protein (~0.1 μg). Lane 2, cell lysate from the *E. coli* strain containing the empty pQE-30 vector. Lane 3, cell lysate from the *E. coli* strain containing the *AtMYB68* cDNA insert. Lane 4, crude protein extract from 10-day old Arabidopsis seedling shoots (10 μg). Lane 5, crude protein extract from roots of the same seedlings (10 μg).
Protein marker sizes are shown at left.

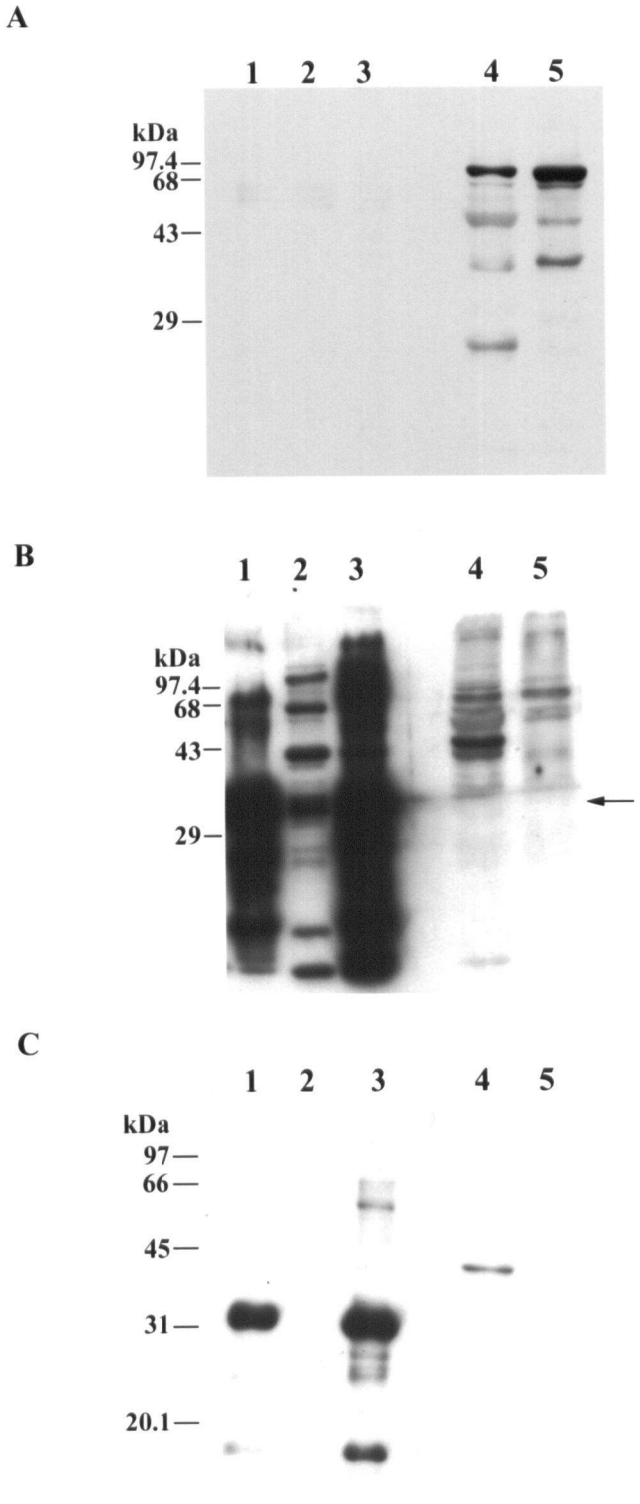
A
1 2 3 4 5
kDa
97.4
68
43
29
B
1 2 3 4 5
kDa
97.4
68
43
29
C
1 2 3 4 5
kDa
97
66
45
31
20.1

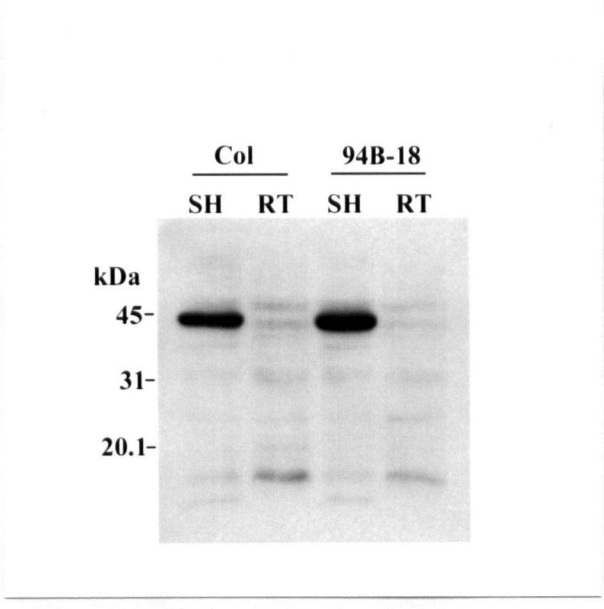

Figure 4-12. Western Blot Analysis of Protein Extracts from an *atmyb68* Knockout Line and Wild Type Seedlings.
Protein crude extracts were from shoots (SH, 15 μg) and roots (RT, 20 μg) of 8-day old hydroponically grown Col and the *atmyb68* knockout line (94B-18). The purified AtMYB68 antibody was used as a probe. Signals were detected by ECL Plus system then visualized by exposure to an x-ray film. Protein marker sizes are shown at left.

4.6 Discussion

As the first step toward understanding the function of *AtMYB68* in Arabidopsis growth and development, expression profiles of *AtMYB68* were generated. At the organ level, both northern and RT-PCR analyses showed that the *AtMYB68* transcript predominantly accumulated in the Arabidopsis root. This result is partially consistent with a previous study (Kranz et al, 1998). In that study, the *AtMYB68* transcript was detected in the root but also in the mature leaf.

However, the reverse northern method used in that study can have cross-hybridization problems. MPSS (defined in Section 3.5) data also shows that the level of the *AtMYB68* transcript was the highest in the root. However, it did not show expression in shoots of the same age as I used in the RT-PCR analysis, other than expression was detected in immature flowers. Since MPSS is a quite new technique, I do not know how to explain this discrepancy. So far no other functionally characterized plant *MYB* gene has been reported to have the same organ-specific expression pattern as *AtMYB68*.

At the tissue/cellular level, GUS activity driven by the *AtMYB68* promoter was stronger in a unique and specialized cell type in the root, the pericycle cells adjacent to the xylem poles. In this study, the GUS reporter gene fused to the *AtMYB68* promoter was used to show the *AtMYB68* transcript at the tissue and cell level. It is worth noting that this project started before the Arabidopsis genome project was completed. At the time I followed general procedures and took a 1.9 kb promoter for a fusion to *GUS* gene. Now we know that the distance from the 5' end of the *AtMYB68* ORF to the stop codon of the previous gene is 4450 bp, so that additional information specifying *AtMYB68* expression could be located in this region. However, the GUS activity data is consistent with the northern and RT-PCR data on accumulation of the *AtMYB68* transcript. All these lines of data showed that the root was the major site of *AtMYB68* expression, and that *AtMYB68* was expressed much less in small groups of cells in the shoot. These results suggest that the *AtMYB68::GUS* fusion reflects the site of *AtMYB68* expression.

It certainly would be good to examine endogenous *AtMYB68* expression at the cell level to confirm the GUS data. Therefore I intended to do *in situ* hybridization. However, for paraplast sectioning, sections with intact root morphology beyond the root tip could not be obtained, since the big cells in the outer layers of the root were too fragile for the xylene treatment. The other sectioning method for *in situ* hybridization, cryosectioning, would be another choice, but the equipment for this technique was not available until recently in the department.

As an alternative to *in situ* hybridization, I also tried to raise an antibody against the recombinant AtMYB68 to do protein immunolocalization. However the antibody raised

apparently strongly cross-reacted to another Arabidopsis protein rather than recognizing native AtMYB68. In the entire Arabidopsis genome, the closest member to AtMYB68 is AtMYB84. However it did not appear that the antibody cross-reacted to AtMYB84, since the transcript of *AtMYB84* accumulated universally at a very low level in all tissues/organs tested (Chapter 5). The signal detected by the AtMYB68 antibody was quite strong and shoot-specific. It is not known what the AtMYB68 antibody reacted to. One would easily suspect that the cDNA cloned into the pQE-30 expression vector was not *AtMYB68*. However this can be excluded, since the 3' cDNA fragment was released directly from the *AtMYB68* full length cDNA clone by restriction enzyme digestion, and the *AtMYB68*-pQE30 clone was confirmed by sequencing.

In response to various external stimuli, the level of the AtMYB68 transcript was up-regulated by ABA, and down-regulated by IAA, cold and desiccation treatments, but the magnitude of changes was not great. In these initial experiments, I only tested one stimulus concentration at one time point for each treatment. It is possible that these do not represent the optimal conditions to show maximal changes. Thus, further experiments with different concentrations and with time courses are required. Another point is that total RNA from the whole seedling is used for the RT-PCR analysis. However the *AtMYB68* transcript mainly accumulates in the root. It would be worth while to examine changes in *AtMYB68* expression in the shoot and root separately.

Many ABA-responsive genes have a highly conserved sequence, PyACGTG(T/G)C, named the ABA-responsive element (ABRE) in the promoter regions (Giraudat et al., 1994; Shinozaki and Yamaguchi- Shinozaki, 2000). Another type of ABRE, known as coupling element, *hex3* or *motif III* containing the core sequence CGCGTG has also been identified (Busk and Pages, 1998). However, neither type of ABREs was found in the 1.9 kb promoter region of *AtMYB68* or further upstream. Another Arabidopsis *MYB* gene *AtMYB2* is also up-regulated by exogenous ABA, and by drought and high salinity treatments. No ABREs are found in the promoter of *AtMYB2* either (Urao et al., 1993).

My expression data gave some insights on possible functions of AtMYB68 and a mechanism that regulates *AtMYB68* expression.

(1) One possible role of AtMYB68. The cell-preferential GUS activity driven by the *AtMYB68* promoter leads to the speculation that AtMYB68 might be related to lateral root formation, since in root development, the pericycle cells adjacent to the xylem poles serve as progenitors for lateral root formation (Steeves and Sussex, 1989; Charlton, 1991). Several cyclin and cyclin-dependent kinase gene promoters driving GUS activity are also detected in pericycle cells, or the cells adjacent to the xylem poles. For example, the Arabidopsis cyclin gene *CycA2;1*, and *cdc2a*, a gene encoding the catalytic subunit $p34^{cdc2}$ of the cyclin-dependent kinase (Burssens et al., 2000; Hemerly et al., 1993). The expression of these cell cycle related genes in this cell type is thought to mark competency for cell division. It is interesting to see that these cell cycle related genes, such as *CycA2;1*, *cyc1a* (*CycB1;1*) and *cdc2a* are also expressed in the stomata guard cells of young leaves, which is similar to that of *AtMYB68* (Burssens et al., 2000; Serna and Fenoll, 1997). The expression of these cell cycle related genes in the stomata guard cells is also thought to mark them for cell totipotency (Serna and Fenoll, 1997).

The similarity of *AtMYB68* cell-type expression with that of cell cycle related genes suggests that AtMYB68 might be related to cell competence for division or cell cycle status. Since GUS activity driven by the *AtMYB68* promoter declined in the upper part of the root, where lateral roots were producing, and was only retained in the lower part of the root, one possibility would be that AtMYB68 is a factor that blocks the cells from re-entering the cell cycle before conditions are ready. When a signal, such as auxin is present at a proper concentration, AtMYB68 could be down-regulated allowing the cells to undergo cell division. However, no clear separation between the site of lateral root primordium emergence and the region of expression of *AtMYB68::GUS* was observed. Given that GUS is a quite stable protein, the GUS pattern may not reflect the real turnover time of AtMYB68. Using GFP tagged AtMYB68 may be better to show the dynamic accumulation of AtMYB68. Although the MYB-binding site has been found in the promoter of the Arabidopsis *CycB1;1* gene (Ito et al., 2001;

Planchais et al., 2002), so far there is no clear evidence to show that any R2R3-type MYB proteins are involved in regulating the cell cycle.

Among two key regulators of lateral root formation examined, the level of the *AtMYB68* transcript was only down-regulated in response to exogenous IAA but not responsive to NO_3^- treatment. This result could be explained by the fact that IAA and NO_3^- affect different stages of lateral root development. Auxin is thought to represent an important factor for lateral root initiation. A threshold concentration of auxin is required for the xylem pole pericycle cells to enter the cell cycle and initiate lateral root development (Casimiro et al., 2001). In contrast, the effect of NO_3^- on lateral root formation affects elongation of emergent lateral roots (Zhang et al., 1999). The down-regulation of *AtMYB68* expression by IAA suggests that *AtMYB68* may be related to initiation of lateral root formation.

The induction of *AtMYB68* expression by ABA could be a part of the mechanism to prevent those competent cells from dividing before conditions are appropriate. ABA inhibition of cell division has been reported (Newton, 1977; Robertson et al., 1990). This inhibition effect might be accomplished by ABA induced expression of the cyclin-dependent kinase inhibitor *ICK1* gene (Wang et al., 1998).

(2) Does the xylem send a signal to determine the cell specificity? Only the pericycle cells adjacent to the xylem poles appear to receive a signal to initiate lateral root formation. However, it is not clear what determines these cells' specialization. Since positional cues produce important signaling in root development (Scheres, 1997), I wished to see if the xylem plays a role in xylem pole pericycle cell differentiation, using expression of *AtMYB68::GUS* as a marker. I demonstrated that cell type-preferential expression of *AtMYB68::GUS* was indeed changed with the altered xylem pattern in the *wol* background. With the xylem produced throughout the root vascular tissue in the *wol* mutant, the expression of *AtMYB68::GUS* was expanded to the entire layer of pericycle cells, where it appeared stronger than that in the wild-type background, and also expanded to the endodermal layer. This result provides evidence that gene expression in these xylem pole pericycle cells is responsive to a positive signal from the

xylem (or alternatively a negative signal from the phloem). However, the link is between *AtMYB68* expression and these cells' role as lateral root founder cells is not known yet. It is also not clear what signal is coming from the root vascular tissue.

(3) Other possible roles for AtMYB68. Apparently, the xylem pole pericycle cells have multiple functions since genes known with different functions are expressed in these cells. One example is the *SOS1* gene. The *SOS1* promoter driving *GUS* expression is more active in the pericycle cells near the xylem poles and the parenchyma cells surrounding the xylem vessels. *SOS1* encodes a Na^+/H^+ antiporter located on the plasma membrane. The role of SOS1 in the cells surrounding the xylem is proposed to load and unload extra Na^+ to the xylem for long-distance transport (Shi et al., 2002).

At the organ level, *AtMYB68* had a root-preferential expression pattern. Expression profiles of 402 potentially stress-related transcription factors, including 121 *MYB* genes from Arabidopsis have revealed that ~15% of these transcription factors are preferentially or specifically expressed in the root, compared with only 6% that are leaf specific. Fifty percent of these root-specific/preferential transcription factors are induced after different types of biotic and abiotic stress treatments (Chen et al., 2002). This data suggests a strong correlation between root-specific/preferential transcription factors and stress responses.

The level of the *AtMYB68* transcript was mostly up-regulated by ABA among the plant hormone treatments. ABA is known to play a primary regulatory role in the plant response to stress. The endogenous ABA level is usually increased to trigger protective or adaptive responses under adverse environment conditions (Zeevaart and Creelman, 1988; Leung and Giraudat, 1998). Many stress-inducible genes are also responsive to ABA (Bray, 1997; Shinozaki and Yamaguchi-Shinozaki, 2000). Expression profiles of 7,000 Arabidopsis genes treated by ABA, drought, cold and high-salinity have shown that there is a distinct set of induced genes upon each treatment, but there are also overlaps between genes induced by different treatments (Seki et al., 2002). The induction of *AtMYB68* expression by ABA also suggests that AtMYB68 might be related to stress responses.

Therefore I further tested expression of *AtMYB68* in response to some abiotic stresses. The down-regulation of *AtMYB68* expression by both desiccation and cold, and the stable level of *AtMYB68* expression upon high salinity, were in contrast to the up-regulation by exogenous ABA. This result suggests that the role of ABA in regulating *AtMYB68* expression is distinct from that of these stresses. The down-regulation of *AtMYB68* expression by desiccation and cold could be a secondary response, as the plant generally slows metabolism under these adverse conditions.

Certainly, it is too early to deduce *AtMYB68* function only from its expression profiles. More evidence is needed from other approaches, which is the purpose of experiments reported in the next chapter.

Chapter 5 *AtMYB68*: a Root Preferentially Expressed *MYB* Gene — Functional Studies

5.1 Introduction

As reviewed in Chapter 1, when gene sequence information is available, reverse genetic approaches, based on T-DNA or transposon insertion mutagenesis, or TILLING (Targeting Induced Local Lesions in Genomes), are possible for a functional analysis. These have been demonstrated to be very useful for Arabidopsis *MYB* gene functional studies, although functions of several *MYB* gene were characterized by the traditional forward genetic approach (Meissner et al., 1999; Penfield et al., 2001; Jin et al., 2000). Another common method for producing loss-of-function mutations in plants, using antisense RNA or RNAi to suppress gene expression, has been also used in the *MYB* gene functional analysis (Vailleau et al., 2002). In the case of genes with redundant functions, producing gain-of-function mutations is another way to reveal gene function. This has also been used successfully in Arabidopsis *MYB* gene functional characterization (Borevitz et al., 2000).

In this chapter, I describe attempts to reveal *AtMYB68* function by disrupting its expression, expressing *AtMYB68* under the control of the 35S promoter, repressing the expression by antisense RNA and searching for insertion mutations in T-DNA tagged populations.

5.2 Overexpression of *AtMYB68* under the Control of the *CaMV 35S* Promoter

To create *AtMYB68* overexpression lines, the full-length *AtMYB68* cDNA of ~1.3 kb in size was inserted behind the *35S* promoter in the sense orientation in the pRT101 vector (Figure 2-2-B). The *35S::AtMYB68* cassette was then cloned into the BIN19 binary vector. After transformation into *Agrobacterium*, the *35S::AtMYB68* construct was transformed into Arabidopsis Col plants by the *Agrobacterium*-mediated floral dip method. The *NPT II* gene in

the BIN19 vector provided kanamycin-resistance as a selectable marker. T1-generation transformants were selected on kanamycin plates. The transformation rate was ~0.2% (15 out of 8,000 with kanamycin-resistance). Kanamycin-resistant T1 plants were allowed to set seeds to generate the T2-generation.

The levels of the *AtMYB68* transcript in *35S::AtMYB68* transgenic lines was detected by a northern blot analysis. The first round of detection was performed in the T2 generation. Total RNA was extracted from T2 kanamycin-resistant seedlings. Figure 5-1-A shows that *35S::AtMYB68* was expressed in all the 12 lines tested. Two transcripts with different sizes were detected. They were apparently caused by two transcription terminators in the transgene. The short transcript was likely due to termination at the internal terminator within the *AtMYB68* cDNA. The long one was likely due to termination at the external 35S polyA terminator within the pRT101 vector. The native *AtMYB68* transcript (observed in Col) was similar in size to the short one from the *35S::AtMYB68* transgene. *AtMYB68* co-suppression lines were not found in these 12 lines based on the northern blot analysis.

Homozygous lines with the *35S::AtMYB68* construct were selected from 3 transgenic lines. A northern analysis of the transcript levels of *AtMYB68* in the homozygous lines is shown in Figure 5-1-B. Total RNA was extracted from whole seedlings for this analysis. The blot showed that *35S::AtMYB68* was expressed at different levels in these 3 homozygous lines. Line 9-3 had the highest expression level followed by lines 6-4 and 15-1. Line 9-3 was selected for phenotypic examination as presented later.

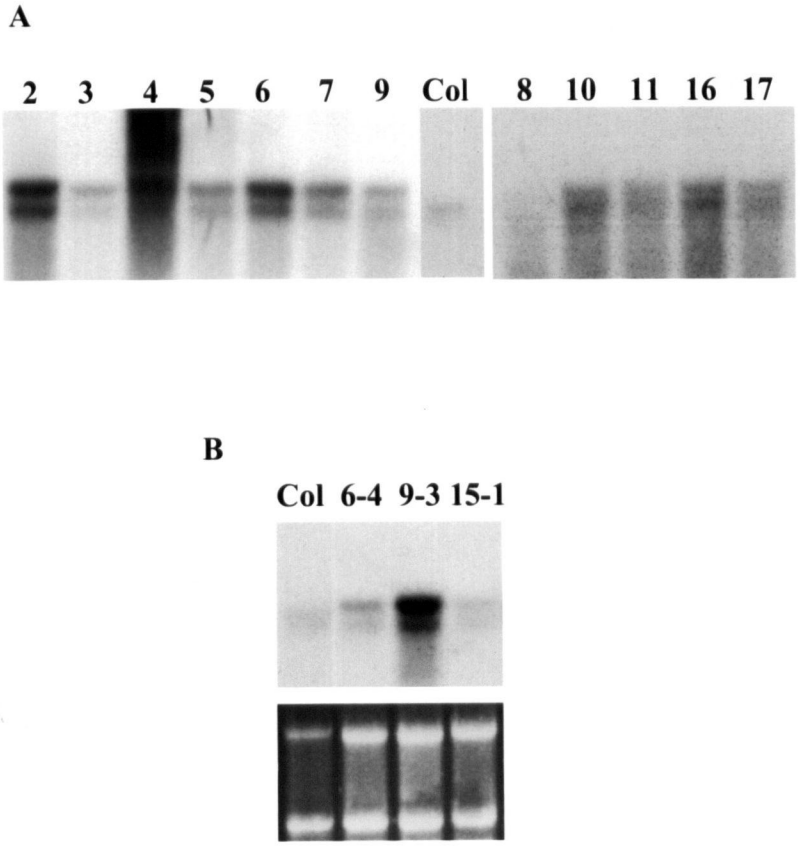

Figure 5-1. Northern Blot Analysis of *AtMYB68* Expression in *35S::AtMYB68* Transgenic Lines.
(A) *AtMYB68* expression in T2-generation plants. Total RNA was extracted from 18-day old kanamycin-resistant seedlings.
(B) *AtMYB68* expression in T3 homozygous lines. Total RNA was extracted from 15-day old seedlings. The ethidium bromide stained gel is shown as a loading control.
10 μg total RNA was loaded in each lane. The numbers above the blots indicate the transgenic lines. Col plants were used for transformation. The two transcripts in transgenic lines were caused by the present of two transcription terminators in the transgene. The short transcript was terminated at the internal *AtMYB68* terminator. The long transcript was terminated at the external 35S polyA terminator introduced by the vector pRT101.

5.3 Repression of *AtMYB68* Expression by Antisense RNA

In order to repress *AtMYB68* expression, transgenic lines in which *AtMYB68* antisense RNA was expressed under the control of the 35S promoter were generated. The 3' end of the *AtMYB68* cDNA encoding the non-conserved region was subcloned behind the *35S* promoter in the antisense orientation in the pRT101 vector (Figure 2-2-C). Then the *35S::AtMYB68-3*(-) construct was cloned into the BIN19 binary vector. After transformation into *Agrobacterium*, the *35S::AtMYB68-3* (-) construct was transformed into Arabidopsis Col plants by the *Agrobacterium*-mediated floral dip method. The *NPT II* gene in the BIN19 vector provided kanamycin-resistance as a selectable marker. T1-generation transformants were selected on kanamycin plates. The transformation rate was 0.85% (34 out of 4,000 with kanamycin-resistance). Kanamycin-resistant T1 plants were allowed to set seeds to generate the T2-generation.

Homozygous lines with the *35S::AtMYB68-3* (–) construct were selected from 6 transgenic lines. The levels of the native *AtMYB68* transcript in the homozygous lines was tested by quantitative RT-PCR (Figure 5-2). Total RNA was extracted from 14-day old seedling roots and subjected to reverse transcription followed by PCR amplification with *AtMYB68* specific primers. 18S rRNA was used as an internal control. The ratio of product intensity of *AtMYB68* to 18S rRNA represents the gene relative expression level. The RT-PCR analysis showed that in 6 homozygous lines tested, lines 1-2 and 11-1 had the *AtMYB68* transcript levels about 2-fold lower than that in the wild type. The other 4 lines generally had the same transcript level as that in the wild type. Since later an *atmyb68* knockout line was identified, these 2 repressed lines were not investigated further.

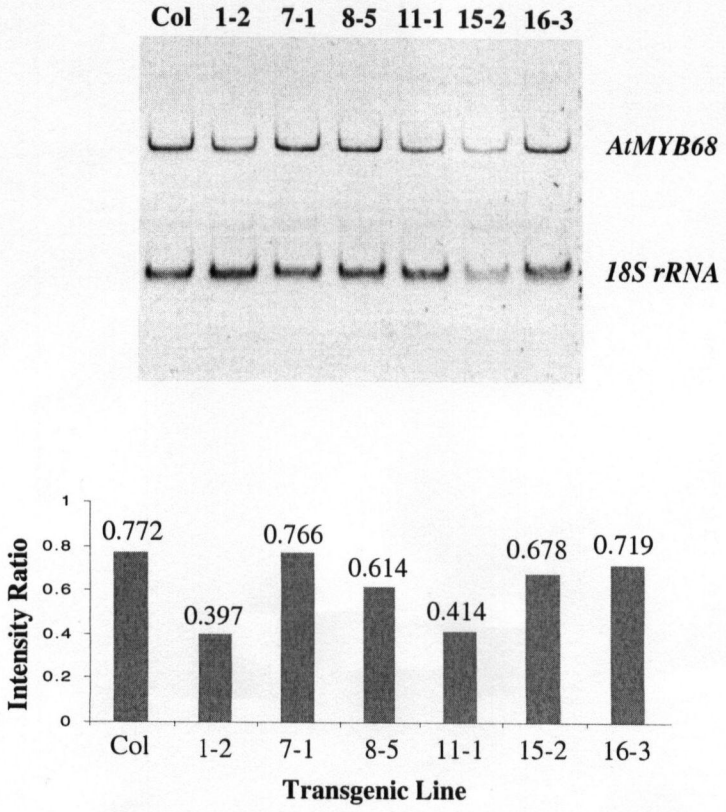

Figure 5-2. RT-PCR Analysis of *AtMYB68* Expression in Homozygous Transgenic Lines Harboring the *35S::AtMYB68* Antisense Transgene.
Total RNA was extracted from 14-day old hydroponically grown seedling roots and subjected to reverse transcription followed by PCR amplification. 18S ribosome RNA was used as an internal control. The ratio of the intensity of *AtMYB68* to 18S rRNA represents the relative *AtMYB68* expression level. The ratios are visualized by bar graphs in the lower panel and values are shown above each bar. The numbers above the gel indicate the transgenic lines. Col plants were used for transformation.

5.4 Screen for *AtMYB68* Knockout Mutations in T-DNA Tagged Populations

As stated in Section 4.1, one T-DNA line with the insertion 536 bp upstream of the ATG codon of *AtMYB68* was identified from the Feldmann T-DNA collection (Pri-Hadash and

Douglas, unpublished data). The level of the *AtMYB68* transcript in the homozygous insertion line, T-14, was tested by a northern blot analysis (Figure 5-3). Total RNA was extracted from 12-day old seedling shoots and roots respectively. The analysis showed that abundance of the *AtMYB68* transcript in the root of line T-14 was the same as that in the wild-type. The *AtMYB68* transcript was not detectable in either shoot RNA. Therefore transcription of *AtMYB68* was not affected in this T-DNA insertion line. No mutant phenotypes were observed in line T-14 under normal growth conditions either (data not shown).

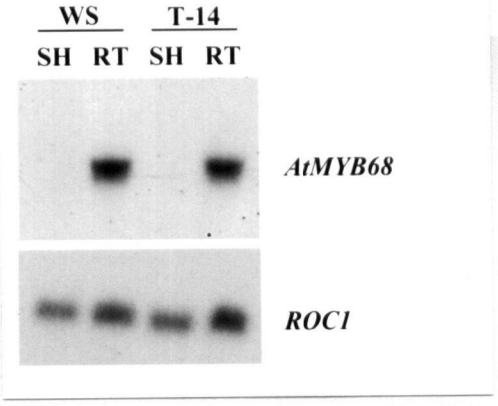

Figure 5-3. Northern Blot Analysis of *AtMYB68* Expression in the T-DNA Insertion Line T-14. Total RNA was extracted from shoots and roots of 12-day old seedlings respectively. 10 μg total RNA was loaded on each lane. The *ROC1* cDNA (encoding Arabidopsis cytosolic cyclophilin) was hybridized to the same blot as a loading control after the blot was stripped. SH, shoot. RT, root. WS ecotype is the wild-type background.

While generating *AtMYB68* overexpression and antisense lines, I continued searching for *AtMYB68* knockout mutations in publicly available T-DNA tagged populations. After Dr. Pri-Hadash finished screening the DuPont and Feldmann collections, I searched the Jack and Wisconsin T-DNA collections by PCR-based strategies (Table 5-1). *AtMYB68* has two small introns, resulting in a total gene size of ~1.6 kb, including potential 5' and 3' regulatory sequences. This ~1.6 kb region was the target sequence in my screening, since a hit in this region would most likely disrupt gene expression.

Table 5-1. Summary of Screens for a T-DNA Insertion in *AtMYB68*

T-DNA Collection	No. of T-DNA line	Position of Insertion	RNA level
DuPont* (Sue Gibson lab)	8,100	None	
Feldmann* (ABRC)	6,000	540 bp upstream of ATG	Normal
Jack (ABRC)	6,000	None	
Wisconsin (U of Wisconsin and ABRC)	60,480	200 bp upstream of ATG+	
Garlic# (TMRI)	100,000	1st intron	Not detectable

* Screened by Dr. Aviva Pri-Hadash

\+ The signal disappeared in 9-line pools.

\# Directly searched on computer.

For screening the Jack collection, which was composed of 6,000 independent T-DNA lines, an *AtMYB68* specific primer slightly outside the 3' end of the coding region combined with T-DNA left and right border primers were used in PCR. The first round of PCR was performed against 6 DNA 1,000-line pools. The PCR reactions were tested by a Southern analysis using the *AtMYB68* cDNA as a probe. No positive signals were detected (data not shown).

Three years ago, the Wisconsin Biotechnology Center provided a screening service for their T-DNA collection, which was composed of 60,480 independent T-DNA lines. We used this service to screen for an *AtMYB68* knockout. *AtMYB68* specific primers targeted slightly outside the 5' and 3' ends of the coding region were sent to them for PCR screening. The first round of PCR searched 30 DNA 2,025-line super pools using the combination of the *AtMYB68* specific primers and a T-DNA left border primer. The PCR reactions were sent to us, and then they were tested on Southern blots using *AtMYB68* genomic DNA as a probe (Figure 5-4). One signal of ~1.7 kb in size that was amplified by the *AtMYB68* reverse primer and the T-DNA left border primer from super pool 7 was detected. There were also other signals detected on the blots, but the sizes were too big and beyond the target region. The signal of ~1.7 kb in size was further re-amplified by the nested primers. The re-amplified signal was gel-purified and sequenced.

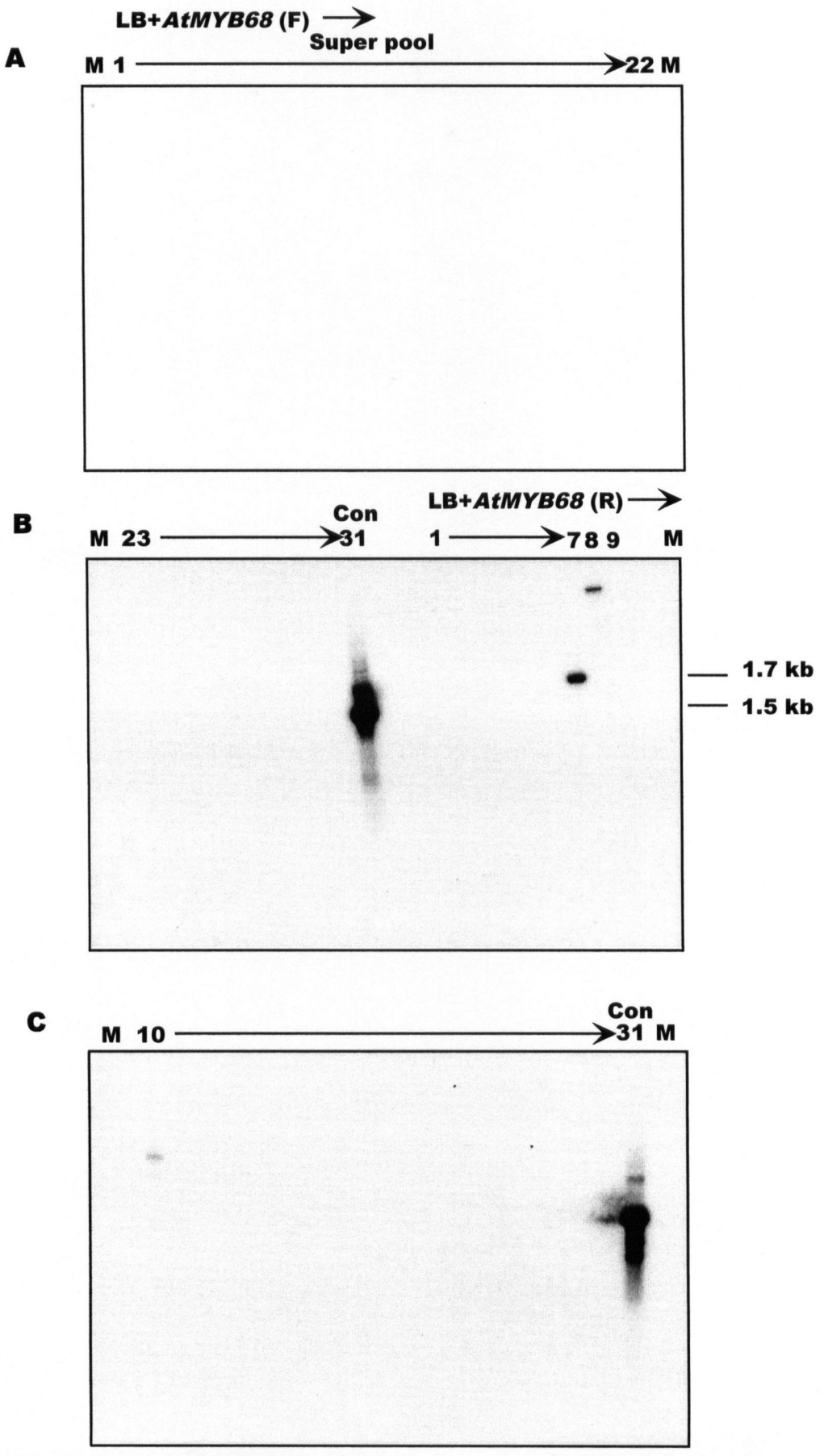
LB+AtMYB68 (F)
Super pool
A
M 1
22 M
B
Con
LB+AtMYB68 (R)
M 23
31
1
7 8 9
M
1.7 kb
1.5 kb
C
Con
M 10
31 M

Sequencing showed that the T-DNA insert was 202 bp upstream of the ATG codon of *AtMYB68*, and there was a 19 bp unknown sequence at the T-DNA-*AtMYB68* junction.

This was a promising insertion position, and then we requested a second round of PCR that searched subpools of super pool 7 (9 pools of 225-line). Again, the PCR reactions were separated on a gel after they were received. A distinct band of ~1.7 kb in size from sub-super pool 61 was observed (Figure 5-5, indicated by arrow). Sub-super pool 61 was re-amplified along with super pool 7 (X7) as a positive control (Figure 5-6). The band of ~1.7 kb in size was re-amplified from sub-super pool 61 (lane 2) using the *AtMYB68* specific and T-DNA left border primers, the same as in super pool 7 (lane 1). A band slightly lower in size was re-amplified using the nested primers (lane 3). No band of the same size was re-amplified using the T-DNA left border primer only (lane 4). These results confirmed that the hit was in sub-super pool 61.

Figure 5-4. Southern Blot Analysis of PCR Amplification for a T-DNA Insertion within *AtMYB68* Using the Wisconsin Collection.
PCR was performed using superpool DNA as templates (superpools 1 to 30) and *AtMYB68* specific primers combined with the T-DNA left border primer (LB) (PCR done by the University of Wisconsin). Each superpool contained 2,025 T-DNA transformed lines. The PCR reactions were separated on a gel and blotted. *AtMYB68* genomic DNA was used to probe blots.
(A) + (B) Left Part, PCR using LB and *AtMYB68* forward primers.
(B) Right part + (C), PCR using LB and *AtMYB68* reverse primers.
Lane 31, the PCR control using *AtMYB68* forward and reverse primers and wild-type WS genomic DNA as a template. M, marker lane with sizes shown at right.

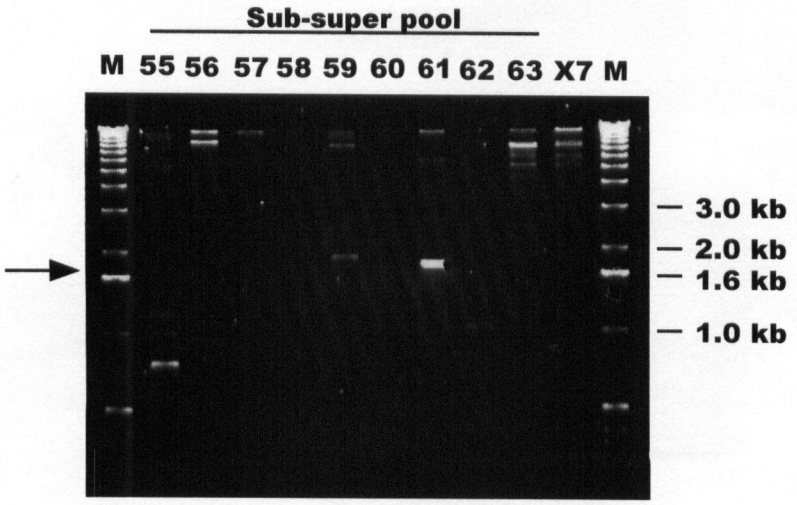

Figure 5-5. Second Round of PCR Amplification for a T-DNA Insertion within *AtMYB68* Using the Wisconsin Collection.
PCR was performed using sub-super pool DNA of the superpool 7 as templates (sub-super pools 55-63) and the *AtMYB68* reverse and the T-DNA left border primers (PCR done by the University of Wisconsin). Each sub-super pool contained 225 T-DNA transformed lines. X7, superpool 7. The arrow indicates the size of the predicted band. M, marker lane with sizes shown at right.

Lastly, the seeds for sub-super pool 61 were ordered, which were composed of 25 pools of 9-line. However one seed pool, J1510, was not sent due to seed shortage. Following the service's instructions, genomic DNA was extracted from 5-day old seedlings of the 24 pools and subjected to PCR amplification using the same conditions as the first two rounds of PCR. The PCR reactions were tested by a Southern analysis as for the first round of PCR. Surprisingly, no signals were detected on the blots except a signal from the control (Figure 5-7). Thus, the signal of the T-DNA insertion in *AtMYB68* that had been detected in the first two rounds of PCR was lost for reasons out of my control. The first two rounds of DNA preps and PCR amplification were performed in Wisconsin, and were beyond my ability to troubleshoot, and I was still

missing one 9-line pool of seeds. Due to these uncertainties and my inability to resolve them, this screening was abandoned.

Figure 5-6. Re-Amplification of an *AtMYB68* -T-DNA Allele from Sub-Super Pool 61 of the Wisconsin Collection.
PCR was performed using the second round PCR reaction from sub-super pool 61 as a template. Superpool 7 DNA was used as a positive control. Lane 1, PCR of superpool 7 DNA using the *AtMYB68* reverse and T-DNA left border primers (LB). Lane 2, PCR of sub-super pool 61 DNA using LB and the *AtMYB68* reverse primers. Lane 3, PCR of sub-super pool 61 DNA using LB and the *AtMYB68* nested primers. Lane 4, PCR of sub-super pool 61 DNA using LB primer only. M, marker lane with sizes shown at left.

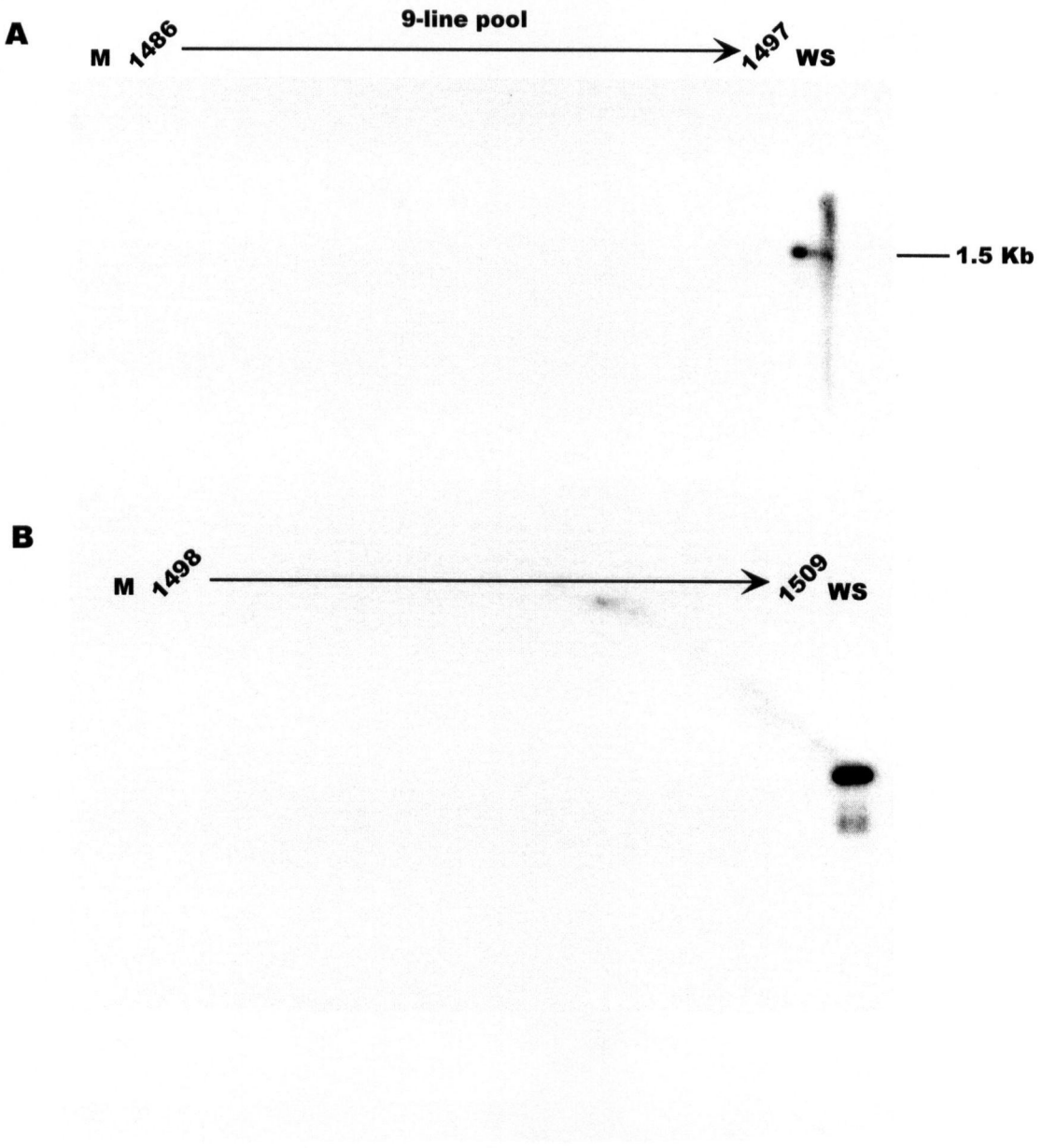

Figure 5-7. Southern Blot Analysis of PCR Amplification for an *AtMYB68*-T-DNA Allele in 9-Line Pools of the Wisconsin Collection.

PCR was performed using 9-line pool DNA as templates (pools 1486-1509) and the *AtMYB68* reverse and T-DNA left border primers. The PCR reactions were separated on a gel and blotted. *AtMYB68* genomic DNA was used to probe blots. WS genomic DNA and the *AtMYB68* specific primers was used in PCR as a control (WS). M, marker lane with sizes shown at right.

(A) 9-line pools 1486 to 1497.

(B) 9-line pools 1498 to 1509.

More recently, by searching on-line databases of sequenced T-DNA junctions, we found that a T-DNA line, Garlic 94B, had the insertion in the *AtMYB68* coding region in the Torrey Mesa Research Institute (TMRI) T-DNA collection. This collection was composed of 100,000 independent T-DNA lines (Table 5-1). The seeds from the line Garlic-94B were ordered. To confirm the insert location, rosette leaves from Garlic 94B plants were pooled. Genomic DNA was extracted from the pooled leaves and subjected to PCR amplification with an *AtMYB68* specific primer and the recommended T-DNA left border primer. The predicted size of the PCR product was ~1.3 kb based on TMRI data. Figure 5-8 shows that only one band of the right size was amplified. This band was gel-purified and sequenced. Sequencing confirmed that the T-DNA insertion was in the predicted location, the first intron of *AtMYB68* (Figure 5-9).

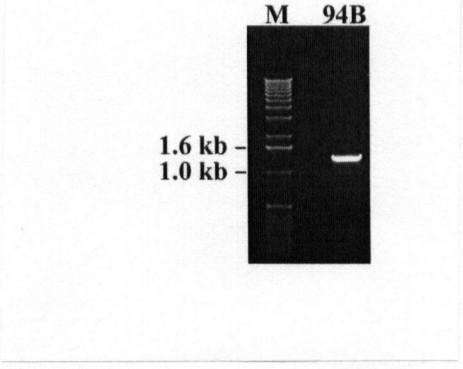

Figure 5-8. PCR Amplification of a T-DNA Insertion within *AtMYB68* in the Garlic 94B Line Using the TMRI Collection.
PCR was performed using genomic DNA extracted from Garlic 94B plants as a template and the *AtMYB68* specific and T-DNA left border primers. M, marker lane with sizes shown at left.

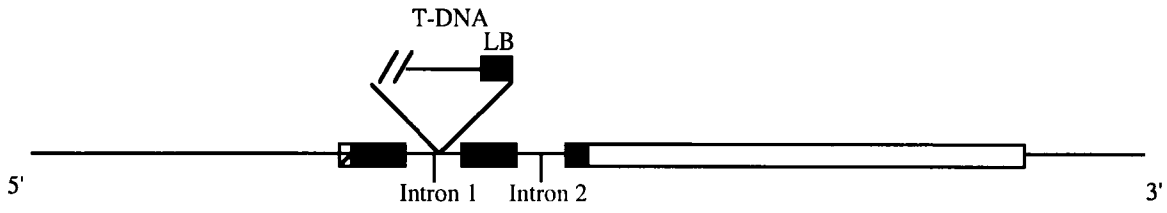

Figure 5-9. Schematic of the T-DNA Insertion within *AtMYB68* from the Garlic 94B Line. The dark and light grey boxes indicate the coding region for the two conserved repeats R2, R3 in the MYB binding domain. The hatched box indicated the conserved 5' region. The open box indicates the non-conserved region.

A homozygous line with the insert was selected from the same generation using a PCR strategy. The first round of PCR selected plants with the insert within the population. This was done by using the *AtMYB68* specific and the T-DNA left border primers in PCR. Figure 5-10-A shows that in a total of 17 plants examined (derived from the Garlic 94B line), a fragment of ~1.3 kb in size was amplified from 13 plants, but not from the other 4 (plants 12, 14, 15 and 17). So these 4 plants did not have the T-DNA insert in *AtMYB68* and they were the wild type siblings. A second round of PCR selected homozygous plants among those with the insert. This was done by using *AtMYB68* specific primers spanning the insertion area for PCR amplification. Since the heterozygous plants would have one copy of a wild-type *AtMYB68* allele, it would be amplified to give a fragment of ~1.5 kb in size. However the *AtMYB68* allele with the insert would be too big to amplify due to the T-DNA insertion, so that no product would be expected in the homozygous plants using these primers. Figure 5-10-B shows that 8 out of 13 plants had a fragment of the predicted size from the wild type copy (plant 4 had the very weak PCR product), suggesting that they were heterozygous. The other 5 plants (plants 5, 8, 11, 18 and 19) did not yield the amplification products. Thus they were presumed to be homozygous for the T-DNA insertion allele. Plant 18 line (referred to 94B-18) was selected for further testing.

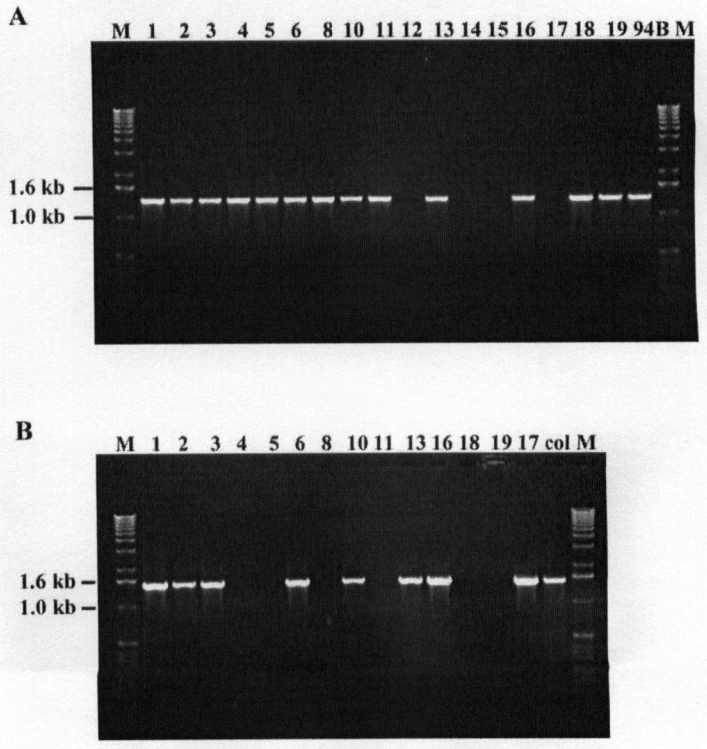

Figure 5-10. PCR Screening for Homozygous Insertion Lines Derived from Garlic 94B.
PCR was performed using genomic DNA from the individual plants derived from Garlic 94B as templates. The numbers above the gels indicate the individual plants. M, marker lane with sizes shown at left.
(A) PCR using the *AtMYB68* specific and T-DNA left border primers. The Garlic 94B DNA pool was used as a positive control.
(B) PCR using the *AtMYB68* specific primers. Col DNA was used as a positive control.

The selectable marker on the binary vector used in the Garlic line transformation was the *BAR* gene, conferring BASTA resistance. Thus the plants in the Garlic line containing a T-DNA insert should also be BASTA-resistant if T-DNA was intact. Therefore BASTA-resistance was also tested in the Garlic-94B line. The result showed that plants from the homozygous line 94B-18 were all BASTA-resistant as expected, but plants from the wild-type sibling line 94B-17 were

also BASTA-resistant. This result indicated that at least one more T-DNA insertion existed in the Garlic-94B line.

The level of the *AtMYB68* transcript in the homozygous line 94B-18 was tested by RT-PCR. Total RNA was extracted from 3-4 days old seedlings. RNA from Col was used as a positive control, and 18S rRNA was used as an internal control for RT-PCR. Figure 5-11-A shows that the level of the *AtMYB68* transcript was not detectable in line 94B-18 on an ethidium bromide stained agarose gel, while the product of the *AtMYB68* transcript from Col was very abundant. When the same reactions were detected on a polyacrylamide gel stained with Syber Green (sensitivity was increased over 100 times), a trace amount of the *AtMYB68* transcript product was seen from line 94B-18. However the abundance was extremely low as compared to Col (Figure 5-11, B), at least 65–fold lower than that in the wild-type. Thus, I referred to the 94B-18 line as an *AtMYB68* 'knockout' line.

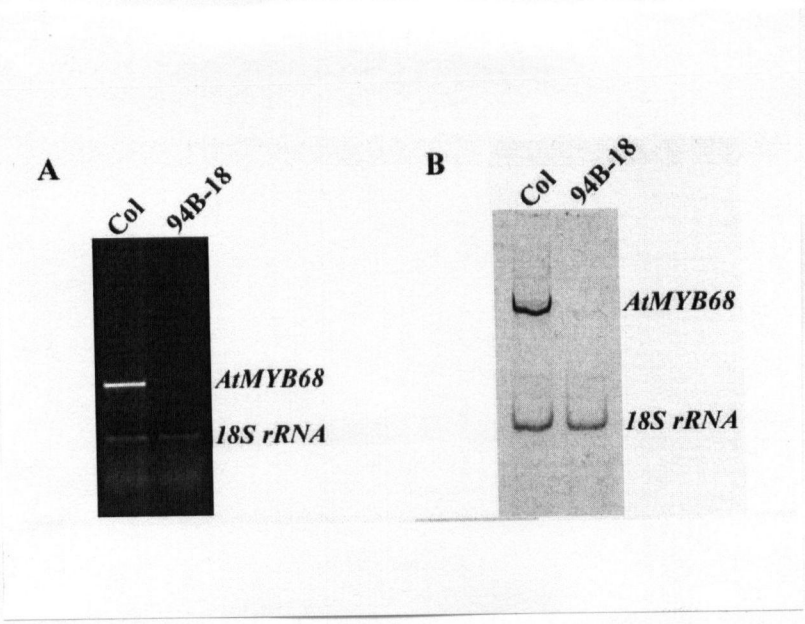

Figure 5-11. RT-PCR Analysis of *AtMYB68* Expression in the T-DNA Insertion Line 94B-18. Total RNA extracted from 3-4 days old seedlings was subjected to reverse transcription followed by PCR amplification. 18S rRNA was used as an internal control for RT-PCR. Col RNA was used as a control.
(A) RT-PCR reactions separated on an ethidium bromide stained agarose gel.
(B) RT-PCR reactions separated on a polyarylamide gel and then stained by Sybre Green.

5.5 Phenotypic Analysis of *AtMYB68* Mutant Lines

Morphological mutant phenotypes were examined in both the *AtMYB68* overexpression line 9-3, and the knockout line 94B-18. As described in the last section, at least one more T-DNA locus other than the insertion in *AtMYB68* exists in the Garlic-94B line. Backcrossing the homozygous line 94B-18 to Col to remove the background T-DNA has been initiated. However due to time limitations, the result of this backcrossing is not included in this thesis. To overcome this problem, a sibling of line 94B-18, line 94B-17, lacking the T-DNA insertion in *AtMYB68*, was used as a control in phenotypic inspection of the knockout line. The genetic background of 94B-17 is identical to the sibling 94B-18. Therefore, any difference on phenotype in line 94B-18 should be solely caused by the disrupted *AtMYB68*.

I first examined phenotypes under normal growth conditions on plates and in soil. No obvious morphological changes were observed in either the overexpression line or the knockout line, except that plants from the overexpression line 9-3 appeared generally shorter than wild-type Col (Figure 5-12, D). Measurements of shoot fresh weight, primary root length and lateral root number were taken from 11-day old seedlings grown on MS plates. These measurements were taken in several batches of seedlings. One set of this data is shown in Table 5-2. No clear statistical differences were shown in different sets of measurements (Table 5-2). The Garlic-94B population generally produced shorter primary roots than Col, but there was no difference in the knockout line 94B-18 and the sibling line 94B-17 (Figure 5-12, A and Table 5-2).

Figure 5-12. Morphology of *AtMYB68* Mutant Plants.
(A) 10-day old seedlings of the *atmyb68* knockout line 94B-18 and controls grown on a plate.
(B) Mature plants of the *atmyb68* knockout line 94B-18 and the control grown in soil.
(C) 11-day old seedlings of the *AtMYB68* overexpression line 9-3 and Col grown on plates.
(D) Mature plants of the *AtMYB68* overexpression line 9-3 and Col grown in soil.
94B-17, a wild-type sibling in the Garlic-94B line. Col, Columbia ecotype.

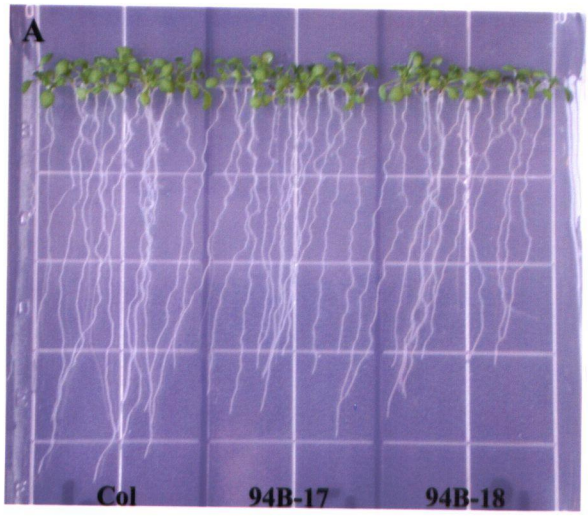

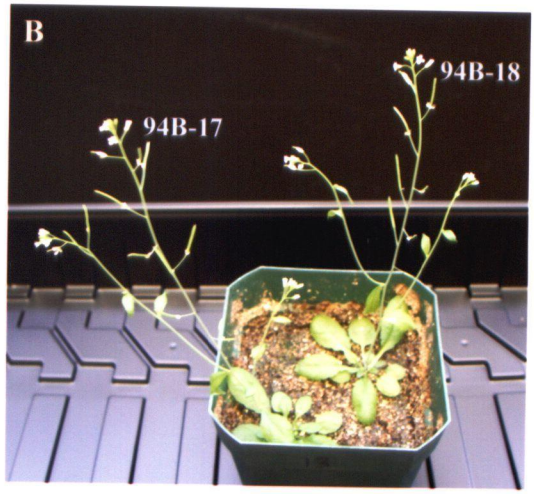

C

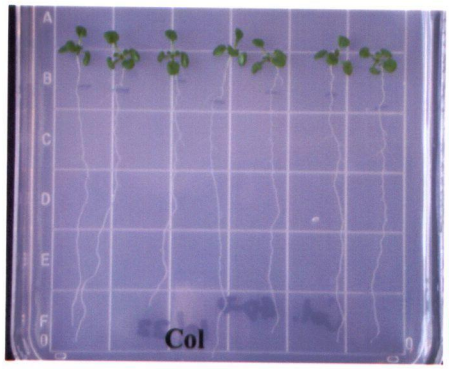

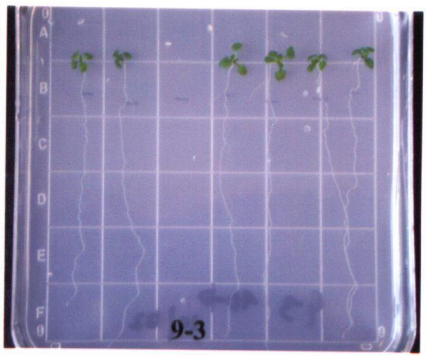

Table 5-2. Growth of *AtMYB68* Mutant Seedlings on Plates*

Line	PRL (mm)	LR No./L $(cm)^{-1}$	SHW (mg)
9-3	64.7±5.6^	1.2±0.2	3.2±1.0
Col	60.0±3.2	1.6±0.3	4.9±0.7
94B-18	59.0±2.7	1.6±0.4	4.7±1.1
94B-17	62.1±3.5	1.0±0.2	4.3±0.8

*Measurements were taken on 11-day old seedlings grown on MS plate plus 3% sucrose.
^ The number indicates SD (n=7).
PRL, primary root length. LR No./L, lateral root number per primary root. SHW, shoot fresh weight.

In Section 4.4, the level of the *AtMYB68* transcript was shown to be up-regulated by ABA, and down-regulated by IAA, cold and desiccation treatments. These treatments served as guidelines for preliminary phenotypic examinations under specific conditions. Phenotypes were examined in response to two plant hormones, ABA and IAA. For the ABA treatment, 1.0 μM ABA was added to medium. Shoot fresh weight, primary root growth and lateral root number were measured after 7 days grown on ABA plates. No significant difference was shown with the measurements in either mutant line (Table 5-3). For the IAA treatment, 1.0 μM IAA was added to medium. The lateral root number was measured after 5 days grown on IAA plates. Again, there was no significant difference in lateral root number increase in response to IAA between the control and *AtMYB68* mutant lines (Table 5-4).

Table 5-3. Seedling growth under ABA treatment*

Line	ABA (μM)	Root growth (%)	LR No	Shoot growth (%)
9-3	0	100	7.7±2.9	100
	1.0	80.0±12.0^	7.6±4.1	86.0±7.31
Col	0	100	10.9±4.02	100
	1.0	95.1±4.80	13.0±2.24	100±16.5
94B-18	0	100	9.7±1.7	100
	1.0	80.8±5.8	5.9±2.5	61.9±6.6
94B-17	0	100	8.4±2.3	100
	1.0	89.4±1.8	7.0±1.5	67.8±5.1

*Measurement were taken after 6 days (for lines 94B-18 and 94B-17), or 7 days (for lines 9-3 and Col) of ABA treatments (1.0 μM).

^ The number indicates SD (n=7).

Root and shoot growth are expressed as the relative growth to the control (0 ABA). LR No, Lateral root

Table 5-4. Seedling lateral root number under IAA treatment (No./L $(cm)^{-1}$)*

IAA (μM)	Overexpression line		Knockout line	
	9-3	Col	94B-18	94B-17
0	1.9±0.51^	2.3±0.49	2.4±0.37	2.6±0.27
1.0	7.3±0.97	7.2±0.41	7.8±0.64	6.9±0.71

*The lateral root number was counted after 5 days of IAA treatments (1.0 μM). No./L, lateral root number per primary root.

^The number indicates SD (n=7).

Phenotypes were also examined under salinity and drought stresses. For the salinity treatment, inhibition of seedling root elongation on 50, 100 and 150 mM NaCl supplemented media was shown by a root-bending assay. For the drought treatment, soil-grown plants were not watered for 2 weeks. Drought tolerance was observed. Plant roots elongate in a wavy pattern when grown on a hard agar surface at an inclined position. This obstacle-touching response is thought to involve auxin signaling (Okada and Shimura, 1992). Thus, this response was also

tested. Under these conditions, no differences between the control and the overexpression or knockout line were observed (data not shown).

Thus, as summarized in Table 5-5, no phenotypic differences were observed between the control and *AtMYB68* mutant lines with respect to normal growth or any of the conditions tested (Table 5-5).

Table 5-5. Summary of Phenotypic Examinations of *AtMYB68* Mutant Lines

Condition	Mutant Phenotype	
	Overexpression line 9-3	Knockout line Garlic 94B-18
Normal growth:		
MS+3% sucrose	No*	No
Soil	No	No
Treatments:		
Abscisic acid	No	No
Indoleacetic acid	No	No
Salinity	No	No
Drought	No	No
Root obstacle-touching	No	No

* Mutant phenotype was not observed. Some data are shown in separate tables.

5.6 Expression Patterns of the Members in AtMYB Phylogenetic Subgroup 14

As stated in Chapter 1, the Arabidopsis R2R3-MYB proteins were categorized into 22 phylogenetic subgroups according to similarity outside the conserved MYB DNA-binding domain (Kranz et al., 1998; Stracke et al., 2001). AtMYB68 was placed in subgroup 14, along with another 5 members, AtMYB84, AtMYB36, AtMYB87, AtMYB37 and AtMYB38 (Figure 5-13). AtMYB84 is the most closely related to AtMYB68 according to this analysis. To gain some insight on how functionally related these family members might be, I wished to compare their expression patterns, and chose AtMYB84 and AtMYB36, another member of this subgroup less closely related to AtMYB68, for the analysis.

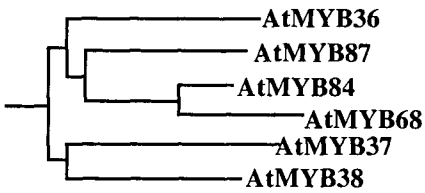

Figure 5-13. Re-Drawing of AtMYB Phylogenetic Subgroup 14 (According to Stracke et al., 2001).

When aligned, it can be seen that the predicted amino acid sequences of these three members were very similar to each other in the conserved amino-terminal MYB DNA-binding domains. Outside the MYB DNA-binding domain, AtMYB68 and AtMYB84 shared two conserved motifs, but they were not well conserved in AtMYB36 (Figure 5-14). Overall, at the amino acid level, AtMYB68 has 57.3% identity to AtMYB84, and 40.5% identity to AtMYB36.

The level of the *AtMYB84* transcript was too low to be detected by a northern blot analysis. Therefore, RT-PCR was used to examine expression patterns of these three genes. Total RNA extracted from Arabidopsis seedlings and mature organs was subjected to the quantitative RT-PCR, using 18S rRNA as an internal control. Figure 5-15 shows that *AtMYB36* had the expression pattern very similar to that of *AtMYB68*. Both were mainly detected in roots and also detectable in 3-day old seedlings, but not detectable in the other organs, including bolting stems, rosette leaves, flowers and siliques. The member most closely related to *AtMYB68, AtMYB84,* had a different expression pattern from the other two. The *AtMYB84* transcript was detected at low levels in all the tissues/organs tested. Northern blot analyses of expression of *AtMYB68* and *AtMYB36* revealed the same result as these RT-PCR data (Figure 4-3 and Figure 3-3-F). These data suggest that *AtMYB36* may be functionally related to *AtMYB68*.

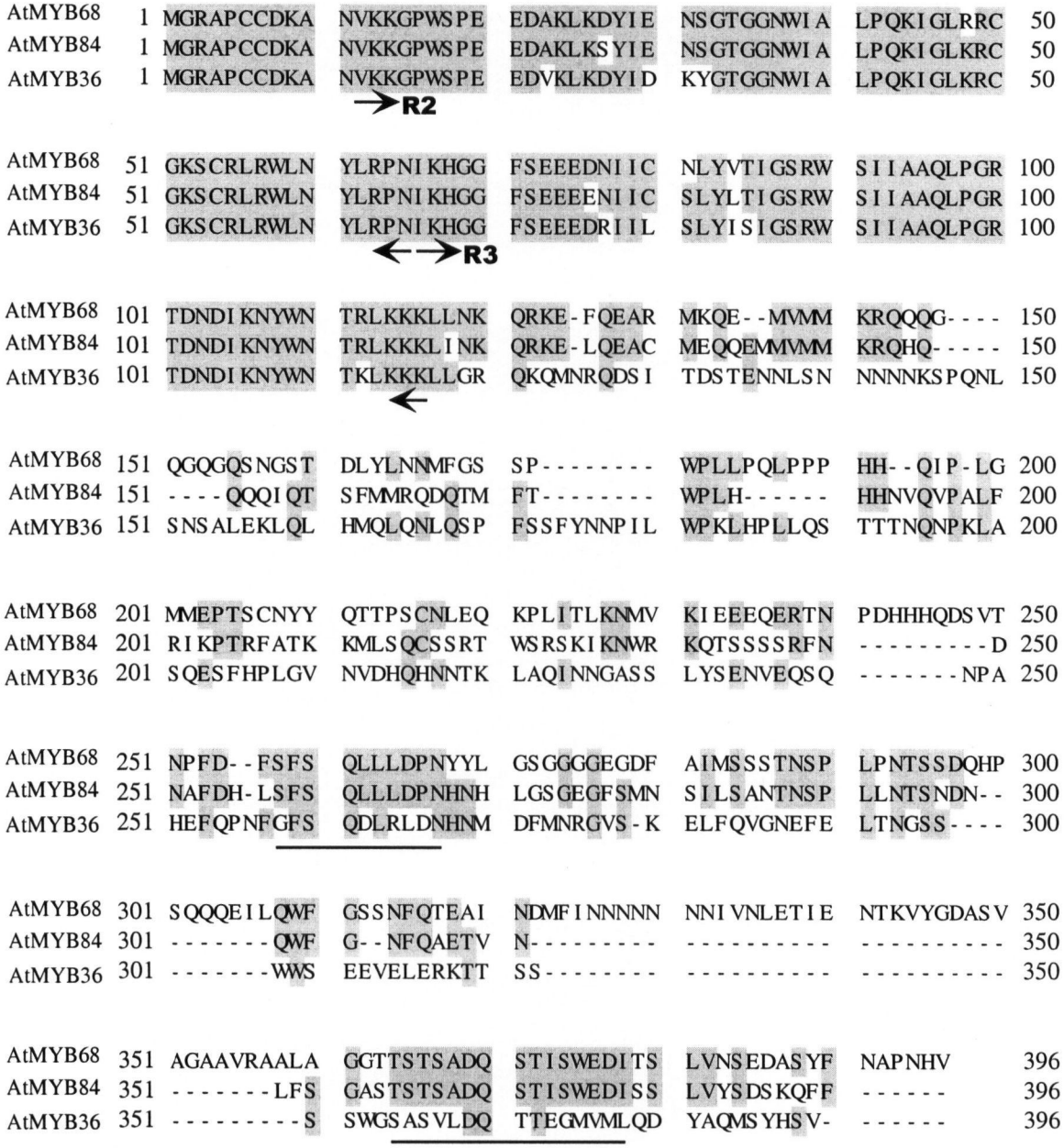

Figure 5-14. Alignment of AtMYB68 with the other Two Members of Phylogenetic Sub-Group 14.

The shaded areas indicate the conserved amino acids. R2 and R3 are the two conserved repeats in the MYB DNA-binding domain. The underlined sequences indicate conserved motifs outside the MYB DNA-binding domain.

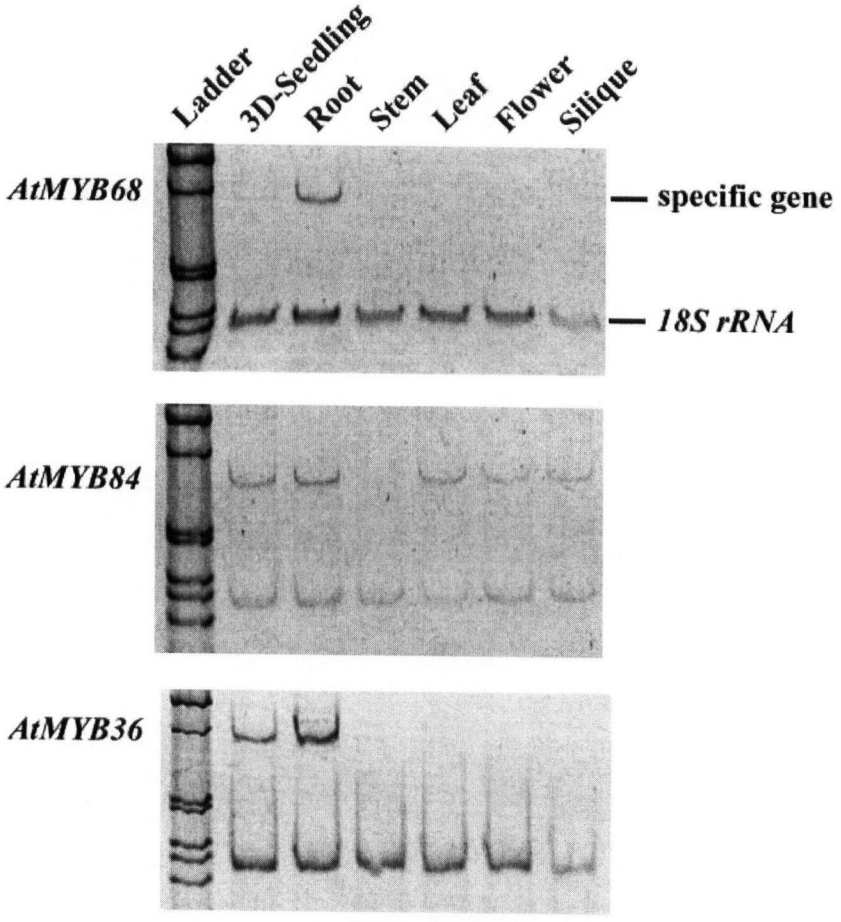

Figure 5-15. RT-PCR Analysis of Expression Patterns of Three Members in the AtMYB Phylogenetic Sub-Group 14.

Total RNA extracted from Col seedlings and mature organs was subjected to reverse transcription followed by PCR amplification. The upper band is the gene specific band. The lower band is 18S rRNA used as an internal control for RT-PCR. Latter, marker lane.

5.7 Discussion

In this chapter, I described the uses of reverse genetic approaches (knockout of gene expression), and overexpression to determine the function of *AtMYB68*. However, neither approach revealed any obvious alterations in morphological phenotype under either normal growth conditions or experimental conditions tested. This result is actually consistent with major trends in functional studies of Arabidopsis *MYB* genes using reverse genetic approaches. In the study done by Meissner et al. (1999), of 47 insertion lines for 36 *AtMYB* genes identified, none exhibited obvious morphological changes, even in the lines in which gene transcription was reduced or abolished. The lack of phenotypic alterations in the mutants is probably due to functional redundancy among *AtMYB* genes.

Functional redundancy has not been documented in plant *MYB* genes, but it has been illustrated in the MADS-box transcription factor gene family. MADS-box transcription factors are also encoded by a large gene family in plants. They control many aspects of plant development, most notably flower development, but also fruit and root development (Theissen et al, 2000). The MADS-box *SHATTERPROOF* genes, *SHP1* and *SHP2* are both required for fruit dehiscence in Arabidopsis. SHP1 and SHP2 share 87% identity in their amino acid sequences, and have similar expression patterns. Single mutations in either of the two genes did not cause phenotypic changes, but the *shp1shp2* double mutant resulted in fruits failed to dehisce (Liljegren et al., 2000).

Another remarkable example of functional redundancy within the MADS-box gene family is that of the *SEPALLATA* genes, which are required for the function of some organ-identity genes. *SEP1*, *SEP2* and *SEP3* are three members closely related to each other. Single insertion mutations or even double mutants caused only subtle changes in phenotype. However, the triple mutant displayed a novel feature: all four flower whorls converted to sepals (Pelaz et al., 2000).

From sequence analysis of the Arabidopsis MADS-box genes, it is estimated that more than 40% of the genes might have redundant (or partially redundant) functions (Riechmann and

Ratcliffe, 2000). Therefore, the examples in the MADS-box gene family should not be regarded as exceptions and a similar scenario might exist in the *AtMYB* gene family as well.

Studies of MADS-box genes revealed that the genes with redundant functions are usually similar in sequence and related to each other in phylogenetic trees (Riechmann and Ratcliffe, 2000). As reviewed in Chapter 1, the same trend has been shown in functional studies of plant *MYB* genes as well, such as *TT2* (*AtMYB123*) and *ZmMYBC1* in the phylogenetic subgroup 5, and *PhMYBAN2*, *PAP1* (*AtMYB75*) and *PAP2* (*AtMYB90*) in the subgroup 6. Therefore, in order to determine if genes in the same phylogenic subgroup as *AtMYB68* could be functionally similar, I examined expression patterns of genes in this subgroup. My results showed that at least one more member of this subgroup, *AtMYB36*, had an expression pattern similar to *AtMYB68*. The member most closely related to *AtMYB68*, *AtMYB84,* had a different but overlapping expression pattern. MPSS data shows that *AtMYB36* expression is root-specific in the organs examined, and it reveals another root-preferential gene in this subgroup, *AtMYB38*. These data support our speculation that the members in this subgroup may not only have related sequences, but also related functions. So far, functional characterizations of members in this subgroup have not been reported. We are not able to infer the *AtMYB68* function based on known examples.

Another possibility for absence of observed phenotypic alterations in the *AtMYB68* mutant lines might be due to the limited number of assays that were performed. In the systematic screen for *AtMYB* mutations by reverse genetics (Meissner et al., 1999), 26 transposon or T-DNA insertion lines, in which many lines had reduced or abolished mRNA levels, were examined under different growth conditions based on plate and greenhouse assays. However, only a minority of these lines revealed discernable changes in response to various stimuli. Since there is no evidence that any of the 125 R2R3-type *AtMYB* genes represents a pseudogene, there must be a function associated to each gene. To find conditions under which gene mutants display phenotypes is a continuing challenge.

It is worth noting that in screening for a T-DNA insertion in *AtMYB68*, we found a total of 3 insertion lines (including the one lost in the Wisconsin collection). Only one of them had an

insert in the ORF, while the other two insertions were in the promoter region >200 bp upstream of the ATG codon. The study by Meissner et al. (1999) had similar results. Only 22 of 47 insertions (including 40 transposon insertion lines and 7 T-DNA insertion lines) were within ORFs. None of 7 T-DNA insertions was located in ORFs, and most of them were within promoter regions ≥500 bp upstream of translation start codons. These data reveal that efficiency to obtain the knockout insertions with this technique may be low. In this study, although the insertion in the first intron of *AtMYB68* reduced the gene expression to an extremely low level, *AtMYB68* expression was not totally abolished. This was also observed by Meissner et al. (1999), who found that many insertions, even those in transcribed regions, only reduced but did not abolish gene expression.

Although to date the function of *AtMYB68* is still unknown, the work presented here definitely provides a good base for future studies. As more and more insertion collections from Arabidopsis are obtained, there is an increasing chance to find a knockout mutation for any particular gene. Besides insertional mutagenesis, other reverse genetics strategies, such as TILLING, are also being used in Arabidopsis (McCallum et al., 2000). Therefore, one strategy is to keep searching for knockouts in members of the same subgroup as *AtMYB68*, and then to cross the knockouts, such as *atmyb36* and *atmyb38*, to create double or even triple mutants to reveal the function of *AtMYB68* and related gene family members.

Recently, microarray technology has been developed, which allows the parallel monitoring of expression of thousands of genes, and some Arabidopsis gene chips are commercially available. Using such a chip, it should be feasible to detect global differences in gene expression in the *atmyb68* knockout line 94B-18 relative to that in wild-type. This might identify downstream genes regulated by *AtMYB68*, and therefore could link *AtMYB68* function to a particular developmental pathway, which would help to reveal *AtMYB68* function.

Bibliography

Abe, H., Urao, T., Ito, T., Seki, M., Shinozaki, K., and Yamaguchi-Shinozaki, K. (2003). Arabidopsis AtMYC2 (bHLH) and AtMYB2 (MYB) function as transcriptional activators in abscisic acid signaling. Plant Cell *15*, 63-78.

Abe, H., Yamaguchi-Shinozaki, K., Urao, T., Iwasaki, T., Hosokawa, D., and Shinozaki, K. (1997). Role of arabidopsis MYC and MYB homologs in drought- and abscisic acid-regulated gene expression. Plant Cell *9*, 1859-68.

Alabadi, D., Oyama, T., Yanovsky, M. J., Harmon, F. G., Mas, P., and Kay, S. A. (2001). Reciprocal regulation between TOC1 and LHY/CCA1 within the Arabidopsis circadian clock. Science *293*, 880-3.

Baranowskij, N., Frohberg, C., Prat, S., and Willmitzer, L. (1994). A novel DNA binding protein with homology to Myb oncoproteins containing only one repeat can function as a transcriptional activator. Embo J *13*, 5383-92.

Becker-Andre, M., Schulze-Lefert, P., and Hahlbrock, K. (1991). Structural comparison, modes of expression, and putative cis-acting elements of the two 4-coumarate: CoA ligase genes in potato. J Biol Chem *266*, 8551-9.

Bender, J., and Fink, G. R. (1998). A Myb homologue, ATR1, activates tryptophan gene expression in Arabidopsis. Proc Natl Acad Sci U S A *95*, 5655-60.

Borevitz, J. O., Xia, Y., Blount, J., Dixon, R. A., and Lamb, C. (2000). Activation tagging identifies a conserved MYB regulator of phenylpropanoid biosynthesis. Plant Cell *12*, 2383-2394.

Bosher, J. M., and Labouesse, M. (2000). RNA interference: genetic wand and genetic watchdog. Nat Cell Biol *2*, E31-6.

Bradford, M. M. (1976). A rapid and sensitive method for the quantitation of microgram quantities of protein utilizing the principle of protein-dye binding. Anal Biochem *72*, 248-54.

Braun, E. L., and Grotewold, E. (1999). Newly discovered plant c-myb-like genes rewrite the evolution of the plant myb gene family. Plant Physiol *121*, 21-4.

Brenner, S., Johnson, M., Bridgham, J., Golda, G., Lloyd, D. H., Johnson, D., Luo, S., McCurdy, S., Foy, M., Ewan, M., Roth, R., George, D., Eletr, S., Albrecht, G., Vermaas, E., Williams, S. R., Moon, K., Burcham, T., Pallas, M., DuBridge, R. B., Kirchner, J., Fearon, K., Mao, J., and

Corcoran, K. (2000). Gene expression analysis by massively parallel signature sequencing (MPSS) on microbead arrays. Nat Biotechnol *18*, 630-4.

Brenner, S., Williams, S. R., Vermaas, E. H., Storck, T., Moon, K., McCollum, C., Mao, J. I., Luo, S., Kirchner, J. J., Eletr, S., DuBridge, R. B., Burcham, T., and Albrecht, G. (2000). In vitro cloning of complex mixtures of DNA on microbeads: physical separation of differentially expressed cDNAs. Proc Natl Acad Sci U S A *97*, 1665-70.

Broccoli, D., Smogorzewska, A., Chong, L., and de Lange, T. (1997). Human telomeres contain two distinct Myb-related proteins, TRF1 and TRF2. Nat Genet *17*, 231-5.

Burssens, S., de Almeida Engler, J., Beeckman, T., Richard, C., Shaul, O., Ferreira, P., Van Montagu, M., and Inze, D. (2000). Developmental expression of the Arabidopsis thaliana CycA2;1 gene. Planta *211*, 623-31.

Busk, P. K., and Pages, M. (1998). Regulation of abscisic acid-induced transcription. Plant Mol Biol *37*, 425-35.

Byrne, M. E., Barley, R., Curtis, M., Arroyo, J. M., Dunham, M., Hudson, A., and Martienssen, R. A. (2000). Asymmetric leaves1 mediates leaf patterning and stem cell function in Arabidopsis. Nature *408*, 967-71.

Cano-Delgado, A. I., Metzlaff, K., and Bevan, M. W. (2000). The eli1 mutation reveals a link between cell expansion and secondary cell wall formation in Arabidopsis thaliana. Development *127*, 3395-405.

Carre, I. A., and Kim, J. Y. (2002). MYB transcription factors in the Arabidopsis circadian clock. J Exp Bot *53*, 1551-7.

Casimiro, I., Marchant, A., Bhalerao, R. P., Beeckman, T., Dhooge, S., Swarup, R., Graham, N., Inze, D., Sandberg, G., Casero, P. J., and Bennett, M. (2001). Auxin transport promotes Arabidopsis lateral root initiation. Plant Cell *13*, 843-52.

Celenza, J. L., Jr., Grisafi, P. L., and Fink, G. R. (1995). A pathway for lateral root formation in Arabidopsis thaliana. Genes Dev *9*, 2131-42.

Charlton, W. A. (1991). Lateral root initiation, in Plant Roots - The Hidden Half. Waisel, Y., Eshel, A., and Kafkafi, U. ed (New York: Marcel Dekker, Inc.), 107-128.

Chen, W., Provart, N. J., Glazebrook, J., Katagiri, F., Chang, H. S., Eulgem, T., Mauch, F., Luan, S., Zou, G., Whitham, S. A., Budworth, P. R., Tao, Y., Xie, Z., Chen, X., Lam, S., Kreps,

J. A., Harper, J. F., Si-Ammour, A., Mauch-Mani, B., Heinlein, M., Kobayashi, K., Hohn, T., Dangl, J. L., Wang, X., and Zhu, T. (2002). Expression profile matrix of Arabidopsis transcription factor genes suggests their putative functions in response to environmental stresses. Plant Cell *14*, 559-74.

Chuang, C. F., and Meyerowitz, E. M. (2000). Specific and heritable genetic interference by double-stranded RNA in Arabidopsis thaliana. Proc Natl Acad Sci U S A *97*, 4985-90.

Church, G. M., and Gilbert, W. (1984). Genomic sequencing. Proc Natl Acad Sci U S A *81*, 1991-5.

Clough, S. J., and Bent, A. F. (1998). Floral dip: a simplified method for Agrobacterium-mediated transformation of Arabidopsis thaliana. Plant J *16*, 735-43.

Cone, K. C., Burr, F. A., and Burr, B. (1986). Molecular analysis of the maize anthocyanin regulatory locus C1. Proc Natl Acad Sci U S A *83*, 9631-5.

Daniel, X., Lacomme, C., Morel, J. B., and Roby, D. (1999). A novel myb oncogene homologue in Arabidopsis thaliana related to hypersensitive cell death. Plant J *20*, 57-66.

de Lange, P., van Blokland, R., Kooter, J. M., and Mol, J. N. (1995). Suppression of flavonoid flower pigmentation genes in Petunia hybrida by the introduction of antisense and sense genes. Curr Top Microbiol Immunol *197*, 57-75.

de Vetten, N., Quattrocchio, F., Mol, J., and Koes, R. (1997). The an11 locus controlling flower pigmentation in petunia encodes a novel WD-repeat protein conserved in yeast, plants, and animals. Genes Dev *11*, 1422-34.

Di Laurenzio, L., Wysocka-Diller, J., Malamy, J. E., Pysh, L., Helariutta, Y., Freshour, G., Hahn, M. G., Feldmann, K. A., and Benfey, P. N. (1996). The SCARECROW gene regulates an asymmetric cell division that is essential for generating the radial organization of the Arabidopsis root. Cell *86*, 423-33.

Dixon, R. A., and Harrison, M. J. (1990). Activation, structure, and organization of genes involved in microbial defense in plants. Adv Genet *28*, 165-234.

Dixon, R. A., and Paiva, N. L. (1995). Stress-Induced Phenylpropanoid Metabolism. Plant Cell *7*, 1085-1097.

Dolan, L., Janmaat, K., Willemsen, V., Linstead, P., Poethig, S., Roberts, K., and Scheres, B. (1993). Cellular organisation of the Arabidopsis thaliana root. Development *119*, 71-84.

Dooner, H. K., Robbins, T. P., and Jorgensen, R. A. (1991). Genetic and developmental control of anthocyanin biosynthesis. Annu Rev Genet *25*, 173-99.

Douglas, C. J. (1996). Phenylpropanoid metablism and lignin biosynthesis: from weeds to trees. Trends in Plant Sci *1*, 171-178.

Douglas, C. J., Ellard, M., Hauffe, K. D., Molitor, E., de Sa, M. M. Reinold, S., Subramaniam, R., and William, F. (1992). General phenylpropanoid metabolism: regulation by environmental and developmental signals, in Phenolic Metabolism in Plants, Stafford, H. A., and Ibrahim, R. K. ed (Plenum Press, New York), 63-89.

Ehlting, J., Buttner, D., Wang, Q., Douglas, C. J., Somssich, I. E., and Kombrink, E. (1999). Three 4-coumarate:coenzyme A ligases in Arabidopsis thaliana represent two evolutionarily divergent classes in angiosperms. Plant J *19*, 9-20.

Fahrendorf, T., Ni, W., Shorrosh, B. S., and Dixon, R. A. (1995). Stress responses in alfalfa (Medicago sativa L.) XIX. Transcriptional activation of oxidative pentose phosphate pathway genes at the onset of the isoflavonoid phytoalexin response. Plant Mol Biol *28*, 885-900.

Feldbrugge, M., Sprenger, M., Hahlbrock, K., and Weisshaar, B. (1997). PcMYB1, a novel plant protein containing a DNA-binding domain with one MYB repeat, interacts in vivo with a light-regulatory promoter unit. Plant J *11*, 1079-93.

Fields, S., and Song, O. (1989). A novel genetic system to detect protein-protein interactions. Nature *340*, 245-6.

Finnegan, E. J., Peacock, W. J., and Dennis, E. S. (1996). Reduced DNA methylation in Arabidopsis thaliana results in abnormal plant development. Proc Natl Acad Sci U S A *93*, 8449-54.

Fuller, S. A., Takahashi, M., and Hurrell, J. G. R. (1997). Purification of monoclonal antibodies, in Current protocols in Molecular Biology. Ausubel, F. M. et al. ed (John Wiley & Sons, Inc.), 11.11.2-11.11.3.

Giraudat, J., Parcy, F., Bertauche, N., Gosti, F., Leung, J., Morris, P. C., Bouvier-Durand, M., and Vartanian, N. (1994). Current advances in abscisic acid action and signalling. Plant Mol Biol *26*, 1557-77.

Goff, S. A., Cone, K. C., and Chandler, V. L. (1992). Functional analysis of the transcriptional activator encoded by the maize B gene: evidence for a direct functional interaction between two classes of regulatory proteins. Genes Dev *6*, 864-75.

Gorlach, J., Raesecke, H. R., Rentsch, D., Regenass, M., Roy, P., Zala, M., Keel, C., Boller, T., Amrhein, N., and Schmid, J. (1995). Temporally distinct accumulation of transcripts encoding enzymes of the prechorismate pathway in elicitor-treated, cultured tomato cells. Proc Natl Acad Sci U S A *92*, 3166-70.

Greider, C. W. (1996). Telomere length regulation. Annu Rev Biochem *65*, 337-65.

Grotewold, E., Drummond, B. J., Bowen, B., and Peterson, T. (1994). The myb-homologous P gene controls phlobaphene pigmentation in maize floral organs by directly activating a flavonoid biosynthetic gene subset. Cell *76*, 543-53.

Grotewold, E., Sainz, M. B., Tagliani, L., Hernandez, J. M., Bowen, B., and Chandler, V. L. (2000). Identification of the residues in the Myb domain of maize C1 that specify the interaction with the bHLH cofactor R. Proc Natl Acad Sci U S A *97*, 13579-84.

Gubler, F., Kalla, R., Roberts, J. K., and Jacobsen, J. V. (1995). Gibberellin-regulated expression of a myb gene in barley aleurone cells: evidence for Myb transactivation of a high-pI alpha-amylase gene promoter. Plant Cell *7*, 1879-91.

Hahlbrock, K. and Scheel, D. (1989). Physiology and molecular biology of phenylpropanoid metabolism. Annu Rev Plant Physiol Plant Mol Biol *40*, 347-369.

Hamilton, A. J., Fray, R. G., and Grierson, D. (1995). Sense and antisense inactivation of fruit ripening genes in tomato. Curr Top Microbiol Immunol *197*, 77-89.

Hemerly, A. S., Ferreira, P., de Almeida Engler, J., Van Montagu, M., Engler, G., and Inze, D. (1993). cdc2a expression in Arabidopsis is linked with competence for cell division. Plant Cell *5*, 1711-23.

Hoeren, F. U., Dolferus, R., Wu, Y., Peacock, W. J., and Dennis, E. S. (1998). Evidence for a role for AtMYB2 in the induction of the Arabidopsis alcohol dehydrogenase gene (ADH1) by low oxygen. Genetics *149*, 479-90.

Ito, M., Araki, S., Matsunaga, S., Itoh, T., Nishihama, R., Machida, Y., Doonan, J. H., and Watanabe, A. (2001). G2/M-phase-specific transcription during the plant cell cycle is mediated by c-Myb-like transcription factors. Plant Cell *13*, 1891-905.

Jackson, D., Culianez-Macia, F., Prescott, A. G., Roberts, K., and Martin, C. (1991). Expression patterns of myb genes from Antirrhinum flowers. Plant Cell *3*, 115-25.

Jin, H., Cominelli, E., Bailey, P., Parr, A., Mehrtens, F., Jones, J., Tonelli, C., Weisshaar, B., and Martin, C. (2000). Transcriptional repression by AtMYB4 controls production of UV-protecting sunscreens in Arabidopsis. Embo J *19*, 6150-61.

Kirik, V., and Baumlein, H. (1996). A novel leaf-specific myb-related protein with a single binding repeat. Gene *183*, 109-13.

Kirik, V., Kolle, K., Misera, S., and Baumlein, H. (1998). Two novel MYB homologues with changed expression in late embryogenesis-defective Arabidopsis mutants. Plant Mol Biol *37*, 819-27.

Kirik, V., Schnittger, A., Radchuk, V., Adler, K., Hulskamp, M., and Baumlein, H. (2001). Ectopic expression of the Arabidopsis AtMYB23 gene induces differentiation of trichome cells. Dev Biol *235*, 366-77.

Klempnauer, K. H., Gonda, T. J., and Bishop, J. M. (1982). Nucleotide sequence of the retroviral leukemia gene v-myb and its cellular progenitor c-myb: the architecture of a transduced oncogene. Cell *31*, 453-63.

Kobayashi, S., Ishimaru, M., Hiraoka, K., and Honda, C. (2002). Myb-related genes of the Kyoho grape (Vitis labruscana) regulate anthocyanin biosynthesis. Planta *215*, 924-33.

Koornneef, M., Dellaert, L. W., and van der Veen, J. H. (1982). EMS- and radiation-induced mutation frequencies at individual loci in Arabidopsis thaliana (L.) Heynh. Mutat Res *93*, 109-23.

Kranz, H., Scholz, K., and Weisshaar, B. (2000). c-MYB oncogene-like genes encoding three MYB repeats occur in all major plant lineages. Plant J *21*, 231-5.

Kranz, H. D., Denekamp, M., Greco, R., Jin, H., Leyva, A., Meissner, R. C., Petroni, K., Urzainqui, A., Bevan, M., Martin, C., Smeekens, S., Tonelli, C., Paz-Ares, J., and Weisshaar, B. (1998). Towards functional characterisation of the members of the R2R3-MYB gene family from Arabidopsis thaliana. Plant J *16*, 263-76.

Krysan, P. J., Young, J. C., and Sussman, M. R. (1999). T-DNA as an insertional mutagen in Arabidopsis. Plant Cell *11*, 2283-90.

Krysan, P. J., Young, J. C., Tax, F., and Sussman, M. R. (1996). Identification of transferred DNA insertions within Arabidopsis genes involved in signal transduction and ion transport. Proc Natl Acad Sci U S A *93*, 8145-50.

Kwok, S. F., Solano, R., Tsuge, T., Chamovitz, D. A., Ecker, J. R., Matsui, M., and Deng, X. W. (1998). Arabidopsis homologs of a c-Jun coactivator are present both in monomeric form and in the COP9 complex, and their abundance is differentially affected by the pleiotropic cop/det/fus mutations. Plant Cell *10*, 1779-90.

Laemmli, U. K. (1970). Cleavage of structural proteins during the assembly of the head of bacteriophage T4. Nature *227*, 680-5.

Larkin, J. C., Oppenheimer, D. G., Pollock, S., and Marks, M. D. (1993). Arabidopsis GLABROUS1 Gene Requires Downstream Sequences for Function. Plant Cell *5*, 1739-1748.

Laskowski, M. J., Williams, M. E., Nusbaum, H. C., and Sussex, I. M. (1995). Formation of lateral root meristems is a two-stage process. Development *121*, 3303-10.

Lee, D., Ellard, M., Wanner, L. A., Davis, K. R., and Douglas, C. J. (1995). The Arabidopsis thaliana 4-coumarate:CoA ligase (4CL) gene: stress and developmentally regulated expression and nucleotide sequence of its cDNA. Plant Mol Biol *28*, 871-84.

Lee, D., Meyer, K., Chapple, C., and Douglas, C. J. (1997). Antisense suppression of 4-coumarate:coenzyme A ligase activity in Arabidopsis leads to altered lignin subunit composition. Plant Cell *9*, 1985-98.

Lee, M. M., and Schiefelbein, J. (2001). Developmentally distinct MYB genes encode functionally equivalent proteins in Arabidopsis. Development *128*, 1539-46.

Lee, M. M., and Schiefelbein, J. (1999). WEREWOLF, a MYB-related protein in Arabidopsis, is a position-dependent regulator of epidermal cell patterning. Cell *99*, 473-83.

Lee, M. W., Qi, M., and Yang, Y. (2001). A novel jasmonic acid-inducible rice myb gene associates with fungal infection and host cell death. Mol Plant Microbe Interact *14*, 527-35.

Leyser, O., and Fitter, A. (1998). Roots are branching out in patches. Trends plant Sci. *3*, 203-204.

Liljegren, S. J., Ditta, G. S., Eshed, Y., Savidge, B., Bowman, J. L., and Yanofsky, M. F. (2000). SHATTERPROOF MADS-box genes control seed dispersal in Arabidopsis. Nature *404*, 766-70.

Locatelli, F., Bracale, M., Magaraggia, F., Faoro, F., Manzocchi, L. A., and Coraggio, I. (2000). The product of the rice myb7 unspliced mRNA dimerizes with the maize leucine zipper Opaque2 and stimulates its activity in a transient expression assay. J Biol Chem *275*, 17619-25.

Logemann, E., Parniske, M., and Hahlbrock, K. (1995). Modes of expression and common structural features of the complete phenylalanine ammonia-lyase gene family in parsley. Proc Natl Acad Sci U S A *92*, 5905-9.

Lois, R., Dietrich, A., Hahlbrock, K., and Schulz, W. (1989). A phenylalanine ammonia-lyase gene from parsley: structure, regulation and identification of elicitor and light responsive cis-acting elements. Embo J *8*, 1641-8.

Lu, C. A., Ho, T. H., Ho, S. L., and Yu, S. M. (2002). Three novel MYB proteins with one DNA binding repeat mediate sugar and hormone regulation of alpha-amylase gene expression. Plant Cell *14*, 1963-80.

Ludwig, S. R., Habera, L. F., Dellaporta, S. L., and Wessler, S. R. (1989). Lc, a member of the maize R gene family responsible for tissue-specific anthocyanin production, encodes a protein similar to transcriptional activators and contains the myc-homology region. Proc Natl Acad Sci U S A *86*, 7092-6.

Maes, T., De Keukeleire, P., and Gerats, T. (1999). Plant tagnology. Trends Plant Sci *4*, 90-96.

Mahonen, A. P., Bonke, M., Kauppinen, L., Riikonen, M., Benfey, P. N., and Helariutta, Y. (2000). A novel two-component hybrid molecule regulates vascular morphogenesis of the Arabidopsis root. Genes Dev *14*, 2938-43.

Malamy, J. E., and Benfey, P. N. (1997). Organization and cell differentiation in lateral roots of Arabidopsis thaliana. Development *124*, 33-44.

McCallum, C. M., Comai, L., Greene, E. A., and Henikoff, S. (2000). Targeting induced local lesions IN genomes (TILLING) for plant functional genomics. Plant Physiol *123*, 439-42.

McCully, M. E. (1975). The development of lateral roots, in The Development and Function of Roots. Torrey, J. G., and Clarkson, D. T. ed (Academic Press: New York), 105-124.

McKinney, E. C., Ali, N., Traut, A., Feldmann, K. A., Belostotsky, D. A., McDowell, J. M., and Meagher, R. B. (1995). Sequence-based identification of T-DNA insertion mutations in Arabidopsis: actin mutants act2-1 and act4-1. Plant J *8*, 613-22.

Meissner, R. C., Jin, H., Cominelli, E., Denekamp, M., Fuertes, A., Greco, R., Kranz, H. D., Penfield, S., Petroni, K., Urzainqui, A., Martin, C., Paz-Ares, J., Smeekens, S., Tonelli, C., Weisshaar, B., Baumann, E., Klimyuk, V., Marillonnet, S., Patel, K., Speulman, E., Tissier, A. F., Bouchez, D., Jones, J. J., Pereira, A., Wisman, E., and et al. (1999). Function search in a large transcription factor gene family in Arabidopsis: assessing the potential of reverse genetics to identify insertional mutations in R2R3 MYB genes. Plant Cell *11*, 1827-40.

Murashige, T., and Skook, F. (1962). Physiol. Plant *15*, 473.

Nesi, N., Debeaujon, I., Jond, C., Pelletier, G., Caboche, M., and Lepiniec, L. (2000). The TT8 gene encodes a basic helix-loop-helix domain protein required for expression of DFR and BAN genes in Arabidopsis siliques. Plant Cell *12*, 1863-78.

Nesi, N., Jond, C., Debeaujon, I., Caboche, M., and Lepiniec, L. (2001). The Arabidopsis TT2 gene encodes an R2R3 MYB domain protein that acts as a key determinant for proanthocyanidin accumulation in developing seed. Plant Cell *13*, 2099-114.

Newton, R. J. (1977). Abscisic acid effects on fronds and roots of *Lemna minor* L. Am. J. Bot. *64*, 45-49.

Noda, K., Glover, B. J., Linstead, P., and Martin, C. (1994). Flower colour intensity depends on specialized cell shape controlled by a Myb-related transcription factor. Nature *369*, 661-4.

Oppenheimer, D. G., Herman, P. L., Sivakumaran, S., Esch, J., and Marks, M. D. (1991). A myb gene required for leaf trichome differentiation in Arabidopsis is expressed in stipules. Cell *67*, 483-93.

Pabo, C. O., and Sauer, R. T. (1992). Transcription factors: structural families and principles of DNA recognition. Annu Rev Biochem *61*, 1053-95.

Payne, C. T., Zhang, F., and Lloyd, A. M. (2000). GL3 encodes a bHLH protein that regulates trichome development in arabidopsis through interaction with GL1 and TTG1. Genetics *156*, 1349-62.

Paz-Ares, J., Ghosal, D., Wienand, U., Peterson, P. A., and Saedler, H. (1987). The regulatory c1 locus of Zea mays encodes a protein with homology to myb proto-oncogene products and with structural similarities to transcriptional activators. Embo J *6*, 3553-8.

Pelaz, S., Ditta, G. S., Baumann, E., Wisman, E., and Yanofsky, M. F. (2000). B and C floral organ identity functions require SEPALLATA MADS-box genes. Nature *405*, 200-3.

Penfield, S., Meissner, R. C., Shoue, D. A., Carpita, N. C., and Bevan, M. W. (2001). MYB61 is required for mucilage deposition and extrusion in the Arabidopsis seed coat. Plant Cell *13*, 2777-91.

Planchais, S., Perennes, C., Glab, N., Mironov, V., Inze, D., and Bergounioux, C. (2002). Characterization of cis-acting element involved in cell cycle phase-independent activation of Arath;CycB1;1 transcription and identification of putative regulatory proteins. Plant Mol Biol *50*, 111-27.

Quattrocchio, F., Wing, J., van der Woude, K., Souer, E., de Vetten, N., Mol, J., and Koes, R. (1999). Molecular analysis of the anthocyanin2 gene of petunia and its role in the evolution of flower color. Plant Cell *11*, 1433-44.

Quattrocchio, F., Wing, J. F., Leppen, H., Mol, J., and Koes, R. E. (1993). Regulatory Genes Controlling Anthocyanin Pigmentation Are Functionally Conserved among Plant Species and Have Distinct Sets of Target Genes. Plant Cell *5*, 1497-1512.

Que, Q., and Jorgensen, R. A. (1998). Homology-based control of gene expression patterns in transgenic petunia flowers. Dev Genet *22*, 100-9.

Rabinowicz, P. D., Braun, E. L., Wolfe, A. D., Bowen, B., and Grotewold, E. (1999). Maize R2R3 Myb genes: Sequence analysis reveals amplification in the higher plants. Genetics *153*, 427-44.

Radwanski, E. R., and Last, R. L. (1995). Tryptophan biosynthesis and metabolism: biochemical and molecular genetics. Plant Cell *7*, 921-34.

Reed, R. C., Brady, S. R., and Muday, G. K. (1998). Inhibition of auxin movement from the shoot into the root inhibits lateral root development in Arabidopsis. Plant Physiol *118*, 1369-78.

Riechmann, J. L., Heard, J., Martin, G., Reuber, L., Jiang, C., Keddie, J., Adam, L., Pineda, O., Ratcliffe, O. J., Samaha, R. R., Creelman, R., Pilgrim, M., Broun, P., Zhang, J. Z., Ghandehari, D., Sherman, B. K., and Yu, G. (2000). Arabidopsis transcription factors: genome-wide comparative analysis among eukaryotes. Science *290*, 2105-10.

Riechmann, J. L., and Ratcliffe, O. J. (2000). A genomic perspective on plant transcription factors. Curr Opin Plant Biol *3*, 423-34.

Riechmann, J. L., and Ratcliffe, O. J. (2000). A genomic perspective on plant transcription factors. Curr Opin Plant Biol *3*, 423-34.

Robertson, J. M., Yeung, E. C., Reid, D. M., and Hubick, K. T. (1990). Developmental responses to drought and abscisic acid in sunflower roots. 2. Mitotic activity. J. Exp. Bot. *41*, 339-350.

Romero, I., Fuertes, A., Benito, M. J., Malpica, J. M., Leyva, A., and Paz-Ares, J. (1998). More than 80R2R3-MYB regulatory genes in the genome of Arabidopsis thaliana. Plant J *14*, 273-84.

Rubin, G. M., Yandell, M. D., Wortman, J. R., Gabor Miklos, G. L., Nelson, C. R., Hariharan, I. K., Fortini, M. E., Li, P. W., Apweiler, R., Fleischmann, W., Cherry, J. M., Henikoff, S., Skupski, M. P., Misra, S., Ashburner, M., Birney, E., Boguski, M. S., Brody, T., Brokstein, P., Celniker, S. E., Chervitz, S. A., Coates, D., Cravchik, A., Gabrielian, A., Galle, R. F., Gelbart, W. M., George, R. A., Goldstein, L. S., Gong, F., Guan, P., Harris, N. L., Hay, B. A., Hoskins, R. A., Li, J., Li, Z., Hynes, R. O., Jones, S. J., Kuehl, P. M., Lemaitre, B., Littleton, J. T., Morrison, D. K., Mungall, C., O'Farrell, P. H., Pickeral, O. K., Shue, C., Vosshall, L. B., Zhang, J., Zhao, Q., Zheng, X. H., and Lewis, S. (2000). Comparative genomics of the eukaryotes. Science *287*, 2204-15.

Rutherford, R., and Masson, P. H. (1996). Arabidopsis thaliana sku mutant seedlings show exaggerated surface-dependent alteration in root growth vector. Plant Physiol *111*, 987-98.

Sablowski, R. W., Baulcombe, D. C., and Bevan, M. (1995). Expression of a flower-specific Myb protein in leaf cells using a viral vector causes ectopic activation of a target promoter. Proc Natl Acad Sci U S A *92*, 6901-5.

Sablowski, R. W., Moyano, E., Culianez-Macia, F. A., Schuch, W., Martin, C., and Bevan, M. (1994). A flower-specific Myb protein activates transcription of phenylpropanoid biosynthetic genes. Embo J *13*, 128-37.

Samuels, A. L., Rensing, K. H., Douglas, C. J., Mansfield, S. D., Dharmawardhana, D. P., and Ellis, B. E. (2002). Cellular machinery of wood production: differentiation of secondary xylem in Pinus contorta var. latifolia. Planta *216*, 72-82.

Schaffer, R., Ramsay, N., Samach, A., Corden, S., Putterill, J., Carre, I. A., and Coupland, G. (1998). The late elongated hypocotyl mutation of Arabidopsis disrupts circadian rhythms and the photoperiodic control of flowering. Cell *93*, 1219-29.

Schellmann, S., Schnittger, A., Kirik, V., Wada, T., Okada, K., Beermann, A., Thumfahrt, J., Jurgens, G., and Hulskamp, M. (2002). TRIPTYCHON and CAPRICE mediate lateral inhibition during trichome and root hair patterning in Arabidopsis. Embo J *21*, 5036-46.

Scheres, B. (1997). Cell signaling in root development. Curr Opin Genet Dev *7*, 501-6.

Scheres, B., Di Laurenzio, L., Willemsen, V., Hauser, M-T., Janmaat, K., Weisbeek, P., and Benfey, P. N. (1995). Mutations affecting the radial organization of the *Arabidopsis* root display specific defects throughout the embryonic axis. Development *121*, 53-62.

Scheres, B., Wolkenfelt, H., Willemsen, V., Terlouw, M., Lawson, E., Dean, C., and Weisbeek, P. (1994). Embryonic origin of the *Arabidopsis* primary root and root meristem initials. Development *120*, 2475-2487.

Schroder, J. (1989). Protein sequence homology between plant 4-coumarate:CoA ligase and firefly luciferase. Nucleic Acids Res *17*, 460.

Schuch, W. (1991). Using antisense RNA to study gene function. Symp Soc Exp Biol *45*, 117-27.

Seki, M., Narusaka, M., Ishida, J., Nanjo, T., Fujita, M., Oono, Y., Kamiya, A., Nakajima, M., Enju, A., Sakurai, T., Satou, M., Akiyama, K., Taji, T., Yamaguchi-Shinozaki, K., Carninci, P., Kawai, J., Hayashizaki, Y., and Shinozaki, K. (2002). Monitoring the expression profiles of 7000 Arabidopsis genes under drought, cold and high-salinity stresses using a full-length cDNA microarray. Plant J *31*, 279-292.

Serna, L., and Fenoll, C. (1997). Tracing the ontogeny of stomatal clusters in Arabidopsis with molecular markers. Plant J *12*, 747-55.

Shi, H., Quintero, F. J., Pardo, J. M., and Zhu, J. K. (2002). The putative plasma membrane Na(+)/H(+) antiporter SOS1 controls long-distance Na(+) transport in plants. Plant Cell *14*, 465-77.

Shinozaki, K., and Yamaguchi-Shinozaki, K. (2000). Molecular responses to dehydration and low temperature: differences and cross-talk between two stress signaling pathways. Curr Opin Plant Biol *3*, 217-23.

Singh, K. B. (1998). Transcriptional regulation in plants: the importance of combinatorial control. Plant Physiol *118*, 1111-20.

Spelt, C., Quattrocchio, F., Mol, J. N., and Koes, R. (2000). anthocyanin1 of petunia encodes a basic helix-loop-helix protein that directly activates transcription of structural anthocyanin genes. Plant Cell *12*, 1619-32.

Spink, K. G., Evans, R. J., and Chambers, A. (2000). Sequence-specific binding of Taz1p dimers to fission yeast telomeric DNA. Nucleic Acids Res *28*, 527-33.

Steeves, T., and Sussex, I. (1989). Patterns in plant development. Cambridge University Press, Cambridge, UK.

Stomp, A-M. (1992). Using the *GUS* gene as a recepter of gene expression, in *GUS* Protocols. Gallagher, S. R. ed (Academic Press, Inc.), 103-113.

Stracke, R., Werber, M., and Weisshaar, B. (2001). The R2R3-MYB gene family in Arabidopsis thaliana. Curr Opin Plant Biol *4*, 447-56.

Sugimoto, K., Takeda, S., and Hirochika, H. (2000). MYB-related transcription factor NtMYB2 induced by wounding and elicitors is a regulator of the tobacco retrotransposon Tto1 and defense-related genes. Plant Cell *12*, 2511-2528.

Tamagnone, L., Merida, A., Parr, A., Mackay, S., Culianez-Macia, F. A., Roberts, K., and Martin, C. (1998). The AmMYB308 and AmMYB330 transcription factors from antirrhinum regulate phenylpropanoid and lignin biosynthesis in transgenic tobacco. Plant Cell *10*, 135-54.

Taiz, L., and Zeiger, E. (2002). Plant Physiology (3rd). Sunderland, MA: Sinauer Associates, Inc.

Theissen, G., Becker, A., Di Rosa, A., Kanno, A., Kim, J. T., Munster, T., Winter, K. U., and Saedler, H. (2000). A short history of MADS-box genes in plants. Plant Mol Biol *42*, 115-49.

Thompson, M. A., and Ramsay, R. G. (1995). Myb: an old oncoprotein with new roles. Bioessays *17*, 341-50.

Timmermans, M. C., Hudson, A., Becraft, P. W., and Nelson, T. (1999). ROUGH SHEATH2: a Myb protein that represses knox homeobox genes in maize lateral organ primordia. Science *284*, 151-3.

Topfer, R., Matzeit, V., Gronenborn, B., Schell, J., and Steinbiss, H. H. (1987). A set of plant expression vectors for transcriptional and translational fusions. Nucleic Acids Res *15*, 5890.

Urao, T., Yamaguchi-Shinozaki, K., Urao, S., and Shinozaki, K. (1993). An Arabidopsis myb homolog is induced by dehydration stress and its gene product binds to the conserved MYB recognition sequence. Plant Cell *5*, 1529-39.

Vailleau, F., Daniel, X., Tronchet, M., Montillet, J. L., Triantaphylides, C., and Roby, D. (2002). A R2R3-MYB gene, AtMYB30, acts as a positive regulator of the hypersensitive cell death program in plants in response to pathogen attack. Proc Natl Acad Sci U S A *99*, 10179-84.

Vassetzky, N. S., Gaden, F., Brun, C., Gasser, S. M., and Gilson, E. (1999). Taz1p and Teb1p, two telobox proteins in Schizosaccharomyces pombe, recognize different telomere-related DNA sequences. Nucleic Acids Res *27*, 4687-94.

Wada, T., Tachibana, T., Shimura, Y., and Okada, K. (1997). Epidermal cell differentiation in Arabidopsis determined by a Myb homolog, CPC. Science *277*, 1113-6.

Walbot, V. (2000). Saturation mutagenesis using maize transposons. Curr Opin Plant Biol *3*, 103-7.

Wang, H., Qi, Q., Schorr, P., Cutler, A. J., Crosby, W. L., and Fowke, L. C. (1998). ICK1, a cyclin-dependent protein kinase inhibitor from Arabidopsis thaliana interacts with both Cdc2a and CycD3, and its expression is induced by abscisic acid. Plant J *15*, 501-10.

Wang, Z. Y., Kenigsbuch, D., Sun, L., Harel, E., Ong, M. S., and Tobin, E. M. (1997). A Myb-related transcription factor is involved in the phytochrome regulation of an Arabidopsis Lhcb gene. Plant Cell *9*, 491-507.

Wang, Z. Y., and Tobin, E. M. (1998). Constitutive expression of the CIRCADIAN CLOCK ASSOCIATED 1 (CCA1) gene disrupts circadian rhythms and suppresses its own expression. Cell *93*, 1207-17.

Weigel, D., Ahn, J. H., Blazquez, M. A., Borevitz, J. O., Christensen, S. K., Fankhauser, C., Ferrandiz, C., Kardailsky, I., Malancharuvil, E. J., Neff, M. M., Nguyen, J. T., Sato, S., Wang, Z. Y., Xia, Y., Dixon, R. A., Harrison, M. J., Lamb, C. J., Yanofsky, M. F., and Chory, J. (2000). Activation tagging in Arabidopsis. Plant Physiol *122*, 1003-13.

Weston, K. (1998). Myb proteins in life, death and differentiation. Curr Opin Genet Dev *8*, 76-81.

Weston, K. (1998). Myb proteins in life, death and differentiation. Curr Opin Genet Dev *8*, 76-81.

Winkler, R. G., Frank, M. R., Galbraith, D. W., Feyereisen, R., and Feldmann, K. A. (1998). Systematic reverse genetics of transfer-DNA-tagged lines of Arabidopsis. Isolation of mutations in the cytochrome p450 gene superfamily. Plant Physiol *118*, 743-50.

Wu, S. J., Ding, L., and Zhu, J. K. (1996). SOS1, a Genetic Locus Essential for Salt Tolerance and Potassium Acquisition. Plant Cell *8*, 617-627.

Yu, E. Y., Kim, S. E., Kim, J. H., Ko, J. H., Cho, M. H., and Chung, I. K. (2000). Sequence-specific DNA recognition by the Myb-like domain of plant telomeric protein RTBP1. J Biol Chem *275*, 24208-14.

Zeevaart, J. A. D., and Creelman, R. A. (1988). Metabolism and physiology of abscisic acid. Annu. Rev. Plant Physiol. Plant Mol. Biol. *39*, 439-473.

Zhang, H., and Forde, B. G. (1998). An Arabidopsis MADS box gene that controls nutrient-induced changes in root architecture. Science *279*, 407-9.

Zhang, H., Jennings, A., Barlow, P. W., and Forde, B. G. (1999). Dual pathways for regulation of root branching by nitrate. Proc Natl Acad Sci U S A *96*, 6529-34.